DEVELOPMENT AND CHARACTERIZATION OF SILICA AND TITANIA BASED NANOSTRUCTURED MATERIALS FOR THE REMOVAL OF INDOOR AND OUTDOOR AIR POLLUTANTS

by

THELGE MANINDU NIRASHA PEIRIS

B.Sc., University of Colombo, Sri Lanka, 2007

AN ABSTRACT OF A DISSERTATION

submitted in partial fulfillment of the requirements for the degree

DOCTOR OF PHILOSOPHY

Department of Chemistry
College of Arts and Sciences

KANSAS STATE UNIVERSITY
Manhattan, Kansas

2012

Abstract

Solar energy driven catalytic systems have gained popularity in environmental remediation recently. Various photocatalytic systems have been reported in this regard and most of the photocatalysts are based on well-known semiconducting material, Titanium Dioxide, while some are based on other materials such as Silicon Dioxide and various Zeolites. However, in titania based photocatalysts, titania is actively involved in the catalytic mechanism by absorbing light and generating exitons. Because of this vast popularity of titania in the field of photocatalysis it is believed that photocatalysis mainly occurs via non-localized mechanisms and semiconductors are extremely important.

Even though it is still rare, photocatalysis could be localized and possible without use of a semiconductor as well. Thus, to support localized photocatalytic systems, and to compare the activity to titania based systems, degradation of organic air pollutants by nanostructured silica, titania and mixed silica titania systems were studied. New materials were prepared using two different approaches, precipitation technique (xerogel) and aerogel preparation technique.

The prepared xerogel samples were doped with both metal (silver) and non-metals (carbon and sulfur) and aerogel samples were loaded with Chromium, Cobalt and Vanadium separately, in order to achieve visible light photocatalytic activity.

Characterization studies of the materials were carried out using Nova BET analysis, DR UV-vis spectrometry, powder X-ray diffraction, X-ray photoelectron Spectroscopy, FT-IR spectroscopy, Transmission Electron Microscopy, *etc*. Kinetics of the catalytic activities was studied using a Shimadzu GCMS-QP 5000 instrument using a closed glass reactor. All the experiments were carried out in gaseous phase using acetaldehyde as the model pollutant.

Kinetic results suggest that chromium doped silica systems are good UV and visible light active photocatalysts. This is a good example for a localized photocatalytic activity. In contrast, our xerogel system shows comparatively high visible light photocatalytic activity for the titania based system, showing the importance of non-localized nature of photocatalysis. The Cobalt doped silica system shows interesting dark catalytic activity towards acetaldehyde and several other pollutants. Thus, in summary, based on the different activities we observed during our studies these materials could be successfully used to improve the quality of both indoor and outdoor air.

DEVELOPMENT AND CHARACTERIZATION OF SILICA AND TITANIA BASED NANOSTRUCTURED MATERIALS FOR THE REMOVAL OF INDOOR AND OUTDOOR AIR POLLUTANTS

by

THELGE MANINDU NIRASHA PEIRIS

B.Sc., University of Colombo, Sri Lanka, 2007

A DISSERTATION

submitted in partial fulfillment of the requirements for the degree

DOCTOR OF PHILOSOPHY

Department of Chemistry
College of Arts and Sciences

KANSAS STATE UNIVERSITY
Manhattan, Kansas

2012

Approved by:

Major Professor
Prof. Kenneth J. Klabunde

Copyright

Abstract

Solar energy driven catalytic systems have gained popularity in environmental remediation recently. Various photocatalytic systems have been reported in this regard and most of the photocatalysts are based on well-known semiconducting material, Titanium Dioxide, while some are based on other materials such as Silicon Dioxide and various Zeolites. However, in titania based photocatalysts, titania is actively involved in the catalytic mechanism by absorbing light and generating exitons. Because of this vast popularity of titania in the field of photocatalysis it is believed that photocatalysis mainly occurs via non-localized mechanisms and semiconductors are extremely important.

Even though it is still rare, photocatalysis could be localized and possible without use of a semiconductor as well. Thus, to support localized photocatalytic systems, and to compare the activity to titania based systems, degradation of organic air pollutants by nanostructured silica, titania and mixed silica titania systems were studied. New materials were prepared using two different approaches, precipitation technique (xerogel) and aerogel preparation technique.

The prepared xerogel samples were doped with both metal (silver) and non-metals (carbon and sulfur) while aerogel samples were loaded with Chromium, Cobalt and Vanadium separately, in order to achieve visible light photocatalytic activity.

Characterization studies of the materials were carried out using Nova BET analysis, DR UV-vis spectrometry, powder X-ray diffraction, X-ray photoelectron Spectroscopy, FT-IR spectroscopy, Transmission Electron Microscopy, *etc*. Kinetics of the catalytic activities was studied using a Shimadzu GCMS-QP 5000 instrument using a closed glass reactor. All the experiments were carried out in gaseous phase using acetaldehyde as the model pollutant.

Kinetic results suggest that chromium loaded silica systems are good UV and visible light active photocatalysts. This is a good example for a localized photocatalytic activity. In contrast, our xerogel system shows comparatively high visible light photocatalytic activity for the titania based system, showing the importance of non-localized nature of photocatalysis. The Cobalt doped silica system shows interesting dark catalytic activity towards acetaldehyde and several other pollutants. Thus, in summary, based on the different activities we observed during our studies these materials could be successfully used to improve the quality of both indoor and outdoor air.

Table of Contents

List of Figures

List of Tables

Acknowledgements

First and foremost, I would like to express my utmost gratitude to my graduate advisor, Professor Kenneth J. Klabunde, at Kansas State University. It is with immense gratitude that I acknowledge the support, encouragement and the freedom during my graduate studies. I consider it an honor to work with such an experienced scientist.

I owe my deepest gratitude to my Graduate Committee Members: Professor Kenneth J. Klabunde, Professor. Stefan Bossmann, Professor. Daniel A. Higgins, Professor. Steven Eckels, and the outside chairperson, Professor Donghai Wang, for their valuable time and suggestions.

A special thanks to Dr. Dan Boyle and the Division of Biology for the assistance and use of the Transmission Electron Microscope, Myles Ikenberry and Dr. Keith Hohn for the XPS measurements, Dr. Daniel Higgins for the Fluorescence Spectrophotometry.

I am grateful to my peer colleagues and post-doctoral fellows for many random conversations during my research studies. Special thanks to Dr. Dambar B Hamal, Dr. Alexander F. Bedilo (Sasha), Dr. Kennedy K. Kalebaila, Dr. Sreeram Singarappu, Dr. Yen-Ting Kuo, Dr. Khadgaman Shrestha, Dr. Deepa Jose, and Yi-Jun Sun.

My sincere thanks to Dr. Thilani Samarakoon and Dhanushka Samarakoon for the continuous friendship and for everything they have done for me over the last five years. A special thank for Chenchen, Dinusha, Dhanushi, and Gayani, for being there for me when ever needed. I feel lucky to have such wonderful friends in my life.

I am grateful to all the Sri Lankan friends in Manhattan, for making me feel K-State a home away from home.

My deepest gratitude goes to my parents for the deep love, care and tremendous sacrifices that they made to ensure that I had an excellent education. For this and much more, I am forever in their debt. Special thank for my brother, Nilina U. Peiris, for the love and friendship throughout my life.

Last but not the least, grateful thank for my husband, Dulan Weerasinghe, and daughter, Nethyu Ama Weerasinghe. They have been my motivation as I hurdle all the obstacles in the completion of this work. I am truly blessed to have them in my life

Dedication

To my parents

Mother, Sandhya Amaradeva and Father, Premachandra Peiris

To my Husband

Dulan J Weerasinghe

To my Daughter

Nethyu Ama Weerasinghe

For their endless love and care in my life

&

To my Country

Sri Lanka

Chapter 1 - Introduction

1.1. Environmental Pollution

Over the last several decades there has been great concern about environmental pollution due to the fact that it is one of the primary causes for various health problems as well as for possible changes in the global climate. Generally, environmental pollution can be defined as contamination of water, land and air due to manmade waste and can be divided in to three major groups; water pollution, soil pollution and air pollution. The world has faced a large number of global and local problems due to the bad condition of the environment created in the last several decades. Some of the problems that have gained the attention of many people are ozone layer depletion, global warming and climate changes. Water pollution and soil pollution usually occurs by similar pollutants due to the close contact of these two environments. Some of the common pollutants in soil and water are heavy metal containing chemicals from industrial effluents, herbicides and pesticides from the agricultural industry. From these three major groups of environmental pollution, air pollution has received the attention of many researchers due to the seriousness of the impact on global climate change, acid rain, smog, and human and animal health.[1]

Air pollution can be sub grouped in to two main categories; as indoor and outdoor. Both categories are equally important as they can create very unhealthy conditions to humans as well as to animals and plants.[1] Outdoor air pollution has gained the attention of many people due to the global effects that it cause. For example depletion of stratospheric ozone and global warming are widely discussed global effects that brought many secondary problems to the earth. On the other hand, indoor air pollution has its own risks to human health though it has received very little attention compared to outdoor air pollution. Usually indoor air pollution occurs due to bad ventilation and water systems. The main indoor air pollutants are radon, household chemicals, biological contaminants, carbon monoxide, pesticides, asbestos and lead, all of which are released by various indoor activities or house hold products.[1,2] Compounds which cause imbalance in the atmosphere are known as air pollutants and can be divided in to two main groups as primary air pollutants and secondary air pollutants. Primary air pollutant is a pollutant emitted directly from a source, and a secondary air pollutant is not directly emitted into the environment, but forms when other pollutants react in the atmosphere. For example tropospheric

ozone is a secondary pollutant produced when hydrocarbons and nitrogen oxides react in the presence of sunlight. Further, according to EPA, the most common air pollutants are Ozone, Particulate matter, Carbon monoxide, Nitrogen Oxides, Sulfur dioxides and lead.
Because of the bad effects of all the forms of environmental pollution, it is important to investigate ways to reduce or eliminate it. The best way to address these issues is to find solutions to already emitted pollutants from the environment and to avoid further release of contaminants to outdoor environment. Finding novel eco-friendly techniques as well as green technology is important to open up new ways to minimize the environmental pollution.

1.2. Solar Energy

Petroleum is the primary energy source of the world to date. Ever growing technologies and industries urge for higher energy demand that is impossible to support with a non-renewable source like petroleum. On the other hand, petroleum products usually undergo incomplete combustion resulting harmful air pollutants such as carbon monoxide, carbon dioxide, and various hydrocarbons. Therefore, clean renewable energy is needed, such as solar energy, wind, geothermal, etc. Out of all these renewable energy sources, solar energy has the most potential. The most important factor about solar energy is that it does not emit any harmful atmospheric pollutants. On the other hand solar energy is important as it is a renewable energy source that can support the increasing demand of energy. Solar energy can be used to heat, or to produce electricity. It can also be converted into chemical energy or can be used to catalyze important reactions. In fact, it has been calculated that the amount of solar energy arriving at the earth's surface in a minute is sufficient to meet the energy demand of the world for a year.
But, the lack of efficient solar energy harvesting and storing methods is one of the main drawbacks that we face today. The maximum electric efficiency attained so far from a solar cell is 43% with multi-junction concentrators. Moreover, high production cost and the higher surface areas required for current solar cells limit their applications in commercial scale. Thus it is very important to discover new cost effective and efficient solar harvesting systems and proper storage systems that help support the increasing energy demand of the world. To meet these energy demands there are thousands of researchers around the globe experimenting on efficient methods to harvest and store solar energy.[3]

1.3. Photocatalysis

Photocatalysis is one of the very successful and active areas of research that have provided important ways to harvest readily available solar energy. Usually, any chemical reaction requires a certain amount of activation energy to initiate the reaction. In normal chemical reactions the activation energy will usually be supplied by simple methods such as heating, mechanical stirring, etc. But, in photochemical reactions, light energy is used. Upon exposure to certain wavelengths of light, photocatalytic material can be used to catalyze specific chemical reactions based on the oxidation and reduction potentials of the photo generated charge carriers. Thus, in photocatalytic reactions, the catalytic material plays an intermediate role between the reactant and the light and promotes desired chemical reactions. There are various steps occurring in a photocatalytic reaction process. The first step is photon absorption to generate electrons and holes with sufficient potentials for the catalytic process. Secondly, charge separation and migration to surface reaction sites. Then suppression of recombination and finally, construction of surface reaction sites for the chemical reaction to be catalyzed.[4] According to the literature, various photocatalytic materials have been employed to drive water splitting to produce hydrogen and oxygen gases, mineralizing harmful organic pollutants, as well as to remove organic dye molecules from industrial effluents. Even though there are many that have been reported, the number of materials that have become successful on industrial scale is very limited.[5]

1.4. Factors Affecting Photocatalytic Activity

There are various factors that determine the efficiency of a photocatalyst. Those can be listed as, particle size, crystal structure, crystallinity and the nature of the boundaries of catalysts, efficiency of charge separation, energy range of the solar spectrum suitable for the excitation of the material, Optimum intensity of the light photons, environment of active sites, etc.

1.4.1. Effects of particle nature on photocatalytic activity

The crystal structure, crystallinity and particle size are important factors that determine the efficiency of a photocatalytic material. These factors are strongly related to charge separation, migration to surface and the charge recombination processes of the photocatalytic process. According to Kudo, A. and co-workers, photo generated electrons and holes tend to recombine in defect sites resulting lower efficiency photocatalytic materials. But, if a photocatalytic material

has higher crystallinity the amount of defects sites are low and the photocatalytic activity becomes efficient. On the other hand, if the size of the particles is smaller they tend to result in higher active photocatalytic materials due to higher surface area available and less number of defects sites. Moreover, when particles become smaller, the charge carrier migration to the surface of the catalyst is fast and less chance for recombination.[4]

1.4.2. Positions of the conduction and valance bands of the semiconductor material

Various semiconducting materials have unique energy positions for their conduction and valance energy bands and energy gaps. Position of these energy levels usually determines the oxidation and reduction ability of generated charge carriers while the energy gap determines the wave length of the photon required to activate the photocatalytic material. It is important to know the redox potential of the chemical reaction which planned to catalyze prior selecting the suitable semiconducting material for the photocatalysis.[4]

1.4.3. Effect of surface area and the nature of the surface on photocatalysis

The nature of the surface of the photocatalytic material is an important factor which determines the efficiency and the selectivity of a photocatalytic process. Since photo generated charge carriers migrate to the surface of the photocatalytic materials in order to react with reactants on the surface, the nature of the surface plays a crucial role when determining the efficiency of the photocatalyst. Moreover, the nature of the surface of the photocatalyst will determine the nature of the reactant compound being absorbed on to the surface. Surface acidity is an important factor that determines the specificity, efficiency and the mechanism of action of a photocatalytic material. For example, acidity of titanium dioxide based materials is strongly related to the amount of surface hydroxyl groups present on the surface and these groups play a major role in trapping photo generated holes and thereby decrease the recombination of electron hole pairs, which in turn increase the quantum efficiency of the photocatalyst.[4,6]

Usually, during the preparation of photocatalytic materials the energy levels of the conduction and valance bands of the materials will be modified or the chemical environment of the active site will be changed by doping with suitable doping agents. These changes to photocatalytic systems usually enhance the light absorption, electron hole pair generation and the overall activity.[6] Surface Area of a material is also playing a major role when deciding the

photocatalytic activity of a material. Usually, most of the photocatalytic processes takes place in the surface of the material. Thus, higher surface area materials will hold larger number of reactive catalytic sites allowing more reactant absorption and thereby enhanced reactivity.[6]

1.5. Titanium Dioxide (Titania/TiO_2) Based Photocatalysts

Most of the successful photocatalytic materials that have been reported consist of a supporting base material. Usually compounds such as zeolite, titania and silica are popular as successful base materials due to their high stability under high temperature and pressure conditions, low toxicity, low cost and the ability to obtain various physico chemical properties simply by changing particle dimensions. Usually, it is believed that the supporting material facilitates the catalytic activity of the catalytic site by enhancing charged carrier separation, providing reduced electron hole recombination and facilitating charge transfer to an adsorbed species.[7]

Titanium dioxide photocatalysis is the most studied and well understood photocatalytic system. Thus, studying the mechanistic details of how titanium dioxide behaves is important. Titanium dioxide, also known as Titania, is a white colored compound that is widely used as a photocatalyst, catalytic support, sensor material, and hydrogen adsorber. It is a semiconductor with a band gap of 3.2 eV, and has been shown to promote mineralization of organic pollutants, water splitting, and carbon dioxide reduction upon exposure to light. Titanium dioxide occurs in nature in three well-known mineral forms known as anatase, rutile and brookite. Among these mineral forms, anatase typically exhibits higher photocatalytic activity than other two forms but in some cases it has been reported that even higher photocatalytic activity is possible with precise mixtures of both anatase and rutile. One such example is commercially available Degussa P25 TiO_2, which consist of 80% anatase phase and 20% rutile phase.[6,7] Because of the relatively wide band gap of titania (3.2 eV), it absorbs light corresponding to wavelengths shorter than 388 nm, which is only 3-4% of the solar energy that reaches the earth.[8] Thus, in principle, photocatalytic activity should be enhanced by adjusting the band gap toward visible light energies by doping, since visible light is readily available in the solar spectrum. Doping has been carried out in earlier research using various methods and materials. Common doping materials used have been noble metals, transition metal oxides, organic dye molecules as well as anionic compounds.[8]

Since Titania is a semiconducting pigment, its valence electrons can be promoted into the conduction band, resulting in the formation of an electron-hole pair upon irradiation with suitable light. But, the created electron hole pair needs to be spatially separated in order to allow the formed electron hole pair to undergo chemical reactions. In titania, charge carrier recombination is usually avoided by immobilizing the created excited electron or hole or both in the trap states available in between the conduction and valance bands.[9] Formed excited electrons usually have a higher effective mass compared to the holes, and moderate reduction potential. So, electrons tend to remain in their free state or in some cases get trapped at the surface. On the other hand, holes usually have high oxidation potential and get trapped at the semiconductor surface. Usually a light excited hole can follow two paths. The holes either oxidize the hydroxyl groups available on the surface of titania to produce hydroxyl radicals or oxidize lattice oxygen atoms from -2 to 0 valence state to create oxygen vacancies in titania. Therefore, in supported photocatalytic materials titania plays two major roles by itself providing a support to the system as well as providing active catalytic sites. Thus, the entire material is involved in photocatalysis, making the photocatalysis process non-localized.[10]

1.6. Insulating Materials Based Systems for Photocatalysis

For many years titania has been recognized as the most useful photocatalyst and various types of applications have been developed based on it. But, recent research has focused more on photocatalytic systems other than titania. Some experiments of this kind have focused on various types of semiconductors, while some dealt with the use of different insulating materials.[11] Compared to the reported titania based photocatalytic systems the number of insulator based materials are less. Silica and Zeolite based materials have been extensively studied in this regard and have successfully used as good photocatalytic materials. Unlike semiconducting titania based materials, insulators consist of a very large band gap that is too large to generate excited electron hole pairs simply using light photons. In most of the reported literature, photoactive sites of insulator based photocatalysis occur due to the presence of highly dispersed metal oxide species of quantum size. According to the findings of Yoshida and coworkers it is possible to obtain photocatalytic abilities because of the presence of surface quantum defects on silica surfaces of silica based photocatalytic systems.[11] More studies have to be carried out in order to understand the photocatalytic mechanism associated with silica based materials.

1.7. Transition Metal Ion Doping to Obtain Visible Light Photocatalysis

It is important to investigate new materials based on titania and silica in order to enhance activities in the visible light range. Therefore, new doping agents as well as new methods of preparation must be studied in order to prepare commercially usable visible light photocatalysts by introducing intermediate energy levels to the conduction and valance bands. Transition metals and metal oxides have been actively used in the past to introduce light absorption in the visible range and have been moderately successful as photocatalysts. Transition metals are very good candidates to absorb in the visible range of the spectrum, as orbital energy transfer usually lies in the visible range. Thus, more careful research in the area of transition metal ions doped titania and silica could result in promising visible light photocatalytic materials to decompose harmful environment pollutants.

1.8. Binary Oxide Systems for Efficient Photocatalysis

Another important approach to enhance the efficiency of a photocatalytic material is use of binary metal oxide systems. Interestingly, there are many reports that discuss enhanced activity of titania when it is associated with another metal oxide such as silica, zirconia, *etc*.[4] Therefore, in most of the cases the binary material was used as a solid acid or as a supporting material to titania. Examples for such metal oxide combinations reported are Al_2O_3/TiO_2, ZrO_2/TiO_2, CdS/TiO_2, $CdSe/TiO_2$, ZnO/TiO_2, SnO_2/TiO_2, PbS/TiO_2, WO_3/TiO_2 and SiO_2/TiO_2. The mixed oxide system of silicon dioxide with titanium dioxide has been widely studied compared to other reported systems because of the promising properties of silica. Silica materials are nontoxic and able to provide high surface area to the photocatalyst, acting as a carrier of titania and helps produce suitable pore structures to favor photocatalytic activity.[10] Moreover, it is believed that the increased photocatalytic efficiency arises due to the improved adsorption of reactants and the concentration of the reactants near the active centers of mixed silica/titania catalysts.

Moreover, according to the article by Ping Cheng and coworkers the photocatalytic efficiency of titania based materials can be enhanced by introducing secondary materials such as silica.[11] Research in this area of binary oxides doped with transition metals is rare. Thus, it is very important to study the effect of various levels of binary oxide materials towards visible light photocatalytic activity. Experiments carried out in this area will lead us to understand the

changes in the active sites of the titania catalysts due to the introduction of secondary oxide species and may complement the findings of Xianzhi Fu and coworkers towards binary oxide photocatalytic systems.[6]

On the other hand, most of the catalytic systems reported in the past are primarily based on some kind of a semiconducting base material. It is believed that semiconducting materials are required to obtain good photocatalytic activities due to the ability of semiconductors to create reactive electron hole pairs upon irradiation of UV or Visible light. But, whether the photocatalysis can be obtained without using semiconducting base materials is an important question that still remains unanswered. Thus, it is very important to synthesize new insulators based materials such as silica doped with suitable transition metal ions in order to study the feasibility of visible light photocatalytic activities. Moreover, this will benefit the area of photo-catalysis because visible light active transition metal doped insulator compounds will open up a new area of photocatalysis where photocatalytic reaction is localized to certain active sites of the system.

1.9. References

1. Environmental Pollution and Impacts on Public Health, United Nations Environment Programme (UNEP)
2. An Office Building Occupant's Guide to Indoor Air Quality, Office of Air and Radiation, EPA, **1997**
3. Climate Change The Role of Cities, United Nations Environment Programme (UNEP), **2009**
4. Kudo, A.; Miseki, Y., Heterogeneous photocatalyst materials for water splitting, *Chem. Soc. Rev.*, **2009**, 38, 253-278
5. Kudo, A., Photocatalysis and solar hydrogen production, *Pure Appl. Chem.*, **2007**, 79, 11, 1917–1927.
6. Fu, X.; Clark, L.; Yang, Q.; Anderson, A. Enhanced Photocatalytic Performance of Titania-Based Binary Metal Oxides: TiO2/SiO_2 and TiO_2/ZrO_2, *Environ. Sci. Technol*. **1996**, 30, 647-653
7. Liang, Y. T.; Vijayan, B.K.; Gray, K.A.; Hersam, M.C.; Minimizing Graphene Defects Enhances Titania Nanocomposite-Based Photocatalytic Reduction of CO2 for Improved Solar Fuel Production, *Nano Lett.* **2011**, 11, 2865–2870
8. Lim, S.H.; Phonthammachai, N.; Pramana, S.S.; White, T.J.; Simple Route to Monodispersed Silica-Titania Core-Shell Photocatalysts, *Langmuir*, **2008**, 24, 6226-6231
9. Yu, M.; Y ao, H.; Jia, H.; Chihc, C.; Chien, C.; Andikal, W., Photocatalytic Activity for Degradation of Nitrogen Oxides over Visible Light Responsive Titania-Based Photocatalysts, *Environ. Sci. Technol*. **2006**, 40, 1616-1621
10. Szczepankiewicz, S.H.; Moss, J.A.; and Hoffmann, M.R.; Electron Traps and the Stark Effect on Hydroxylated Titania Photocatalysts, *J. Phys. Chem. B*, **2002**, 106, 7654-7658

11. Cheng, P.; Zheng, M.; Jin, Y.; Huang, Q.; Gu, M.; Preparation and characterization of silica-doped titania photocatalyst through sol–gel method, *Materials Letters*, **2003**, 57, 2989– 2994
12. Yoshida, H.; Active sites of silica-based quantum photocatalysts for non-oxidative reactions, *Catalysis Surveys from Asia*, **2005**, 9, 1

Chapter 2 - Comparison of Photocatalytic Activities of Novel Silica and Titania Based Materials co-doped with both Metals and Non-Metals

2.1. Introduction

The interest of titania based photocatalytic studies gained attention after its first discovery of photocatalytic water splitting by Fujishima, Akira and coworkers.[1,2] They introduced the photocatalytic activity of titanium dioxide under UV light irradiation. Since then, a large number of studies have been carried out in order to improve titania in various ways to harvest solar energy efficiently. Preparation of various sizes, various shapes, as well as various preparation methods have been employed to enhance properties that affect the photocatalytic ability.[3,4,5] Titania, because of its very large band gap, absorbs the UV region of solar spectrum, which is about 8% of the whole solar spectrum. Thus, many attempts have been made to modify titania, so that it absorb in the visible region of the solar spectrum to achieve efficient photocatalysis. Doping of titania with various types of materials have been carried out in order to prepare new titania based materials to harvest visible wave lengths. Various types of transition metals as well as non-metals, such as carbon, nitrogen, and sulfur have been successfully used in this regard. Use of titania as a combination of mixed oxides is another approach to enhance the visible light activity. Silica doped titania and various zeolites mixed with titania systems are good examples for such systems. [6-9]

Here in, we discuss the preparation and activity comparison of both metal and non-metal co doped titania, silica and mixed titania silica systems for degradation of organic pollutants under UV and visible light irradiation.

2.2. Experimental Methods

2.2.1. Preparation of Ag, (C, S) doped titania and silica photocatalysts

Silver, Carbon and Sulfur co-doped titania and silica photocatalysts were prepared using $Ti[OCH(CH_3)_2]_4$ and TEOS as the starting materials for the titania and silica based systems respectively in ethanol medium. First, an amount of 0.124 mol NH_4SCN was dissolved in 200 mL of C_2H_5OH. A 0.031 mol of either $Ti[OCH(CH_3)_2]_4$ or TEOS or a mixture of both,

depending on the desired material to be synthesized, was added under vigorous stirring. Then, the desired amount of $AgNO_3$ (Ag=0, 1, 3, and 5 mol%) was dissolved in 0.125 mol of deionized water and 1 ml of NH_4OH solution. This mixture was added drop wise into the starting base material-ammonium thiocyanate solution and stirred for 5 min at room temperature; the solvent was then evaporated in a rotavap. The samples were dried overnight and calcined at 500 ^oC for two hours in air.

2.2.2. Characterization studies

As prepared samples were characterized using various techniques. Brunauer-Emmet-Teller (BET) effective surface area and pore size distribution of the samples were tested using a Quantachrome NOVA 1200 gas absorption/desorption analyzer after degassing the samples at 150 ^oC for two hours. Scintag-XDS-2000 spectrometer with Cu Kα radiation with applied voltage of 40 kV and current of 40 mA was used to obtain powder XRD analysis of the samples to determine the crystalline nature. Samples were scanned 2θ from 0^o to 75^o with a scan rate of 1^o per minute. Diffuse reflectance UV-Visible spectra were measured at room temperature in air on a Cary 500 scan UV-Vis-NIR photometer over the range from 200 to 800 nm. Polytetrafluoroethylene (PTFE) powder of 1 μm particle size was taken as a reference material for diffuse reflectance studies.

2.2.3. Kinetic studies of photocatalysis

The as prepared Ag/(C-S) TiO_2, Ag/(C-S) SiO_2, and Ag/(C-S) TiO_2-SiO_2 mixed systems were tested for photocatalytic degradation of acetaldehyde under UV light and visible light separately. The rate of decomposition of acetaldehyde and production of carbon dioxide (CO_2) was followed using a glass reactor with a quartz window and Shimadzu GCMS-QP 5000 instrument. Acetaldehyde degradation was studied as a model pollutant and the temperature of the glass reactor was maintained at 25 ^oC by circulating water in the outer jacket of the reactor system during all the kinetic experiments. For all the kinetic studies, 0.10 g of the prepared sample was uniformly placed on the special glass chamber allowing UV or visible light to directly contact the prepared photocatalytic material. Then the air filled system was sealed and 0.10 ml of liquid acetaldehyde was introduced to the bottom of the reactor to avoid any direct contact of liquid acetaldehyde and the photocatalytic material. During the experiment acetaldehyde slowly gets evaporated due to its near room temperature boiling point, and gaseous acetaldehyde gets

absorbed on to the reaction sites of the catalyst. Photocatalysts were then illuminated with UV or visible light using a 1000 w xenon lamp. Glass filters was used to obtain visible region wavelengths (>420 nm) and UV region (320 nm – 400 nm) by cutting off unnecessary light. The progress of any reaction was detected by injecting 35 µl of gas samples from the sealed reactor to the Shimadzu GCMS-QP 5000 instrument every 20 minutes. All the kinetics experiments were carried out at least two times in order to confirm the accuracy of the results and were compared with commercially available titania P25 and prepared blank samples, where no dopant elements were present.

2.3. Results and Discussion

2.3.1. Structure of the photocatalytic system

BET surface area values obtained for as prepared samples are given in the Table 1 below. According to the obtained results, titania doped samples show the highest surface area values while silica samples show very low values giving somewhat different from what is reported in most of the literature. Even though silicon dioxide (SiO_2/Silica) based samples in most of the cases was used to take advantage of their higher surface area, there are few reports that talk about lower surface area silica as well. In reality, the surface area of silica based materials depends on the method of preparation and the materials used for the preparation. Further, it appears according to the results reported in the table 2.1, doped silver causes sintering of SiO_2 and mixed systems.[10]

Table 2.1: BET surface area values of as prepared photocatalysts

Ratio of TiO_2: SiO_2	Surface Area Data (m^2g^{-1})			
	1% Ag	3% Ag	5% Ag	0% Ag
1:0	60	50	55	44
1:1	10	9	11	15
0:1	2.5	3.5	21	25

In the current studies photocatalyst were prepared using a simple precipitation method by co-hydrolyzing the basic lattice material (Silica, Titania or the mixture of both) with the corresponding doping elements using base catalyzed hydrolysis. The precipitation technique results in xerogels and helps prepare materials more cost-effectively and less time consuming methods to obtain higher yielding photocatalysts. Hydrolysis of both titania and silica precursors can be generally explained using well-known sol-gel process. In solution, respective alkoxides get hydrolyzed and condensed to generate new polymeric materials composed of M O M (M represent Ti or Si) bonds according to the following reaction schemes.[11]

$$M\ OR\ H_2O \underset{\text{Esterification}}{\overset{\text{Hydrolysis}}{\rightleftharpoons}} M\ OH\ ROH \qquad (1)$$

$$M\ OR\ HO\ M \underset{\text{Alcoholysis}}{\overset{\text{Alcohol Condensation}}{\rightleftharpoons}} M\text{-O-}M + ROH \qquad (2)$$

$$M\ OH\ HO\ M \underset{\text{Hydrolysis}}{\overset{\text{Water Condensation}}{\rightleftharpoons}} M\ O\ M\ H_2O \qquad (3)$$

So, after complete hydrolyzation of the sol-gel prepared material solvent drying using a rotavap results in collapse of the formed network structure leaving lower surface area materials. Compared to the well-known aerogel synthesis process there is no need of higher temperature and pressure conditions during this synthesis method which makes the process very cost efficient.[12]

Calcination of the catalyst at 500 ^{o}C for two hours is important due to several reasons. Generation of photocatalytically active crystalline phases mainly takes place and removal of left over solvents from the photocatalytic structure, generation of right crystalline state and the removal of unwanted organic compounds occur during this step.

The powder XRD patterns obtained for the prepared photocatalysts are given in Figures 2.1-2.3 with corresponding powder XRD patterns obtained after catalytic studies under UV and visible light respectively. Figure 2.1 shows the powder XRD pattern of the 5%Ag (C,S) doped titania based system prepared in our lab. The XRD pattern clearly resembles the peak pattern of Anatase crystalline titania present in the system. Additionally, three unique peaks, that are not usually present in XRD peaks of anatase titania, can be clearly identified in the region of 2θ value, 28 to 34, which is according to reported literature belongs to crystalline silver sulfate species. Thus, it

is clear from powder XRD characterization studies, doped sulfur exist in the form of sulfate in these systems.[13,14]

Figure 2.1: Powder XRD patterns obtained for the (a) 5% Ag/(C,S) TiO_2 photocatalyst, (b) the catalyst after 140 minutes in acetaldehyde environment under UV light, (c) The catalyst after 140 minutes in acetaldehyde environment under visible light.

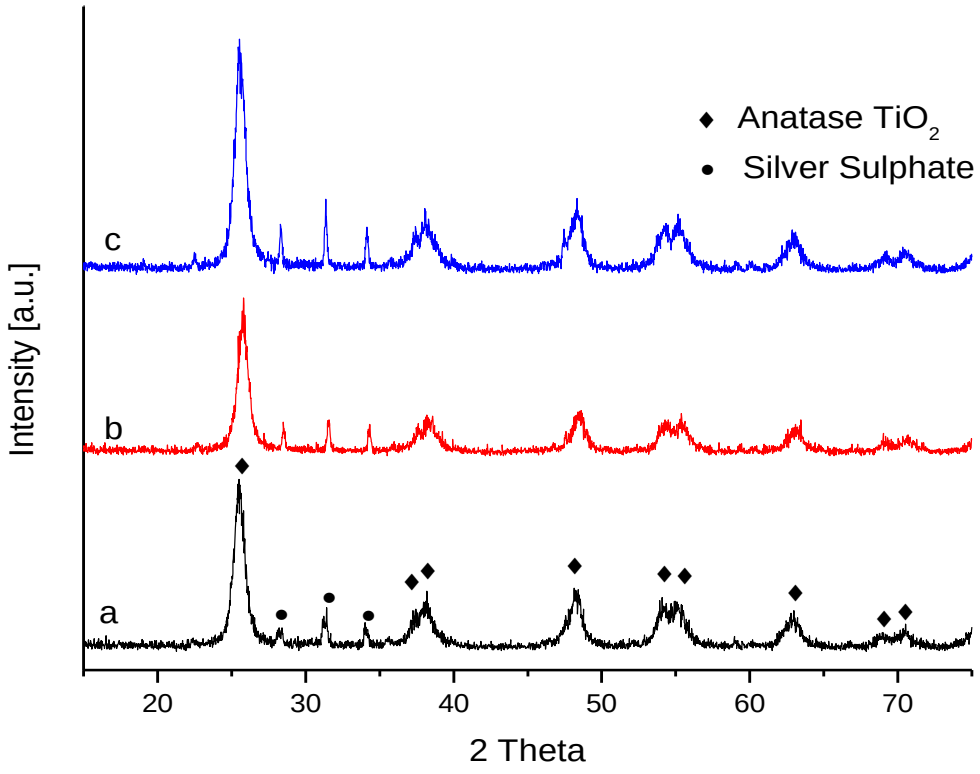

Figure 2.2: Powder XRD patterns obtained for the (a) 5% Ag/(C,S) doped SiO_2 photocatalyst, (b) the catalyst after 140 minutes in acetaldehyde environment under UV light, (c) The catalyst after 140 minutes in acetaldehyde environment under visible light.

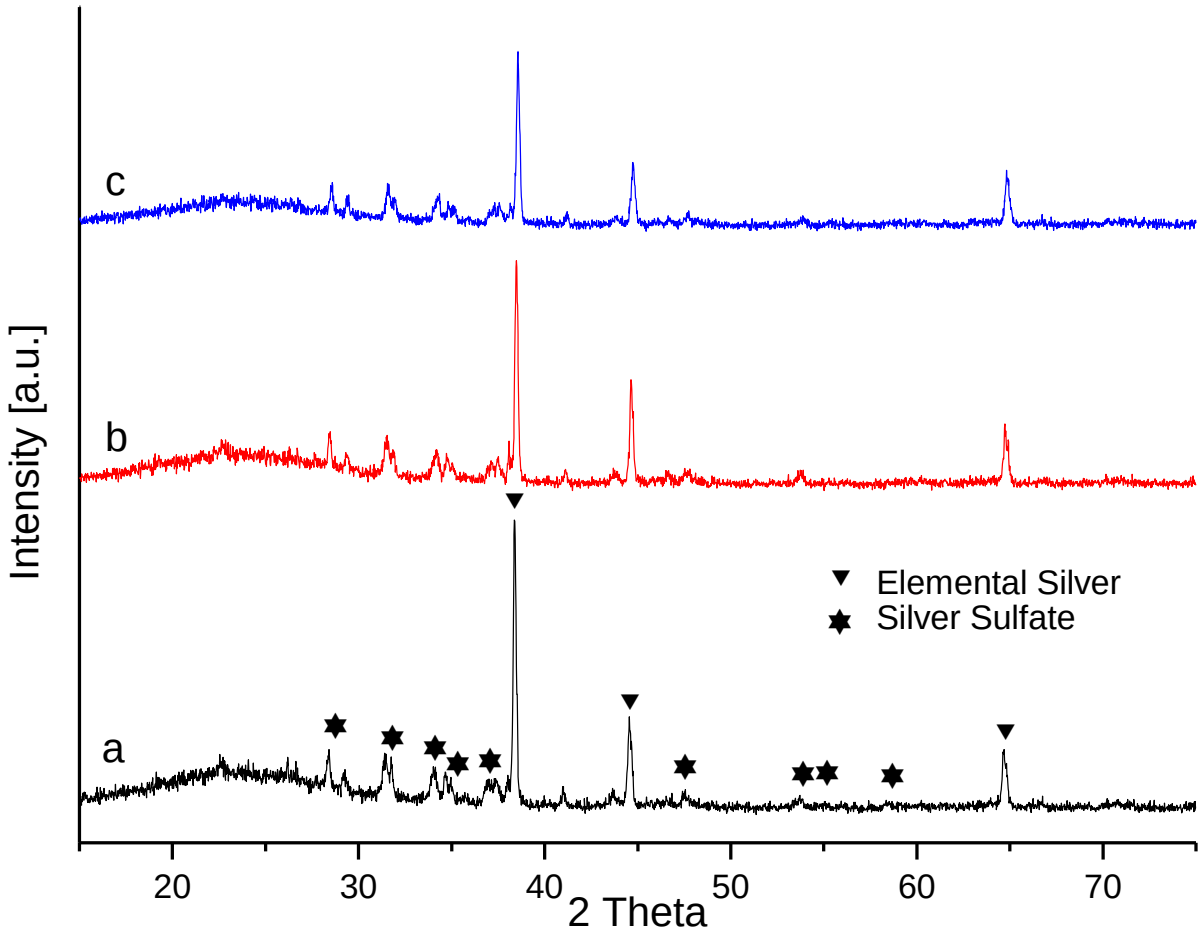

The powder XRD pattern obtained for the silica based photocatalytic systems (Figure 2.2) show a broad peak correspond to amorphous silica and characteristic peaks for elemental silver and peak patterns for crystalline silver sulfate species indicating that silver exists in two major forms in the system[13,14]. One interesting observation that can be seen by comparing silica based photocatalytic systems to titania system is that the relative high intensity observed for the crystalline peaks of elemental silver for silica based system. Even though it is very difficult to distinguish elemental silver peaks in the 1% Silver doped sample, few XRD peaks with small intensities could be identified in the 5% Ag (C,S) TiO_2 system. Since both systems were prepared using the same synthesis procedure keeping the base material as the only difference, the presence of differing amounts of silver must occur due to an involvement of the matrix material.

The XRD pattern of the mixed TiO_2 and SiO_2 system also show peak patterns for elemental silver, and silver sulfate species present in the system. Further, it shows peak patterns for both anatase titania and amorphous silica present in the system.

Figures 2.1-2.3 include powder XRD patterns obtained for all three types of samples after UV and Visible light photocatalytic studies. In all the XRD patterns no significant difference could be observed before and after the catalytic processes which is a clear indication of the stability of the catalyst during its photocatalytic activities.

Figure 2.3: Powder XRD patterns obtained for the (a) 5% Ag/(C,S) doped TiO_2-SiO_2 photocatalyst, (b) the catalyst after 140 minutes in acetaldehyde environment under UV light, (c) The catalyst after 140 minutes in acetaldehyde environment under visible light.

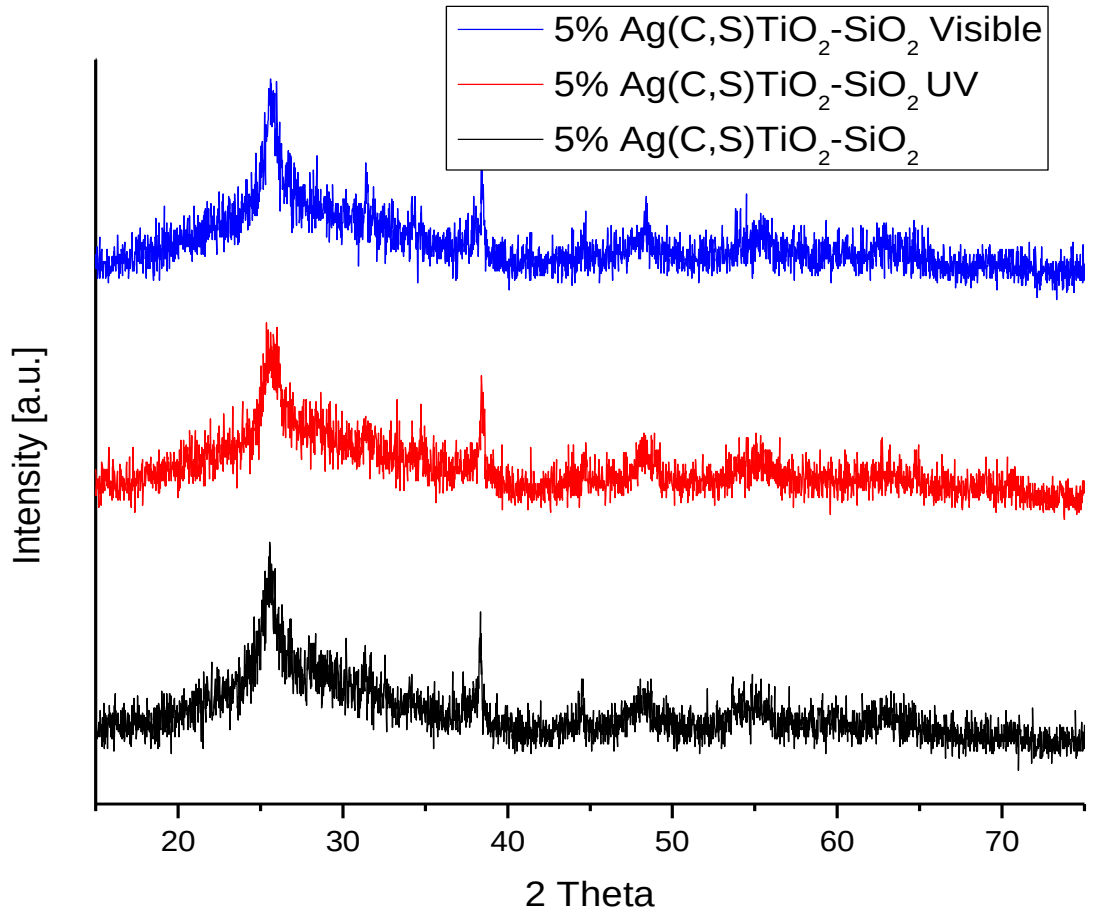

Diffuse reflectance UV-visible characterization studies were also carried out for the as prepared photocatalysts to study the effect of various ratios of silica and titania on light absorption.

According to the obtained spectra all the samples show red shifts of the absorption compared to that of commercially available P25 which is expected as a result of doped silver and non-metals. But, the light absorption in the visible region of the spectrum varies in the order of TiO_2 << mixed SiO_2-TiO_2 ≈ SiO_2.

Figure 2.4: Diffuse reflectance UV-vis studies of as prepared photocatalysts

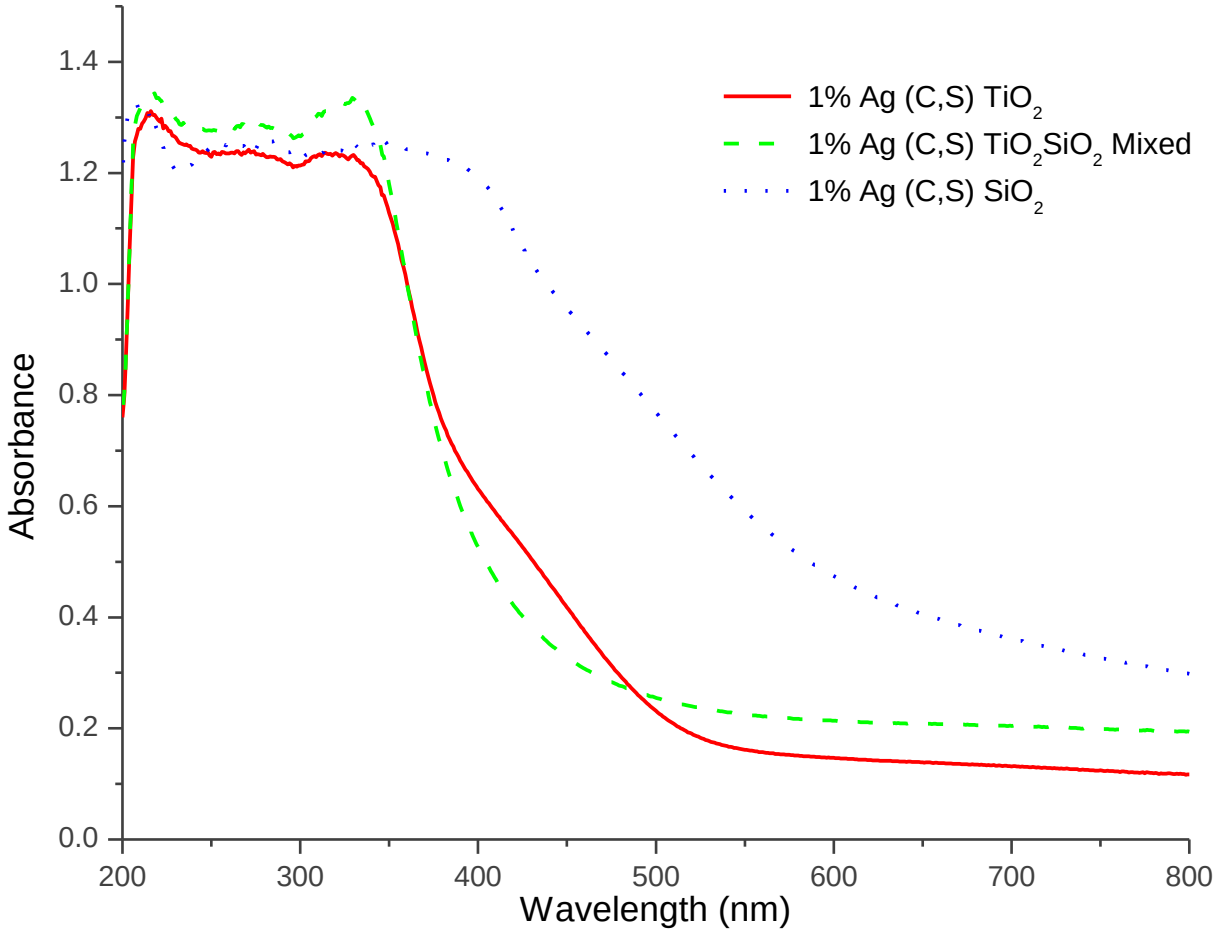

2.3.2. Kinetics of photocatalytic degradation

Photocatalytic ability of as prepared samples was tested using acetaldehyde as a model pollutant. Acetaldehyde is a common air pollutant that is usually emitted into the air due to the smoke produced from combustion in automobiles and tobacco smoke. Acetaldehyde is a main pollutant mostly in industrial and ambient environments due to the release of acetaldehyde as a byproduct of thermal degradation of various polymers. Therefore, study of effective ways to eliminate acetaldehyde is important. Further, acetaldehyde degradation is mostly an oxidation process; there is a high chance for the catalyst which is active towards acetaldehyde to be active towards

oxidation of other complex pollutants as well. In the presence of oxygen complete oxidation of acetaldehyde takes place according to the reaction scheme 4 below and resulting in carbon dioxide and water as products.

(4)

Even though a complete oxidation is expected, several side reactions can also take place due to the polymerization and other reactions of acetaldehyde. Acetic acid is one of the main byproducts that usually results in oxidation studies of acetaldehyde.

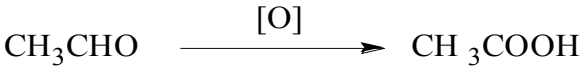

(5)

Moreover, there are some reports of polymerization of acetaldehyde to generate higher molecular weight compounds such as Paraldehyde, 2,4,6-trimethyl-1,3,5-trioxane and Metaldehyde, the tetramer of the acetaldehyde. But, these polymers tend to form in aged acetaldehyde samples and usually do not affect the quality of kinetic results as GCMS is an excellent technique to separate and distinguish compounds with different molecular weights.[15-17]

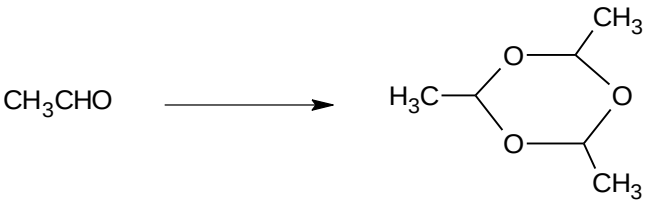

(6)

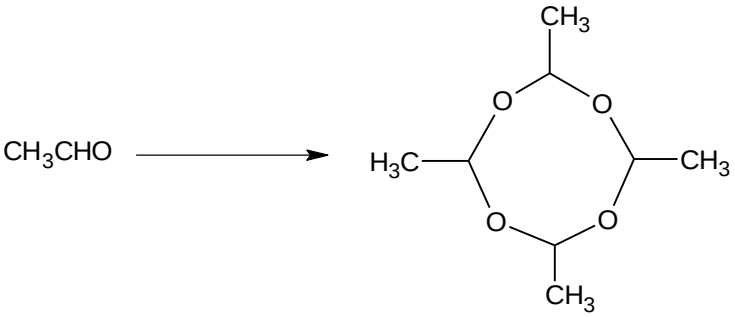

(7)

Figure 2.5 shows photocatalytic reaction progress of as prepared 1%Ag(C,S) doped systems under UV and visible light irradiations. All three samples show good acetaldehyde degradation ability while the mixed sample shows the highest photocatalytic oxidation of acetaldehyde compared to the systems which have titania and silica as the main lattice structure. According to recent studies carried out by Qifeng Chen and co-workers[18], introduction of silica into titania matrices results in formation of unbalanced positive charges due to the replacement of some of

the Ti^{4+} ions. These unbalanced positive charges in the system adsorb more hydroxyl groups onto their surface increasing the number of reactive sites present on the surface.[18] The number of reactive sites are important as they usually play a major role in adsorption and the conversion of the pollutant into CO_2. This could be a major reason for the enhanced photocatalytic activity observed for our mixed system under UV light. The catalytic rates observed for the titania based and silica based systems showed reasonable results as semiconducting titania is showing higher photocatalytic efficiency compared to that of insulating silica based system. Titania, with its 3.2 eV band gap successfully absorbs radiation in the UV region of the solar spectrum making it is an ideal candidate under UV light compared to silica. Thus, the reactivity differences observed can be easily understood. The photocatalytic activities obtained under visible light (Figure 2.5b) does not follow the same order as under UV light. Above all, the photocatalytic activity of all the samples is high compared to that of visible light due to the higher energy of UV light. But, the order of reactivity is also different from UV light studies. The titania doped system showed significantly high photocatalytic activity compared to the other two systems. The results obtained with the 5% Ag loading samples show similar order as 1% Ag doped samples as indicated in the figure 2.6a and 2.6b.

Figure 2.5: Photocatalytic acetaldehyde degradation studies of as prepared 1%Ag(C,S) doped TiO_2, 1%Ag(C,S) doped SiO_2 and 1%Ag(C,S) doped mixed systems (a) under UV light (b) under visible light irradiation.

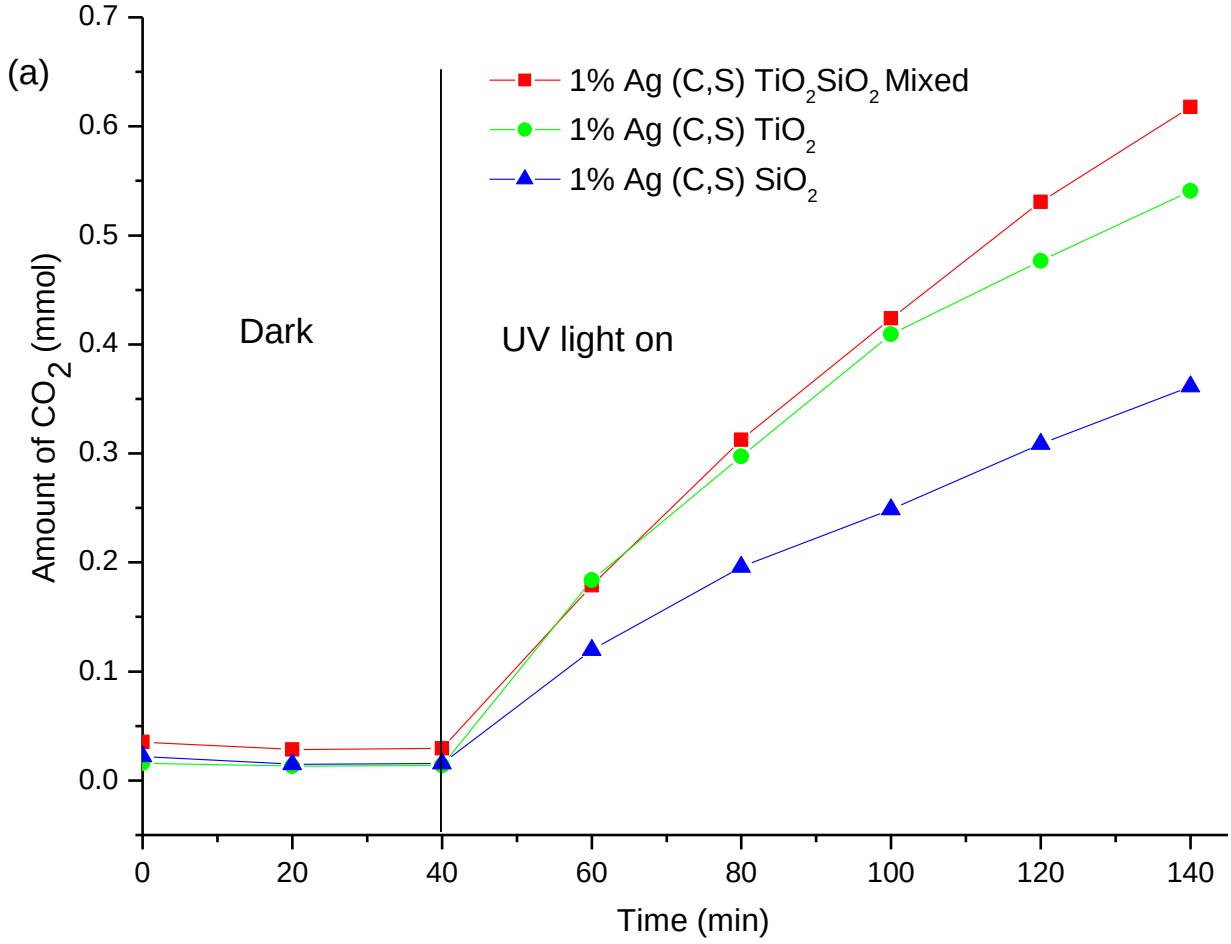

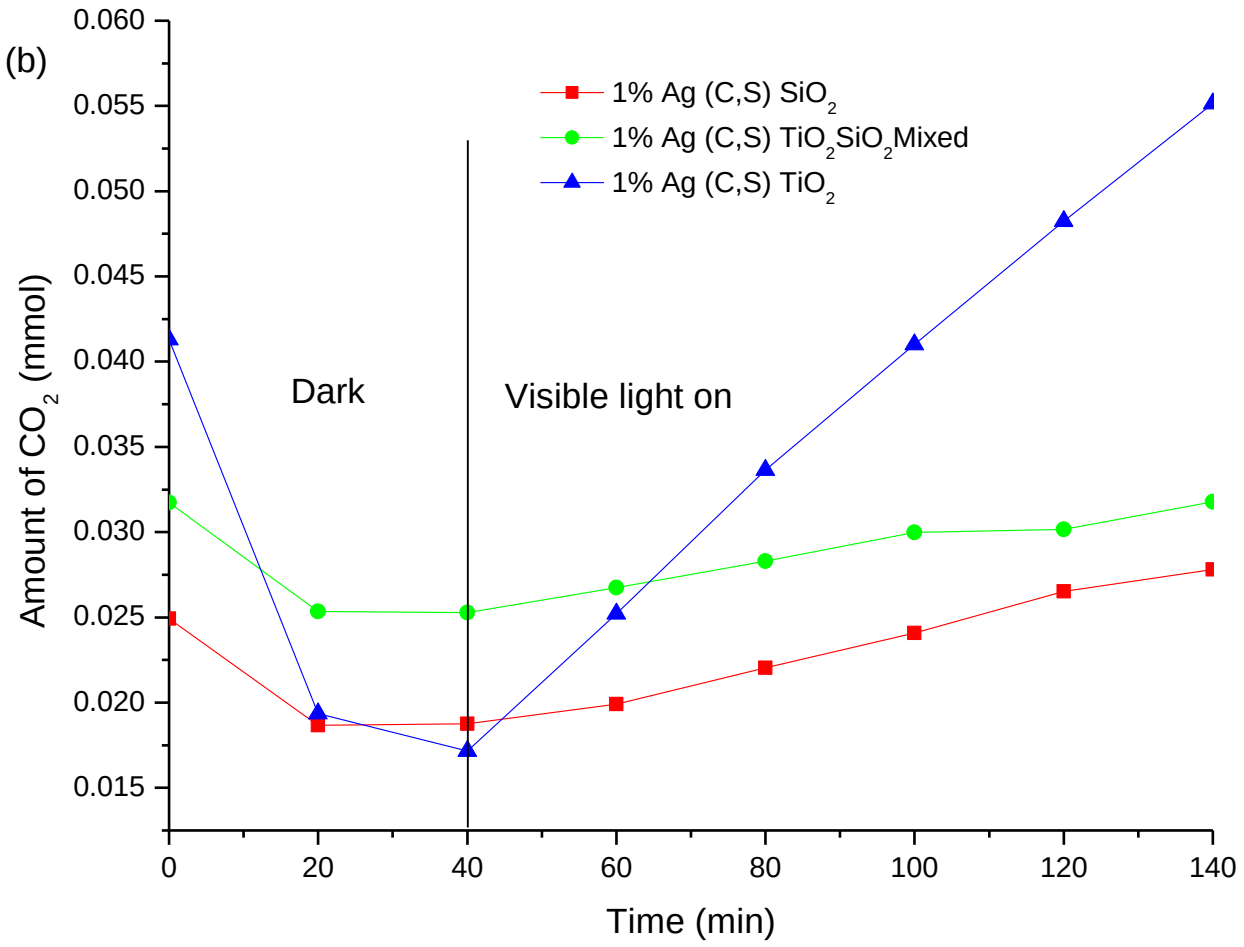
(b)
1% Ag (C,S) SiO2
1% Ag (C,S) TiO2SiO2Mixed
1% Ag (C,S) TiO2
Dark
Visible light on
Amount of CO2 (mmol)
Time (min)
0.060
0.055
0.050
0.045
0.040
0.035
0.030
0.025
0.020
0.015
0
20
40
60
80
100
120
140

Figure 2.6: Photocatalytic acetaldehyde degradation studies of as prepared 5%Ag(C,S) doped TiO_2, 5%Ag(C,S) doped SiO_2 and 5%Ag(C,S) doped mixed systems (a) under UV light (b) under visible light irradiation.

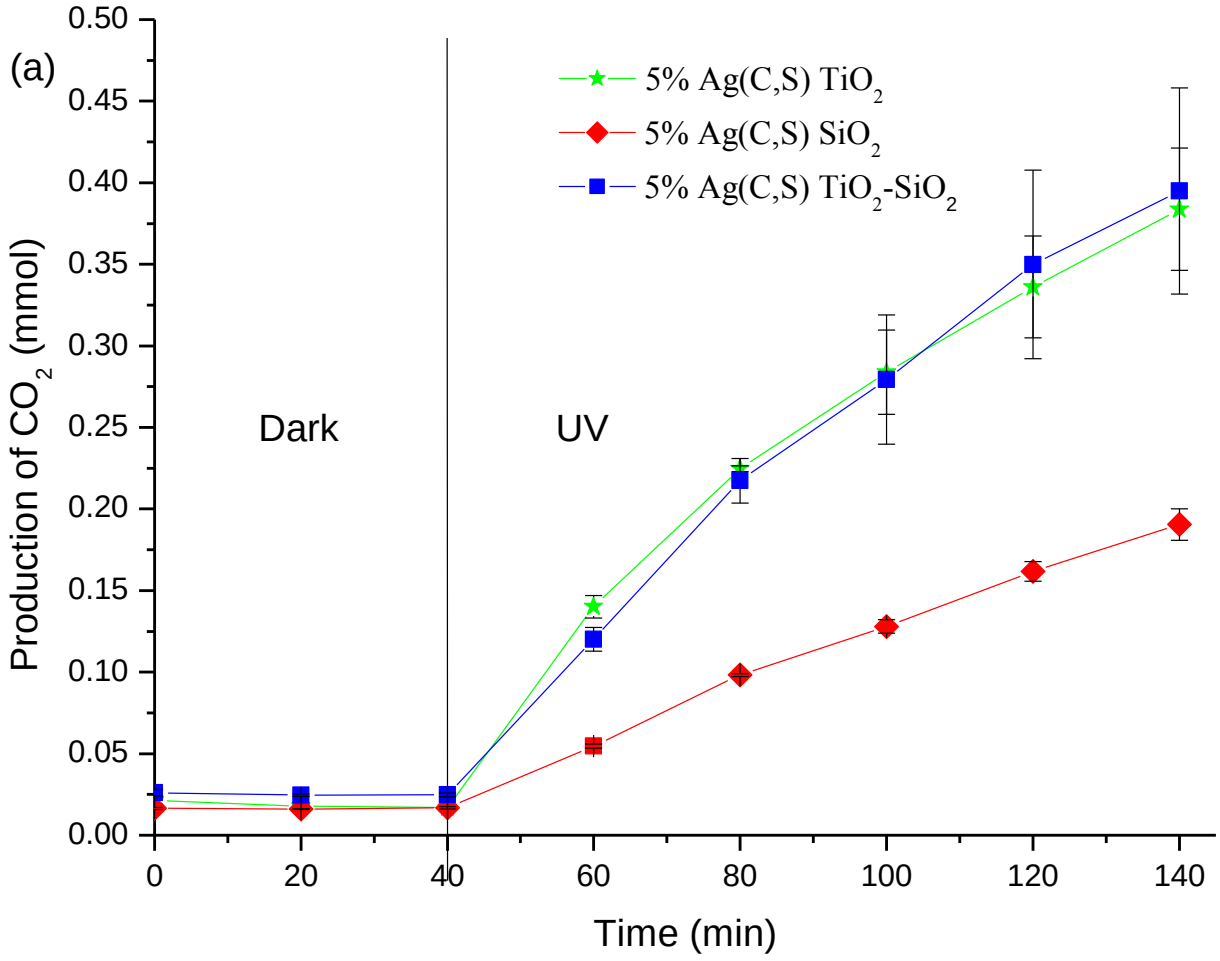

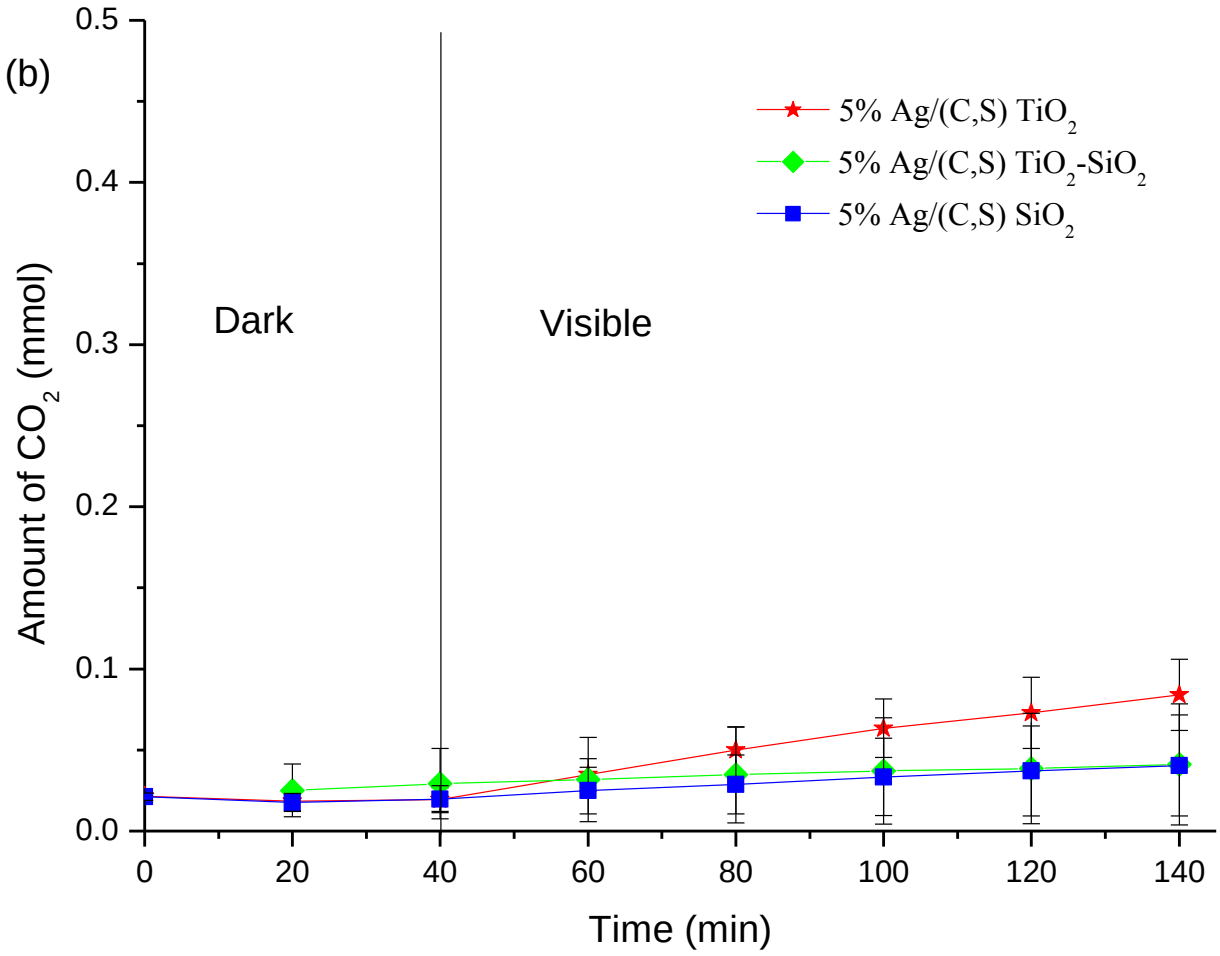

Photocatalytic activity of titania based systems with different amounts of silver loadings were plotted together in order to study the effect of silver loading towards oxidation of acetaldehyde. The results are shown in figure 2.7 comparing catalytic performances separately under UV and visible light irradiations. According to the results shown in the figure it is clear that the photocatalytic performance is highest for the 1%Ag doped sample for both under UV and visible irradiations. According to the previous studies carried out in our laboratory the presence of silver is essential to obtain the photocatalytic activity. Thus, in line with earlier studies 1% silver is the optimum amount of silver that is needed to be present in the system to achieve good photocatalytic activities[13]

Figure 2.7: Photocatalytic performance of 1%Ag(C,S) TiO_2, 3%Ag(C,S) TiO_2, and 5%Ag(C,S) TiO_2, (a) under UV light (b) under visible light irradiation.

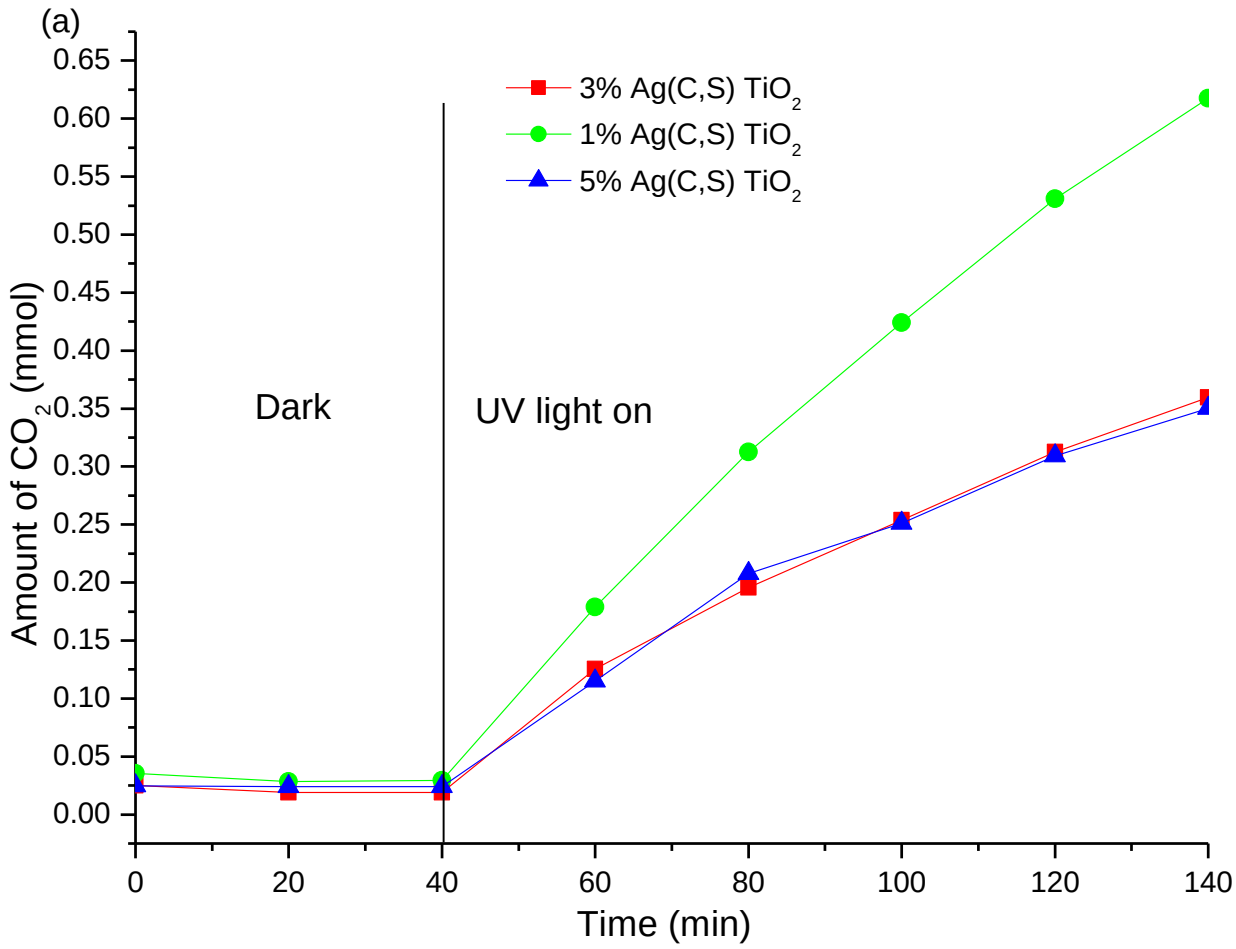

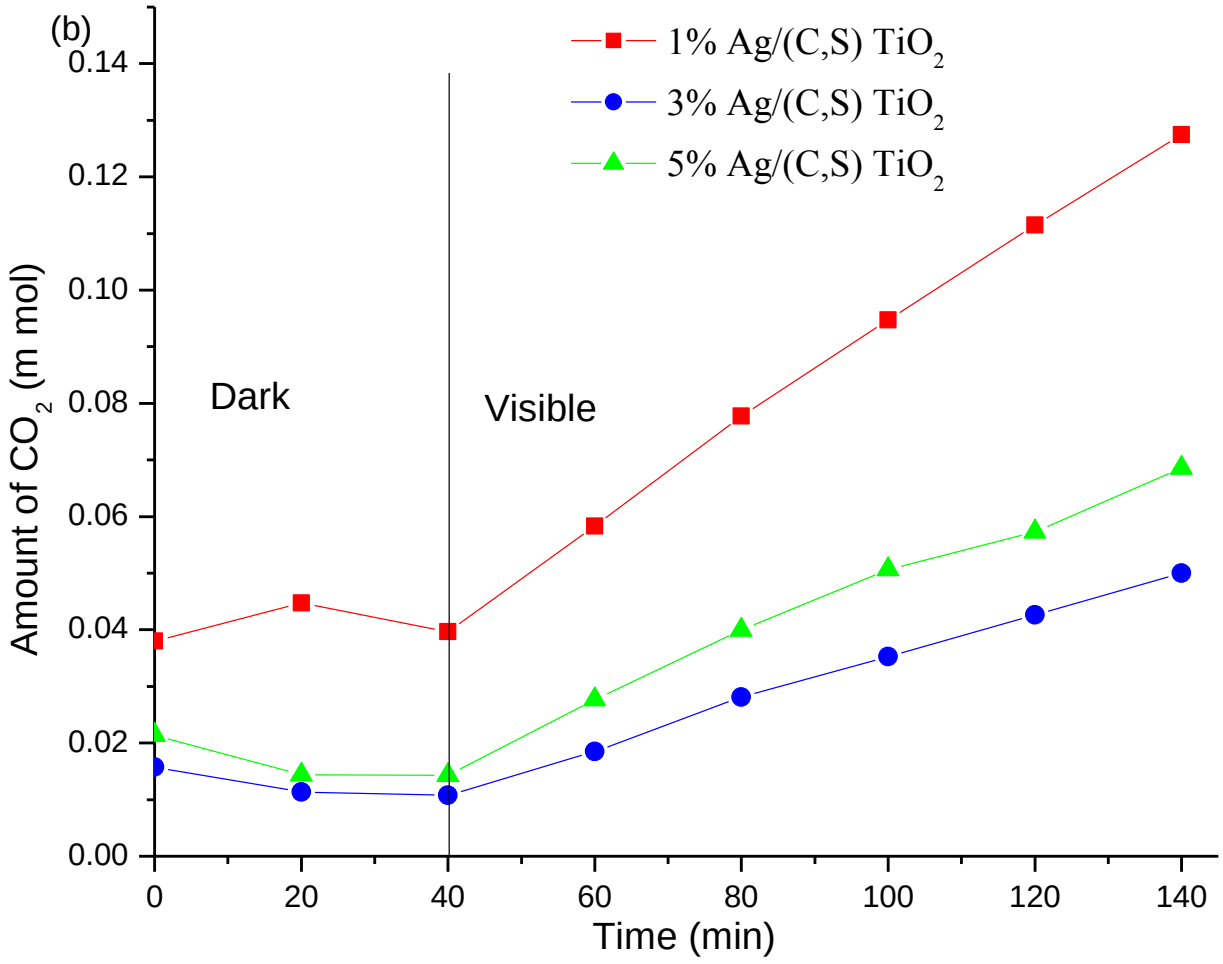

2.4. Mechanism/s of Photocatalytic Activity

Photocatalytic mechanism of titania based systems are well studied and understood. But, when titania is doped with various types of metal and non-metal dopants, the mechanism of photocatalytic activity can also change based on the alignment of the new energy levels introduced by the dopant atoms.[19-21] Usually, non-metal doping, especially carbon and sulfur in our system, into titania introduce energy bands in the band gap of titania closer to the valance band, resulting in decrease in the energy gap creating a doped system visible light active.[22,23] On the other hand, there are literature reports about the ability of sulfur to increase surface acidity of titania there by enhancing pollutant absorption.[24] Generally, upon exposure to visible region of light, excited electron and hole pairs will be created from doped titania photocatalysts according to the reaction scheme 8 below.

$$TiO_2 + hv \longrightarrow e^-_{(CB)} + h^+_{(VB)} \qquad (8)$$

According to our powder XRD results it is clear that the 1% Ag(C,S) TiO_2 photocatalyst consists of both ionic and elemental silver. Elemental silver is known to enhance photocatalytic activity of titania by introducing a new Fermi energy level just below the conduction band of titania facilitating generated electron hole pairs while doped Ag^{1+} ions enhance the photocatalytic activity by trapping excited electrons.[25,26] The observed decrease in photocatalytic activity with higher loading of silver could occur due to its activity as an electron hole recombination center and acting as a barrier to the incoming radiation and the pollutant.[25,27]

2.5. Summary

Novel photocatalytic systems based on silica and titania co-doped with both metals and nonmetals were successfully studied. Characterization studies revealed that these samples consist of both ionic and metallic silver (Ag and Ag^{+1}) and sulfur in the form of sulfate. Interesting photocatalytic activities were observed under both UV and visible light conditions. Mixed silica and titania, and titania based samples showed nearly similar and the high activities under UV light and titania based photocatalysts showed the highest activity under visible light. Silica based systems did not show any interesting acetaldehyde degradations. Even though the surface areas of these materials are low, the employed preparation technique allows low cost and efficient photocatalyst preparation.

2.6. References

1. A. Fujishima, K. Honda, S. Kikuchi, Photosensitized electrolytic oxidation on semiconducting n-type TiO_2 electrode, Kogyo Kagaku Zasshi, **1969**, 72, 108–113
2. A. Fujishima, K. Honda, Electrochemical photolysis of water at a semiconductor electrode, Nature, **1972**, 238, 37–38
3. Wu, J.; Zhang, T., Large-Scale Preparation of Ordered Titania Nanorods with Enhanced Photocatalytic Activity, *Langmuir*, **2005**, 21, 6995-7002
4. Suprabha, T.; Roy, H.G.; Thomas, J.; Kumar, K.P.; Mathew, S., Microwave-Assisted Synthesis of Titania Nanocubes, Nanospheres and Nanorods for Photocatalytic Dye Degradation, *Nanoscale Res Lett*, **2009**, 4, 144–152
5. Ke, A.; Peng, C.W.; Lee, C.Y.; Chiuc, H.T.; Sheud, H.S., {110}-exposed rutile titanium dioxide nanorods in photocatalytic performance, Cryst.Eng.Comm, 2009, 11, 1691–1695
6. Dagan, G.; Sampath, S.; Lev, O., Preparation and Utilization of Organically Modified Silica-Titania Photocatalysts for Decontamination of Aquatic Environments, *Chem. Mater.*, **1995**, 7, 446-453
7. Cheng, P.; Zheng, M.; Jin, Y.; Huang, Q.; Gu, M., Preparation and characterization of silica-doped titania photocatalyst through sol–gel method, Materials Letters, 2003, 57, 2989– 2994

8. Guo, Y.; Yang, S.; Zhou, X.; Lin, C.; Wang, Y.; Zhang, W., Enhanced Photocatalytic Activity for Degradation of Methyl Orange over Silica-Titania, *Journal of Nanomaterials,* **2011**, 9
9. Zhang, G.; Choi, W.; Kim, S.H.; Hong, S.B., Selective photocatalytic degradation of aquatic pollutants by titania encapsulated into FAU-type zeolites, *Journal of Hazardous Materials,* **2011**, 188 198–205
10. Naik, B.; Ghosh, N.N., A Review on Chemical Methodologies for Preparation of Mesoporous Silica and Alumina Based Materials, *Recent Patents on Nanotechnology*, **2009**, 3, 213-224
11. Brinker, C.J., Hydrolysis and condensation of silicates: effects on structure, *Journal of Non-Crystalline Solids*, **1988**, 100, 31-50
12. Rupp, W.; Hu¨sing, N.; Schubert, U., Preparation of silica–titania xerogels and aerogels by sol–gel processing of new single-source precursors, *J. Mater. Chem.,* **2002**, 12, 2594–2596
13. Hamal, D.B.; Haggstrom, J.A.; Marchin, G.L.; Ikenberry, M.A.; Hohn, K.; Klabunde, K.J., A Multifunctional Biocide/Sporocide and Photocatalyst Based on Titanium Dioxide (TiO_2) Codoped with Silver, Carbon, and Sulfur, *Langmuir*, **2010**, 26, (4), 2805–2810
14. Preuksarattanawut, T.; Asavavisithchai, S.; Nisaratanaporn, E., Fabrication of silver hollow microspheres by sodium hydroxide in glycerol solution, *Materials Chemistry and Physics*, **2011**, 130, 481– 486
15. Pauling, L.; Carpenter, D.E., The Crystal Structure of Metaldehyde, *J. Am. Chem. Soc.*, **1936**, 58, (7), 1274–1278
16. Giang, P.A.; Smith, F.F., Colorimetric Determination of Metaldehyde Residues on Plants, *J. Agric. Food Chem.*, **1956**, 4, (7), 623–625
17. Carpenter, D. C.; Brockway, L. O.; The Electron Diffraction Study of Paraldehyde, *J. Am. Chem. Soc.*, **1936**, 58, (7), 1270–1273
18. Chen, Q.; Shi, H.; Shi, W.; Xu, Y.; Wu, D.; Enhanced visible photocatalytic activity of titania–silica photocatalysts: effect of carbon and silver doping, *Catal. Sci. Technol.*, **2012**, 2, 1213–1220
19. Kim, S.; Hwang, S.J.; Choi, W., Visible Light Active Platinum-Ion-Doped TiO_2 Photocatalyst, *J. Phys. Chem. B*, **2005**, 109, 24260-24267
20. Zhou, J.; Zhang, Y.; Zhao, X. S.; Ray, A.K., Photodegradation of Benzoic Acid over Metal-Doped TiO_2, *Ind. Eng. Chem. Res*. **2006**, 45, 3503-3511
21. Zhang, Y.; Zhang, H.; Xu, Y.; Wang, Y., Europium doped nanocrystalline titanium dioxide: preparation, phase transformation and photocatalytic properties, *J. Mater. Chem.*, **2003**, 13, 2261–2265
22. Konstantinova,E.A.; Kokorin, A.I.; Sakthivelc, S.; Kisch, H.; Lips, K., Carbon-Doped Titanium Dioxide: Visible Light Photocatalysis and EPR Investigation, *Chimia*, **2007**, 61, 810–814
23. Umebayashi, T.; Yamaki, T.; Tanaka, S; Asai, K., Visible Light-Induced Degradation of Methylene Blue on S-doped TiO_2, *Chemistry Letters*, **2003**, 32, (4), 330-331
24. Ciambelli, P.; Sannino, D.; Palma, V.; Vaiano, V., The Effect of Sulphate Doping on Nanosized TiO_2 and MoO_x/TiO_2 Catalysts in Cyclohexane Photooxidative Dehydrogenation, *International Journal of Photoenergy*, **2008**, 8

25. Seery, M.K.; George, R.; Floris, P.; Pillai, S.C.; Silver doped titanium dioxide nanomaterials for enhanced visible light photocatalysis, *Journal of Photochemistry and Photobiology A: Chemistry*, **2007**, 189, 258–263
26. Iliev, V.; Tomova, D.; Bilyarska, L.; Eliyas, A.; Petrov, L., Photocatalytic properties of TiO_2 modified with platinum and silver nanoparticles in the degradation of oxalic acid in aqueous solution, *Applied Catalysis B: Environmental*, **2006**, 63, 266–271
27. Xin, B.; Jing, L.; Ren, Z.; Wang, B.; Fu,, H., Effects of Simultaneously Doped and Deposited Ag on the Photocatalytic Activity and Surface States of TiO_2, *J. Phys. Chem. B*, **2005**, 109, 2805-2809

Chapter 3 - Comparison of Catalytic Activities of Nanostructured Silica and Titania Based Materials Loaded with Various Transition Metal Ions

3.1. Introduction

Transition metal ions have been widely used in photocatalytic studies because of many favorable properties.[1] Most of the transition metal ions absorb in the visible region of the spectrum making them ideal candidates to use when designing novel photocatalytic materials. Further, various properties such as oxidation/reduction abilities can be changed or tuned simply by changing the transition metal used or changing the oxidation state of them. Transition metals and their respective ionic species show various properties depending on the number of d electrons available on their outermost electronic shell. Thus, there are a large number of reports on use of transition metal ions loaded systems for catalytic, and photocatalytic environmental remediation applications.[2,3] Therefore, it is very interesting to study the effects of the loaded transition metal ions and the host materials on textural, optical, and catalytic properties.

Photocatalysis based on silica materials had not been of much interest to researchers due to the very large band gap and inert property of silica. But, silica based materials gained the attention of many researchers after the discovery of M41S type of molecular sieves due to their high surface area (~1000 m^2/g) and narrow pore size distribution with long range ordering.[4] It is believed that higher surface area available on silica based materials improve guest absorption and provide suitable environments for transition metal ions to bind to create active catalytic sites.[5] further, one of the main disadvantages associated with titania based photocatalytic materials is their lower surface area. Thus, there are many attempts of combining titania with silica in order to obtain higher photo catalytic activities.[5,6]

Here in, we have synthesized novel silicon dioxide (SiO_2) and titanium dioxide (TiO_2) based systems separately loaded with three different transition metal ions, cobalt, chromium and vanadium ions using well-known aerogel synthesis methods. One of the main objectives of this study is to compare structural and photocatalytic differences that could be obtained using different types of transition metal ions and to compare titania and silica based systems that were prepared by the same synthesis process.

3.2. Experimental Methods

3.2.1. Preparation of new photocatalytic systems

Well known aerogel preparation method was employed to prepare silicon dioxide (SiO_2), titanium dioxide (TiO_2) and mixed (1:1) silica-titania samples. All the prepared samples were loaded with chromium, cobalt and vanadium ions. As starting material tetraethylorthosilicate (TEOS) and titanium isopropoxide ($Ti(ipr)_4$) were used respectively to prepare silica and titania lattices. These precursors were co-hydrolyzed in the presence of the transition metal ion to be loaded. Required amounts of Chromium(III) nitrate ($Cr(NO_3)_3.9H_2O$), Cobalt(II) acetylacetonate, and Vanadium(III) acetylacetonate were used as transition metal ion precursors for the preparation of chromium loaded, cobalt loaded, and vanadium loaded systems, respectively. All the chemicals were analytical grade and used without further purification. During the preparation of samples an amount equivalent to 0.5 mol percent of the dopant material was dissolved in 140 ml of methanol and 20.0 ml of TEOS solution and stirred well. Corresponding titania based samples were prepared by dissolving the same amount of transition metal ion precursor in 140 ml of methanol and 26.6 ml of $Ti(ipr)_4$. The 1:1 mixed silica and titania samples were prepared using corresponding silica and titania precursor amounts for the molar ratios expected for the final products. Then, a mixture of 0.5 ml of water and 2.5 ml concentrated nitric acid was added drop wise to hydrolyze the silica and/or titania precursors. The solution mixture was then aged for about 15 minutes and super critical drying was carried out in an autoclave. Then the autoclave was quickly vented soon after the temperature reached 265 ^oC. Finally, the resulting aerogel was calcined in air at 500 ^oC for 2 hours.

3.2.2. Characterization studies

Brunauer-Emmet-Teller (BET) measurements of surface area and pore size distribution of the prepared samples were carried out using Quantachrome NOVA 1200 gas absorption/desorption analyzer after degassing the samples at 150 ^oC for two hours. Powder XRD analysis of the samples was carried out to determine the crystalline nature of samples using a Scintag-XDS-2000 spectrometer with Cu Kα radiation with applied voltage of 40 kV and current of 40 mA. Samples were scanned 2θ from 0^o to 75^o with a scan rate of 0.5^o per minute. Diffuse reflectance UV-Visible spectra were measured at room temperature in air on a Cary 500 scan UV-Vis-NIR photometer over the range from 200 nm to 800 nm. The sample cell was made of two transparent

CaF2 discs, a Teflon O-ring and screw-type combination in which catalysts were packed between two discs and the O-ring. Polytetrafluoroethylene (PTFE) powder of 1 μm particle size was taken as a reference material for diffuse reflectance studies.

3.2.3. Kinetic studies of photocatalytic systems

Prepared aerogel materials were tested for both UV and visible light photocatalytic activities using suitable glass filters. Kinetics of the photocatalytic degradation was studied using a Shimadzu GCMS-QP 5000 instrument and a glass reactor. Acetaldehyde was used as a model pollutant and the temperature of the glass reactor was maintained at 25 ^{o}C by circulating water in the outer jacket of the reactor system during all the kinetic experiments. In a typical experiment 0.10 g of the prepared sample was uniformly placed on the special glass chamber allowing UV or visible light to directly contact the prepared photocatalytic material by passing through the quartz window on top of the reactor. Then the air filled system was sealed and 0.10 ml of liquid acetaldehyde was introduced to the bottom of the reactor to avoid any direct contact of liquid acetaldehyde and the photocatalytic material. During the experiment acetaldehyde slowly gets evaporated due to its near room temperature boiling point, and gaseous acetaldehyde gets absorbed on to the reaction sites of the catalyst. Photocatalysts were then illuminated with UV (320 nm – 400 nm) or visible light($\lambda > 420$ nm) using a 1000 w xenon lamp and glass filters by cutting off unnecessary light. The progress of any reaction was detected by injecting 35 μl of gas samples from the sealed reactor to the Shimadzu GCMS-QP 5000 instrument every 20 minutes. All the kinetics experiments were carried out at least two times in order to confirm the accuracy of the results and were compared with commercially available titania P25 and prepared blank samples, where no dopant elements were present.

3.3. Results and Discussion

3.3.1. Structure and Characterization

Table 3.1: BET surface area values obtained for the 0.5 (mol)% transition metal ion loaded samples

Surface Area (m^2/g)	Chromium	Cobalt	Vanadium
SiO_2	717	487	374
TiO_2	84	93	97.5
SiO_2TiO_2 (1:1)	345	328	347

BET surface area values obtained for the as prepared samples were given in the table 3.1 and clearly indicate the very high effective surface area values we obtained for our samples. Similar to reported literature, silica based samples show very high surface area values compared to that of titania samples. Still, the effective surface area values obtained for the titania based samples are also high compared to the reported titania surface area values in literature. Moreover, BET values reported in the table 3.1 indicate high effective surface area values obtained for the 1:1 silica titania mixed systems.[5,6]

Powder XRD patterns obtained for the as prepared nine systems are given in figures 3.1-3.3. Powder XRD patterns are identical for systems with same matrix materials irrespective of the loaded transition metal ion. Titania based systems and mixed systems show XRD patterns corresponding to anatase titania crystallinity. Silica based systems show a broad peak for all three systems indicating amorphous silica material present in our samples.[7,8] For any sample no crystalline peaks could be detected arising from any crystalline states of the loaded transition metals. This can be due to fine dispersion of transition metals/metal oxides in the main matrix material or due to the formation of metal-Silica or metal- titania composite structures without forming any crystalline species. Detailed powder XRD studies are needed to understand structural details of these materials.

Figure 3.1: Powder XRD patterns of Chromium loaded (a) TiO_2, (b) SiO_2, and (c) Mixed SiO_2:TiO_2 systems

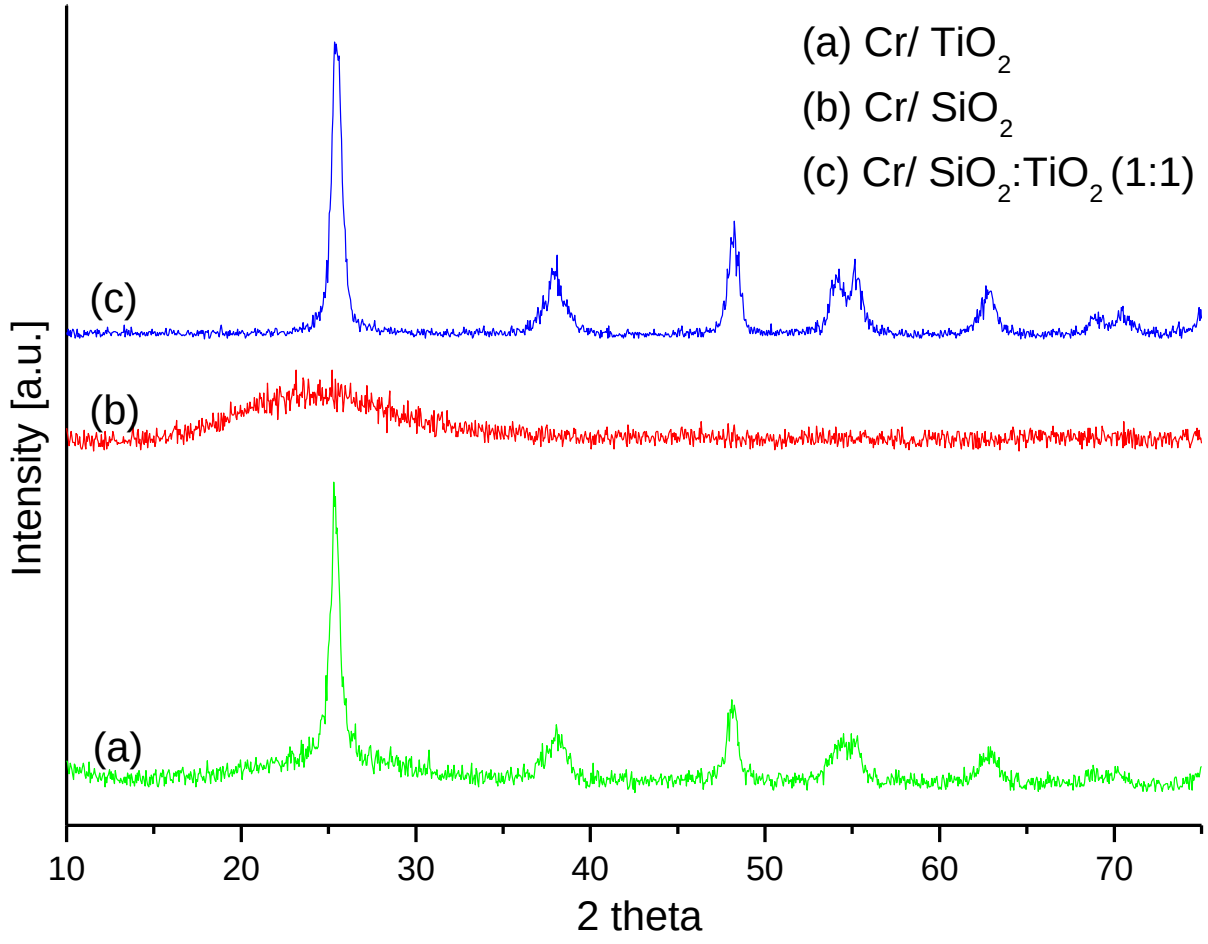

Figure 3.2: Powder XRD patterns of Cobalt loaded (a) TiO_2, (b) SiO_2, and (c) Mixed SiO_2:TiO_2 systems

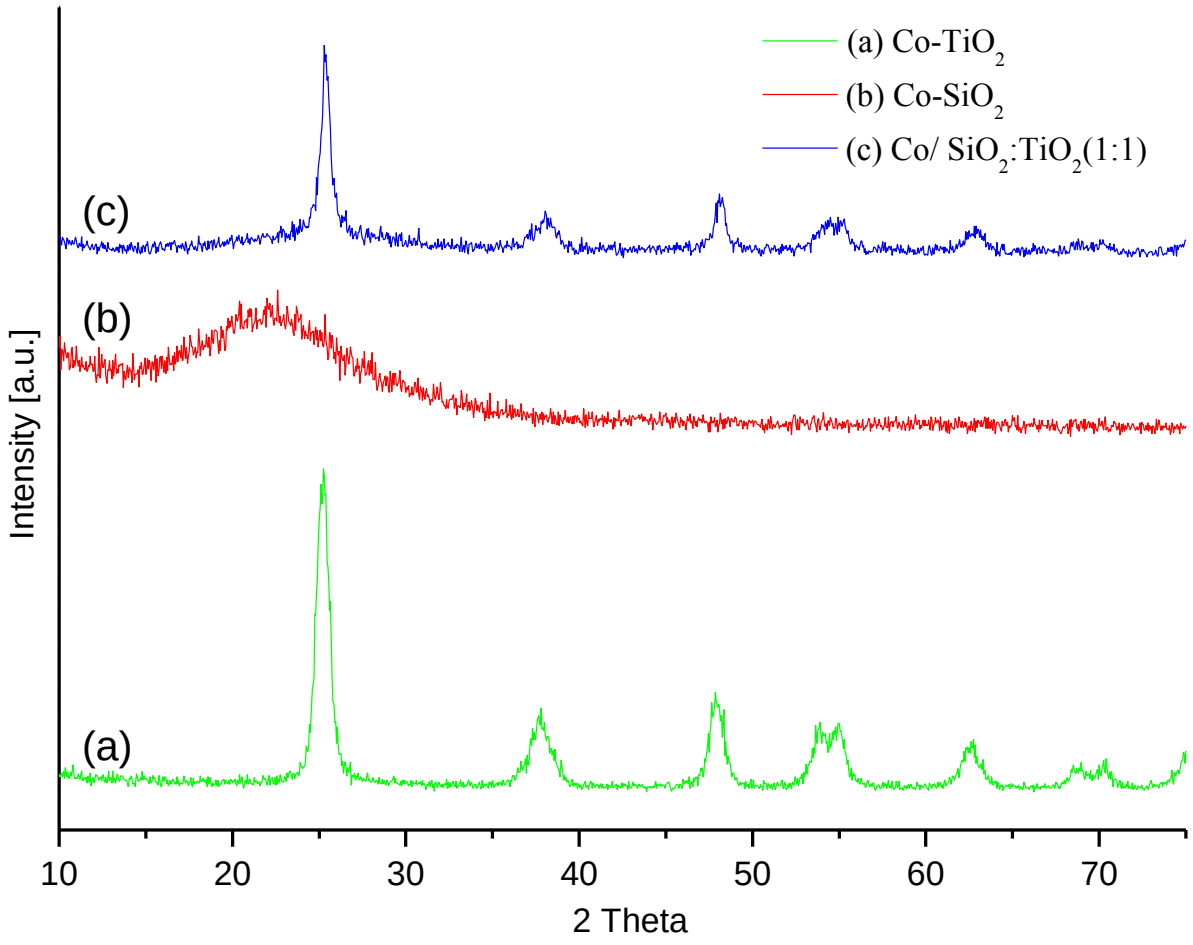

Figure 3.3: Powder XRD patterns of vanadium loaded (a) TiO_2, (b) SiO_2, and (c) Mixed SiO_2:TiO_2 systems

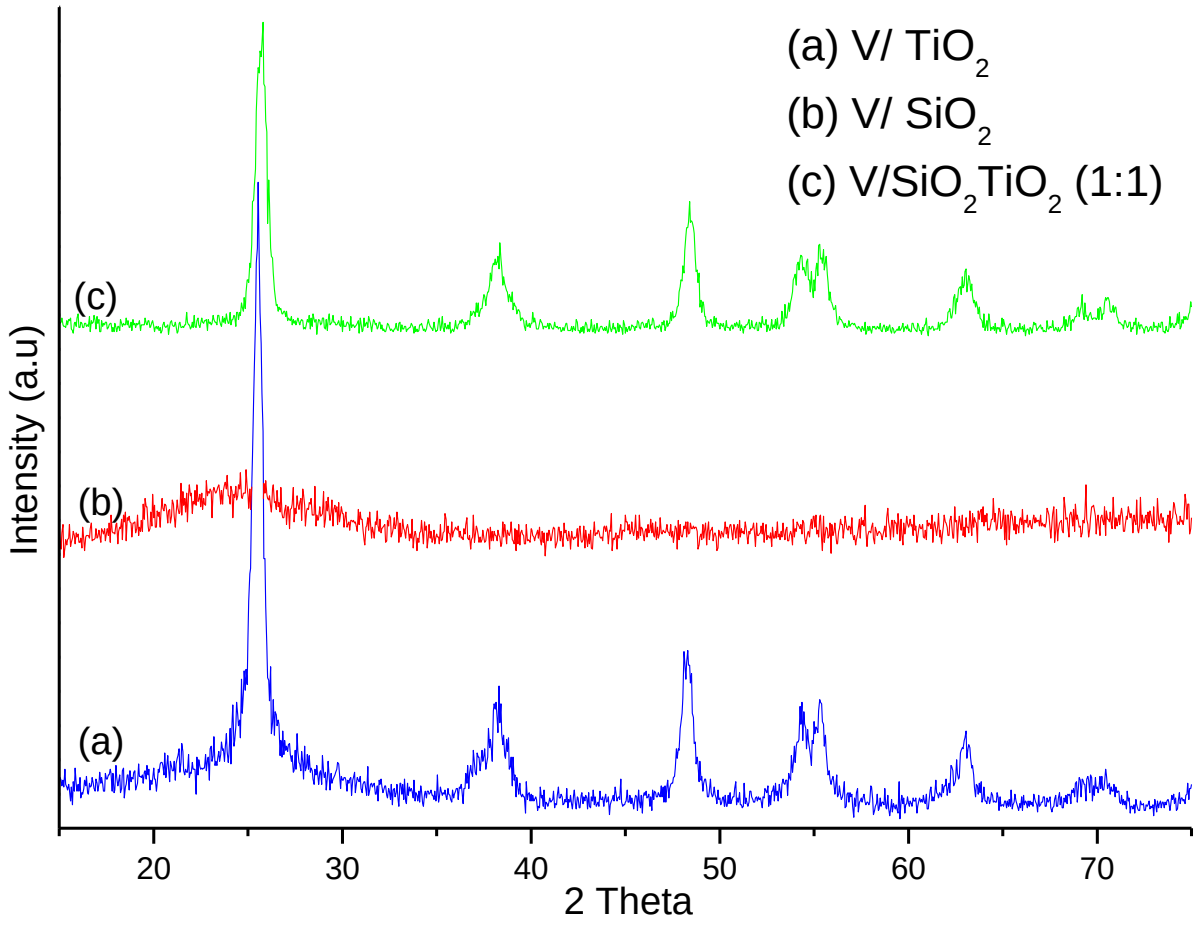

Diffuse reflectance UV-vis spectra obtained are indicted in figures 3.4-3.6 separately for the three transition metal ions loaded systems. Transition metal ion doping of the titania system enhances absorption towards the visible region can be observed by comparing the absorption pattern of pure titania. A red shift in the absorption can be recognized for the silica titania mixed systems. Both Chromium and Cobalt loaded silica based systems show unique absorption patterns in the visible region which arise due to the loaded transition metal ions. Detailed explanation of these two special systems will be given in the next two chapters where in depth studies based on these two systems are explained.

Figure 3.4: Diffuse reflectance UV-vis spectroscopic studies of chromium loaded samples

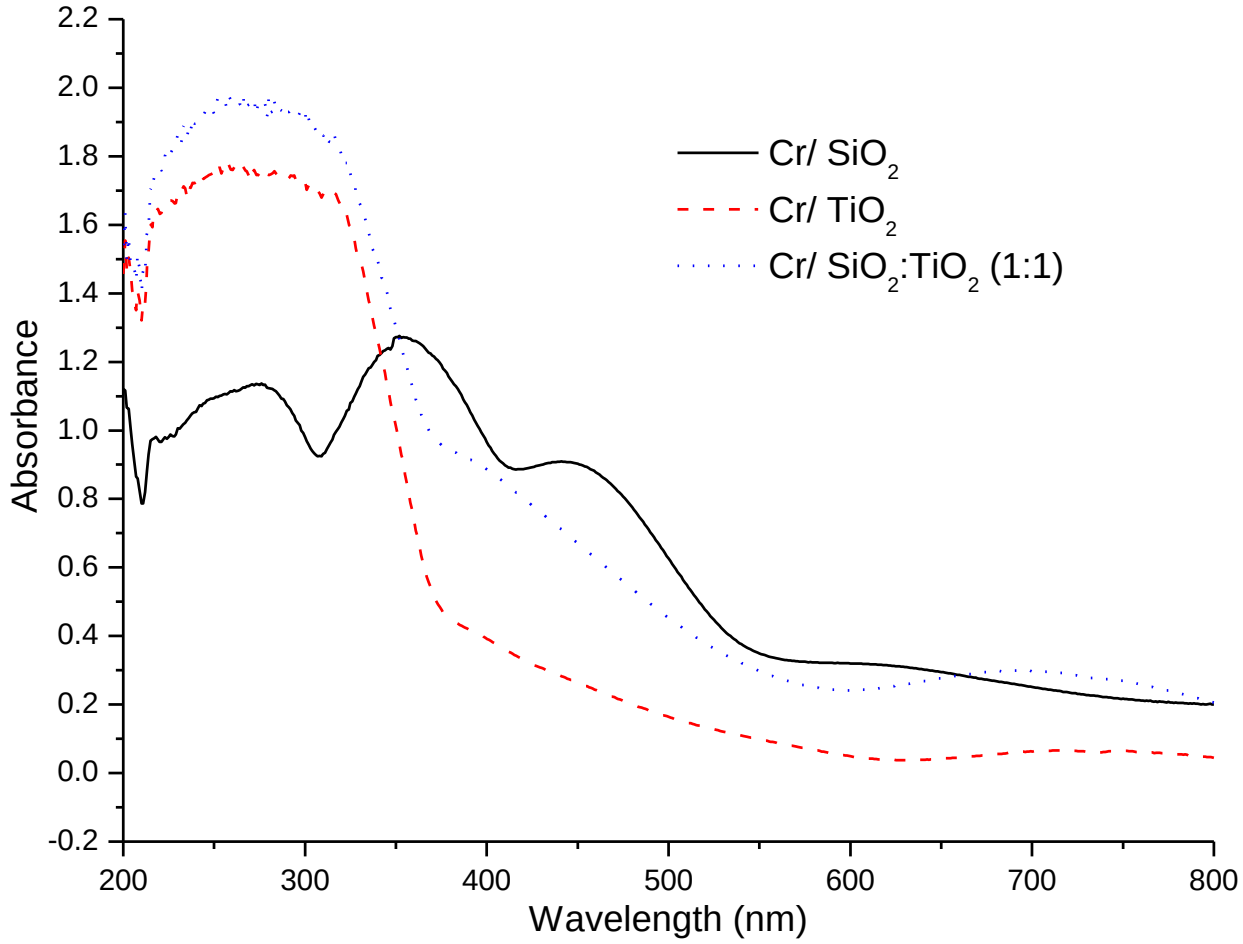

Even though unique absorption patterns can be seen for the other two systems, vanadium loaded silica shows very low absorption in the visible region (Figure 3.6). This observation is further supported by the white color observed for the as prepared vanadium silica sample. Chromium loaded systems have bright yellow coloration and the cobalt loaded silica sample is blue in color which perfectly match with the absorption patterns observed.

Figure 3.5: Diffuse reflectance UV-vis spectroscopic studies of chromium loaded samples

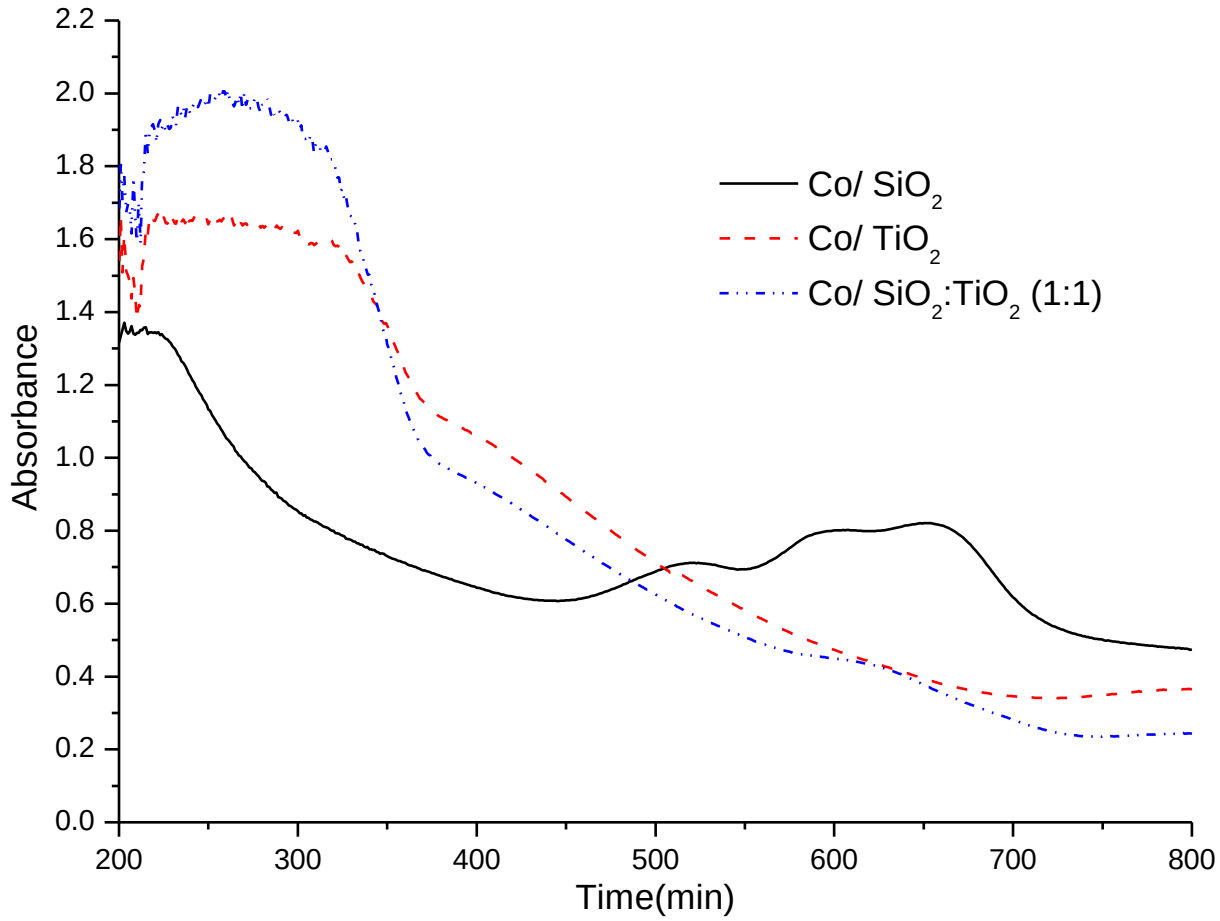

Figure 3.6: Diffuse reflectance UV-vis spectroscopic studies of vanadium loaded samples

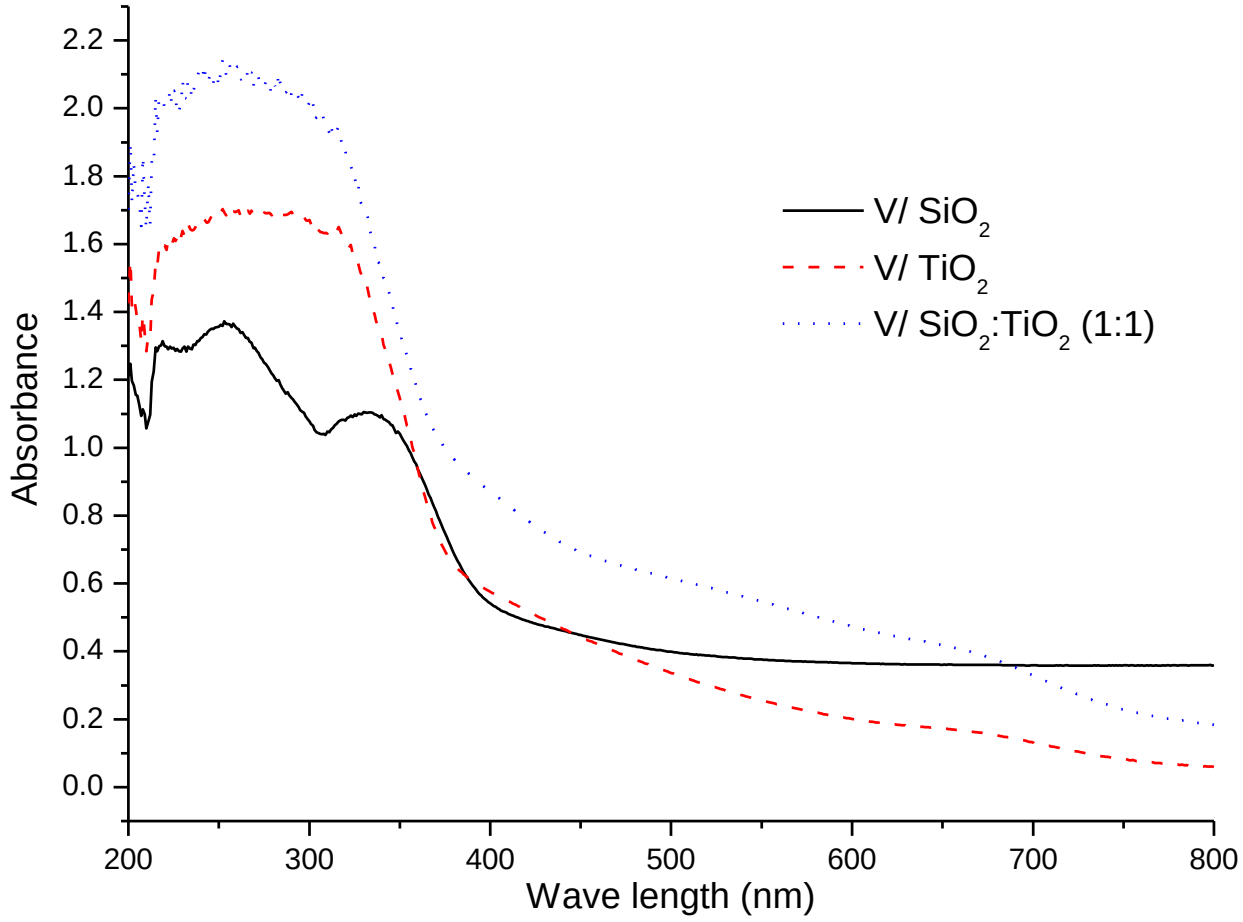

3.3.2. Kinetics of Photocatalytic Degradation

Acetaldehyde degradation of chromium loaded samples

The photocatalytic studies were carried out using acetaldehyde as the model pollutant. Complete degradation of acetaldehyde was assumed according to the following reaction scheme and the produced CO_2 was measured using GCMS.

$$CH_3CHO + O_2 \longrightarrow 2\,CO_2 + H_2O \qquad (1)$$

Figure 3.7 summarizes the results obtained from acetaldehyde photo degradation studies of as prepared 0.5(mol)% chromium loaded silica, titania and mixed photocatalytic systems under UV light. According to the kinetic results obtained, chromium ion loaded silica shows the highest photocatalytic degradation ability towards acetaldehyde under UV light. The blank silica sample,

without any chromium ion doping, shows minimal acetaldehyde degradation, indicating the importance of loaded chromium in the photocatalytic performance.

Furthermore, the acetaldehyde degradation under UV light without any catalyst (No Catalyst) is higher than that of in the presence of pure silica (Blank/SiO_2). Blank titania also shows significant CO_2 production and this is expected for titania based compounds under UV light.[9,10] Chromium doping into titania seems to be not very important in UV light based catalysis as there is only a slight increase in the activity compared to the blank titania based sample. The highest active sample, chromium loaded silica aerogel, as shown in both figures 3.7 and 3.8, shows very interesting photocatalytic behaviors under UV and visible wavelengths that only start its activity upon exposure to light confirming the photocatalytic nature of the material.

Figure 3.7: Kinetics of photocatalytic degradation of acetaldehyde using 0.5%(mol) chromium loaded silica, titania, mixed systems, blank samples and commercially available titania P25 under UV light irradiation

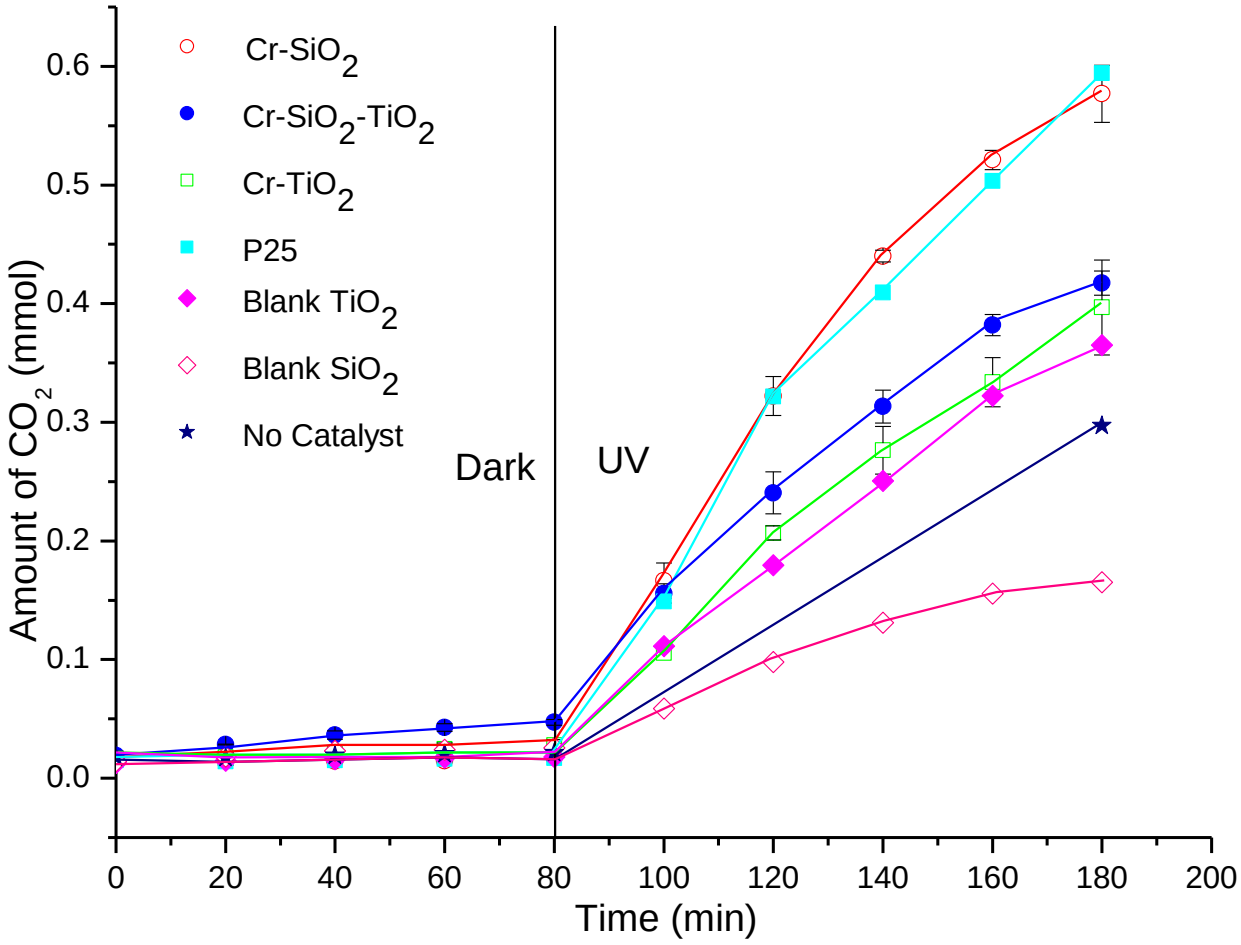

The photocatalytic activity under visible light is of more interest to us since a larger percentage of solar radiation consists of visible light.[11] Thus, all the samples were tested for visible light photo degradation of acetaldehyde and the results obtained are plotted in figure 3.8. According to the kinetic results, acetaldehyde degradation under visible light without any catalyst is very low. Therefore, it can be assumed that all the carbon dioxide observed is due to the photocatalytic behavior of the catalyst material. The blank silica sample showed no photocatalytic activity, as expected, because of the inability of insulating silicon dioxide (SiO_2) to act as a photocatalytic material by itself. The titania sample prepared in our labs shows a slight activity compared to commercially available P25 which may be arising due to the compositional changes of different crystalline phases, surface area differences and the particle sizes of titania.[10,12] According to the powder X-ray diffraction studies the titania based samples prepared in our lab consisted of 100% anatase crystalline titania. But, commercially available P25 titania is a mixture of both anatase and rutile crystalline phases.[10,12] The 0.5(mol)% Cr-SiO_2-TiO_2 systems and the 0.5(mol)% Cr-SiO_2 systems show very high photocatalytic activities under visible light compared to all the other systems. The higher surface area of our silica SiO_2 samples could be one major reason for the observed higher photocatalytic activity.

Figure 3.8: Kinetics of photocatalytic degradation of acetaldehyde using 0.5%(mol) chromium loaded silica, titania, mixed systems, blank samples and commercially available titania P25 under visible light irradiation

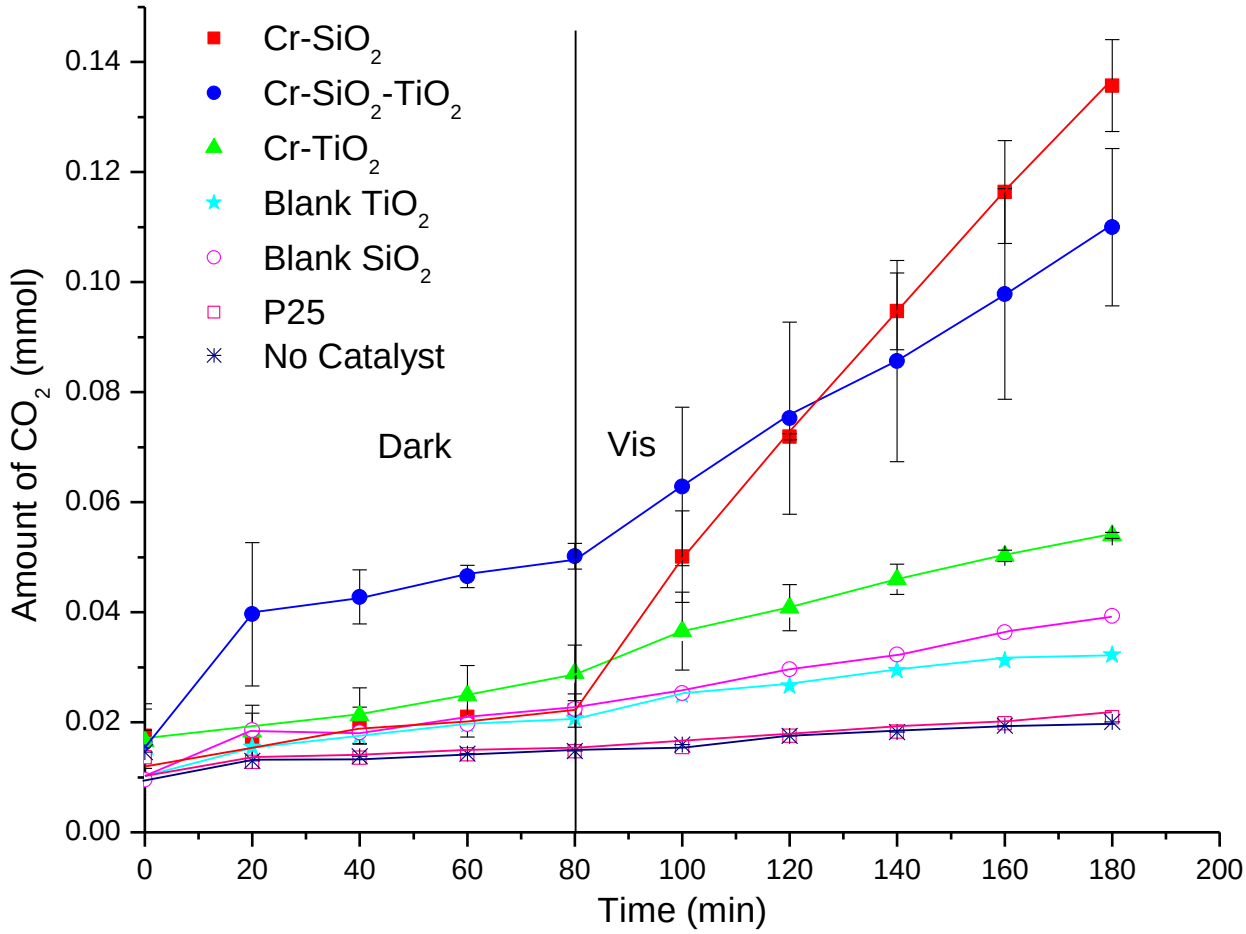

The 0.5(mol)% Cr-SiO_2-TiO_2 systems and the 0.5(mol)% Cr-SiO_2 systems show very high photocatalytic activities under visible light compared to all the other systems.

Acetaldehyde degradation of cobalt loaded samples

Figures 3.9 and 3.10 summarize the results obtained for the catalytic degradation of the model pollutant, acetaldehyde, by as prepared 0.5(mol)% Co-SiO_2 catalyst and compare the catalytic activity of the catalyst to its photocatalytic relatives made from titania, mixed titania/silica systems and commercially available photocatalytic material P25 under UV and Visible lights.

Figure 3.9: Kinetics of photocatalytic degradation of acetaldehyde using 0.5%(mol) cobalt loaded silica, titania, mixed systems, blank samples and commercially available titania P25 under UV light irradiation

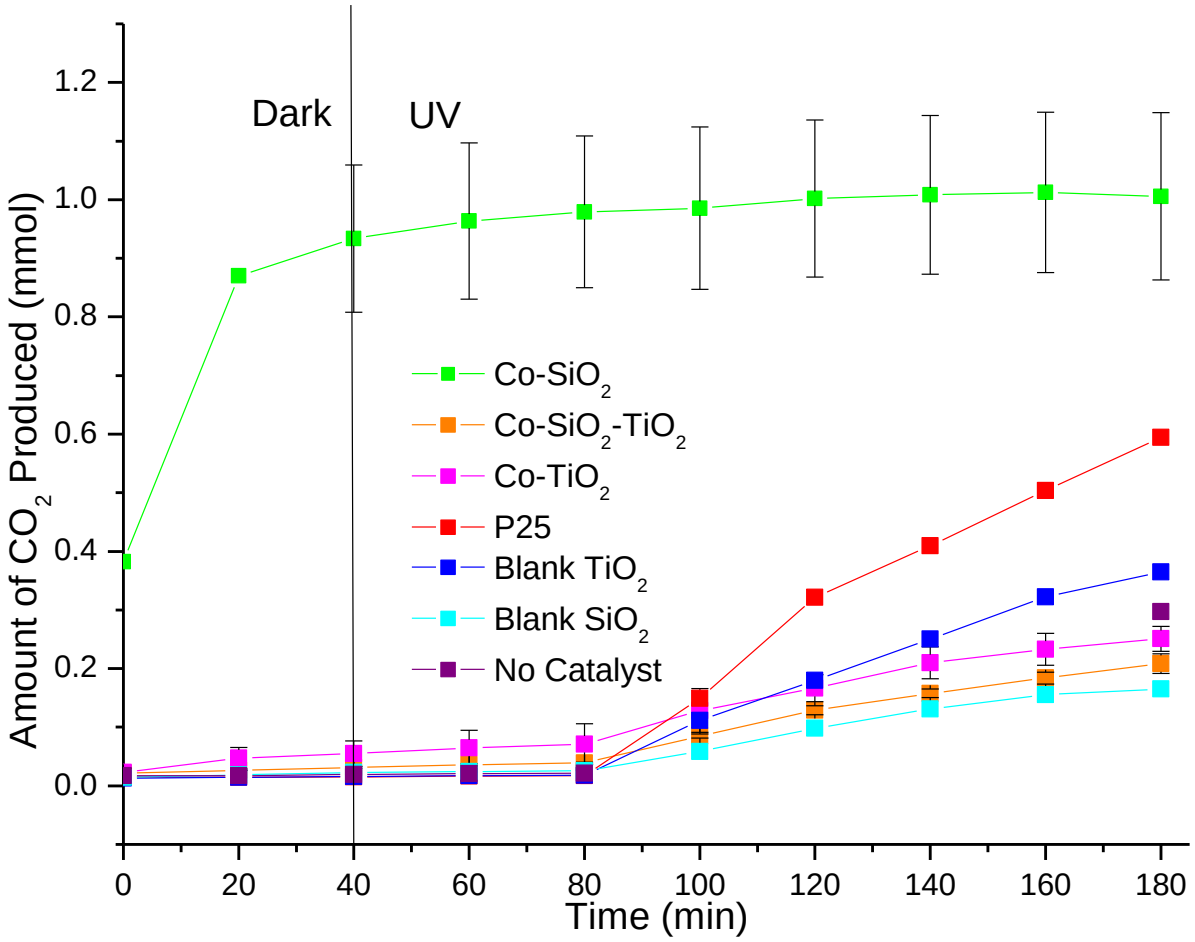

According to the kinetic results (figure 3.9-3.10) it is very clear that the Co-SiO_2 system has the highest activity towards acetaldehyde degradation. The catalyst does not require any light source to initiate or maintain the reaction. One interesting observation unique to the Co-SiO_2 catalyst is conversion of almost all the acetaldehyde present in the system into CO_2 within the first 40 minutes of the reaction. But, after the first 40 minutes of the reaction no additional CO_2 production occurred. This can be due to two main reasons; lack of reactants or the catalyst deactivation, which will be discussed later.

Figure 3.10: Kinetics of photocatalytic degradation of acetaldehyde using 0.5%(mol) cobalt loaded silica, titania, mixed systems, blank samples and commercially available titania P25 under visible light irradiation

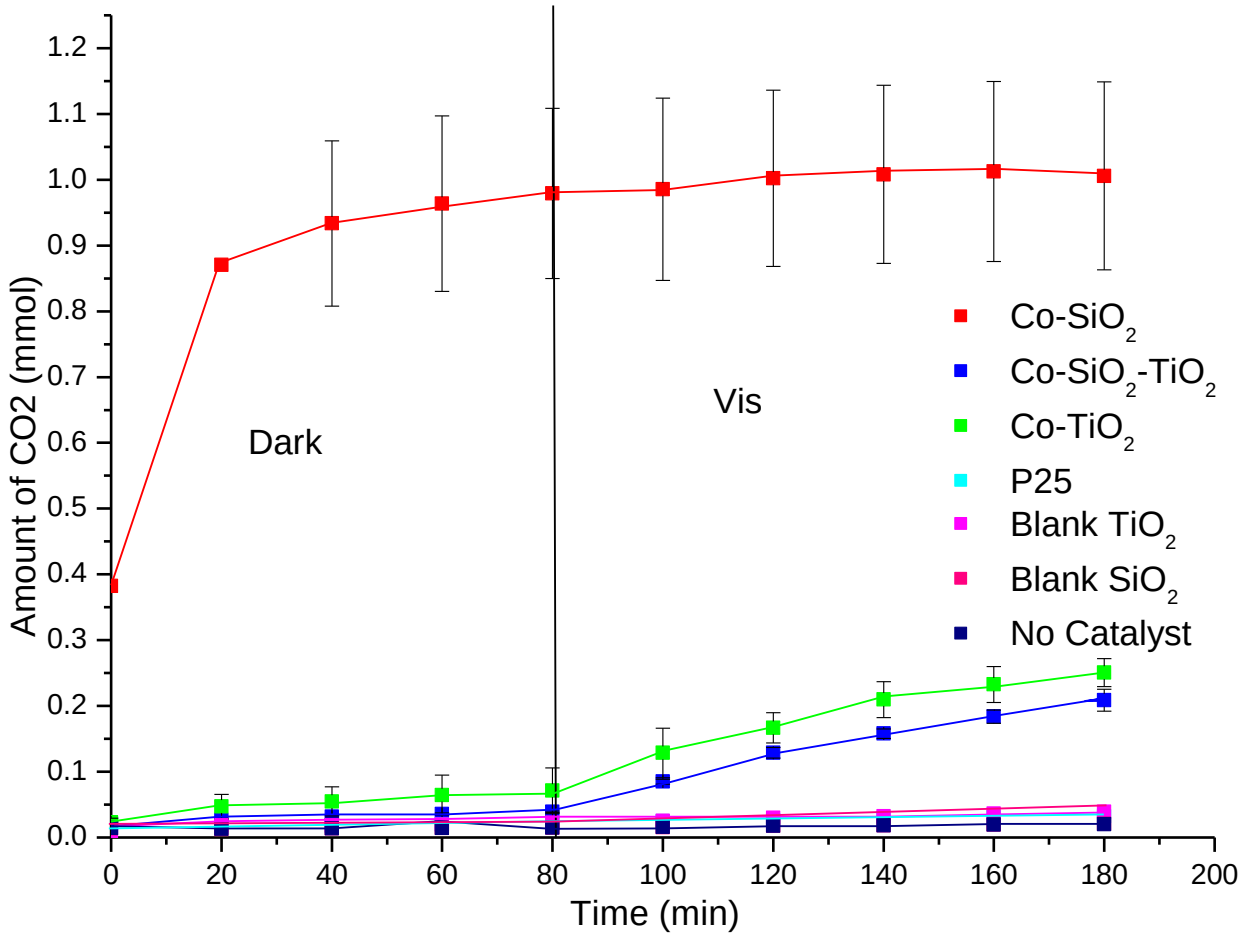

Acetaldehyde degradation of vanadium loaded samples

Photocatalytic acetaldehyde degradation using vanadium loaded systems under UV and visible light irradiation are given in figures 3.11 and 3.12. Unlike chromium loaded and cobalt loaded samples, vanadium loaded samples did not show promising photocatalytic activities under UV and visible light conditions. According to the results indicated in figure 3.11 below, under UV light irradiation, commercially available P25 showed the highest catalytic activity, while the vanadium loaded silica sample was only able to produce about half of the amount of carbon dioxide that was produced by P25. Similar to the other two transition metal loaded silica systems we used, the vanadium loaded silica system shows highest activity. The observed very low

activity under visible light seems to have a direct relationship with the low diffuse Reflectance UV-Vis absorption in the visible region.

Figure 3.11: Kinetics of photocatalytic degradation of acetaldehyde using 0.5%(mol) vanadium loaded silica, titania, mixed systems, blank samples and commercially available titania P25 under UV light irradiation

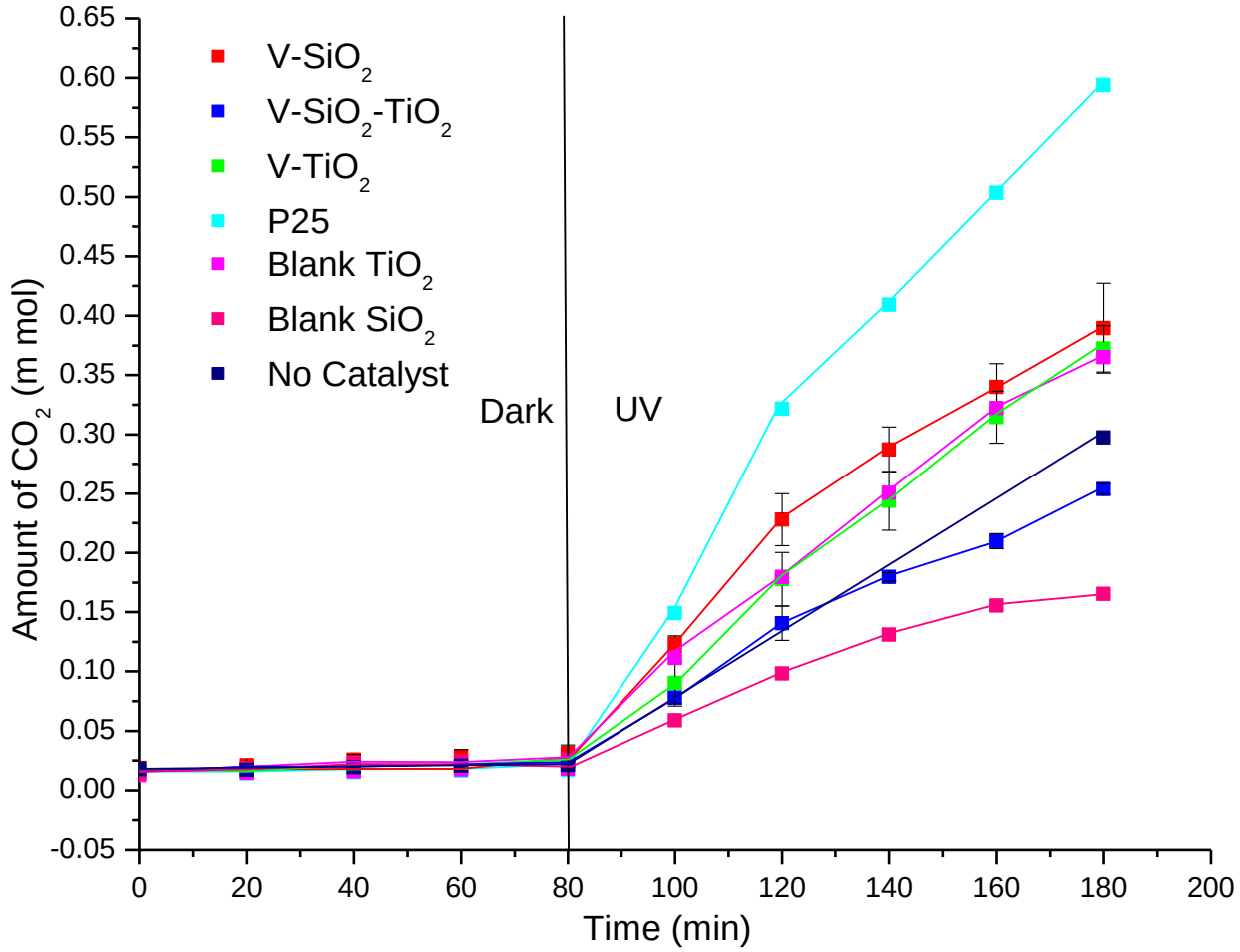

Figure 3.12: Kinetics of photocatalytic degradation of acetaldehyde using 0.5%(mol) vanadium loaded silica, titania, mixed systems, blank samples and commercially available titania P25 under visible light irradiation

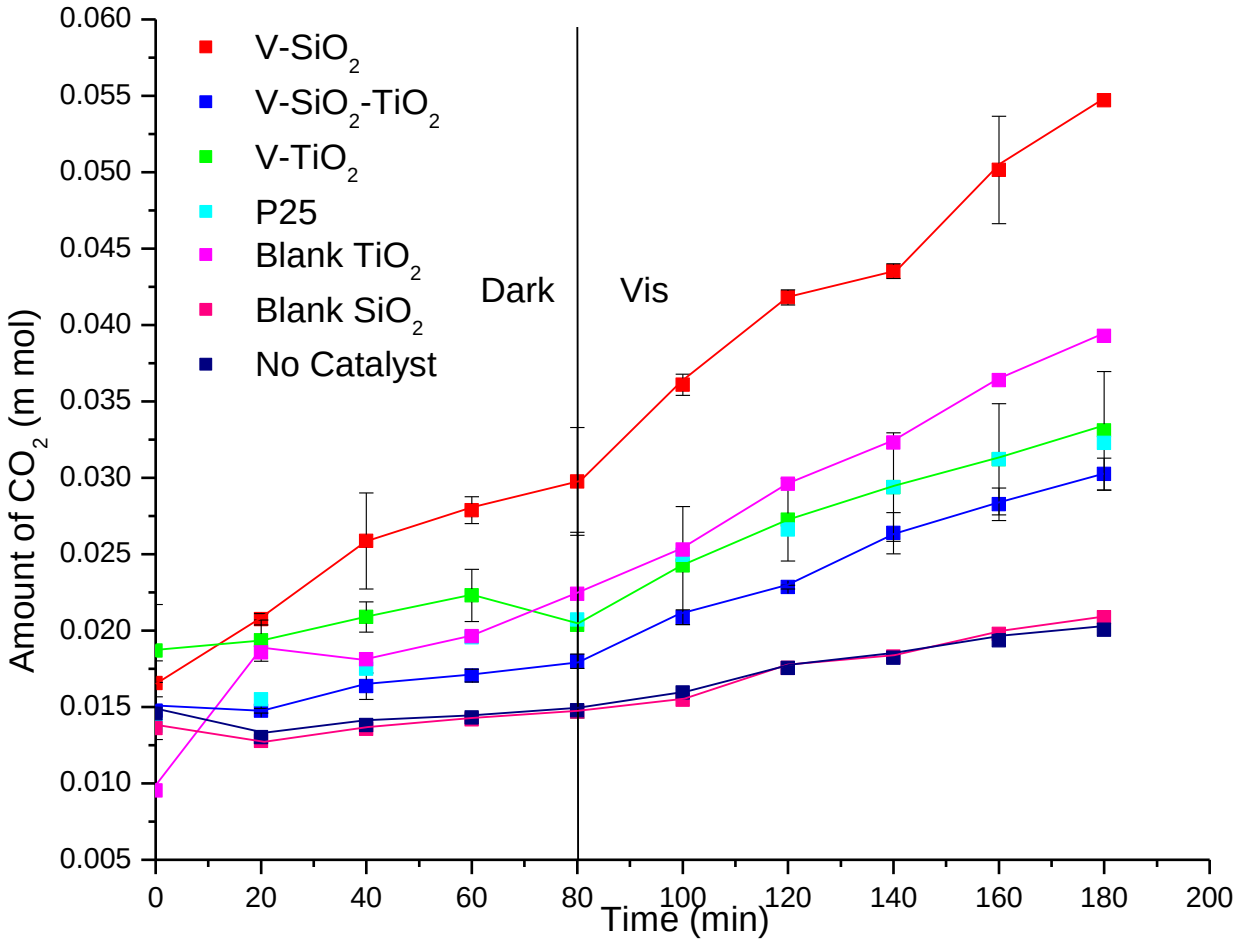

3.3.3. Calculation of Catalytic Turnover

Turnover number and the rate of catalysis were calculated based on the kinetic information obtained under visible light irradiation. For calculation purposes the amount of loaded chromium was used as the catalytic active sites assuming that all the loaded chromium was involved equally in catalytic oxidation process. Equations 2 and 3 were used for the calculations.

$$\text{Turnover Number} = \frac{\text{Amount of } CO_2 \text{ produced (mol)}}{\text{Amount of the catalyst present (mol)}} \qquad (2)$$

$$\text{Turnover Frequency} = \frac{\text{Turnover Number}}{\text{Time}} \ (\text{min}^{-1}) \qquad (3)$$

Table 3.2: Turnover numbers obtained for the catalysts for four hours of reaction for each metal ion site

Catalyst	Turnover number of Chromium loaded Systems	Turnover number of Cobalt loaded Systems	Turnover number of vanadium loaded Systems
SiO_2	16.8	79.0	4.8
TiO_2	4.8	15.0	3.2
SiO_2/TiO_2	12.6	8.7	2.8

Table 3.3: Turnover frequencies obtained for the catalysts for four hours of reaction for each metal ion site

catalyst	Turnover frequency of chromium loaded systems	Turnover frequency of cobalt loaded systems	Turnover frequency of vanadium loaded systems
SiO_2	0.28	7.9	0.08
TiO_2	0.08	0.25	0.05
SiO_2/TiO_2	0.21	0.145	0.046

3.4. Mechanism of Photocatalytic Activity

To briefly review the general mechanism of titania based photocatalysis under UV light, positively charged holes and negatively charged electrons are created in valence and conduction bands of titania respectively as described by Eq 1.

$TiO_2 + h\nu \rightarrow TiO_2 (e^- \text{ and } h^+)$ …… Eq 1

$OH^- + h^+ \rightarrow {}^{\bullet}OH$ …… Eq 2

$O_2 + e^- \rightarrow O_2^{\bullet -}$ …… Eq 3

In the second step positively charged holes are trapped by surface hydroxyl groups of titania generating reactive hydroxyl radicals (Eq 2). In the meantime negatively charged electrons can interact with oxygen in the valence band to generate reactive oxygen species (Eq3). The oxidation ability of $^{\bullet}OH$ radicals is very high so that they easily react with various organic pollutants.[13,14]

3.4.1. Mechanism of transition metal (Cr/Co) loaded TiO_2 photocatalyst

Even though the above equations explain the behavior of semiconducting titania under UV light, a modified mechanism is needed to explain the visible light activity of transition metal ion loaded titania photocatalysts. There are various ways that loaded transition metals help improve the visible light photocatalytic activity[15,16]. The most accepted way of inducing visible light activity into the titania network is by introducing new localized electronic states and surface structures. These changes to the titania network can eventually change the electronic structure, absorption properties, redox potential and charge carrier mobility of the photocatalyst, *etc*.[14] Introduction of such energy states and surface structures in the band gap induces a red shift in the band gap transition and visible light absorption through charge carrier transfer between a dopant and conduction band(CB) or valence band(VB) or a d—d transition in the crystal field[17]. The charge transfer transition between Cr ion 3d electrons and conduction band of titania is known to be responsible for the red shift evident in UV-Vis spectra. According to the studies carried out by Umebayashi and co-workers, for chromium loaded titania photocatalysts two types of electron transitions are possible. The first transition is a donor transition from the Cr t_2g level into the CB which can be explained using Eq 4, and the other transition is the acceptor transition from the VB to the Cr t_2g level given by Eq 5.[14,16,17,18]

$M^{n+} + h\nu \rightarrow M^{(n+1)+} + e^{-}_{CB}$ ……..… Eq4

$M^{n+} + h\nu \rightarrow M^{(n-1)+} + h^{+}_{VB}$ ……..… Eq5

Furthermore, loaded transition metal ions can also enhance the efficiency of TiO_2 by providing electron (or hole) trapping/defect sites and thereby decreasing generated electron hole pair recombination when the energy levels for $Mn^{+}/M^{(n-1)+}$ lies below the conduction band edge and the energy level for $M^{n+}/M^{(n+1)+}$ above the valence band edge. This can be illustrated using the following equations [16-19]

$M^{n+} + e^{-} \rightarrow M^{(n-1)+}$ ……..…… Eq 6

$M^{n+} + h^{+} \rightarrow M^{(n+1)+}$ …….. Eq 7

Therefore, considering all the possible effects of transition metals and as well as according to the mechanism proposed by Devi and co-workers it is possible to explain the enhanced visible light photocatalytic activity of chromium and cobalt loaded Titania photocatalysts using the following equations.

Charge trapping:

$Ti^{4+} + e^{-} \rightarrow Ti^{3+}$ …… Eq8

$M^{n+} + e^{-} \rightarrow M^{(n-1)}$ …… Eq9

$M^{n+} + h^{+} \rightarrow M^{(n+1)+}$…… Eq10

$OH^{-} + h^{+} \rightarrow OH^{\bullet}$ ……..… Eq11

Charge release and migration:

$Ti^{4+} + M^{(n-1)} \rightarrow Ti^{3+} + M^{n+}$ …… Eq 12

$M^{(n+1)+} + OH^{-} \rightarrow M^{n+} \quad OH^{\cdot}$ ……..… Eq 13

Recombination:

$e^{-} + h^{+} \rightarrow$ heat ……...… Eq 14

$Ti^{3+} \quad OH^{\cdot} \rightarrow Ti^{4+} + OH^{-}$ ……..… Eq 15

$M^{(n-1)} + h \rightarrow M^{n+}$ ……..… Eq 16

$M^{(n-1)} \quad OH^{\cdot} \rightarrow M^{n+} + OH^{-}$ …… Eq 17

$M^{(n+1)+} + e^{-} \rightarrow M^{n+}$ ……..… Eq18

$M^{(n+1)+} + Ti^{3+} \rightarrow M^{n+} + Ti^{4+}$ …… Eq19

Interfacial charge transfer process:

e^{-} (or Ti^{3+}, $M^{(n-1)}$) $O \rightarrow O^{-}$ ……..… Eq20

h^{+} (or $OH^{\bullet}$, $M^{(n+1)+}$) $^{+} R \rightarrow R^{+}$ …… Eq 21

3.5. Summary

We have synthesized novel silicon dioxide (SiO_2) and titanium dioxide (TiO_2) based systems loaded with different transition metal ions such as cobalt, chromium and vanadium ions using well-known aerogel synthesis methods. These samples were characterized with BET surface area analysis, X-ray diffraction studies and diffuse reflectance UV-vis spectroscopic measurements. Catalytic and photocatalytic activities were determined using acetaldehyde as a model pollutant. For better comparison of the catalytic activities, kinetic results obtained for all the photocatalysts

except the dark catalyst 0.5% Co-SiO_2 catalyst, were plotted together in figure 3.13. Among all the catalysts, even though the 0.5% Co-TiO_2 catalyst shows the highest CO_2 production, it shows a significant amount of CO_2 production under dark conditions and does not show an increase in CO_2 production upon exposure to visible light. But, 0.5% Cr-SiO_2 system shows nearly zero CO_2 at the beginning and shows rapid CO_2 production in the visible region. The in-depth dark catalytic activity of 0.5% Co-SiO_2 system will be discussed in chapter 5.

Figure 3.13: Photocatalytic performances of all the as prepared transition metal ion systems except dark active Co/Silica system under visible light

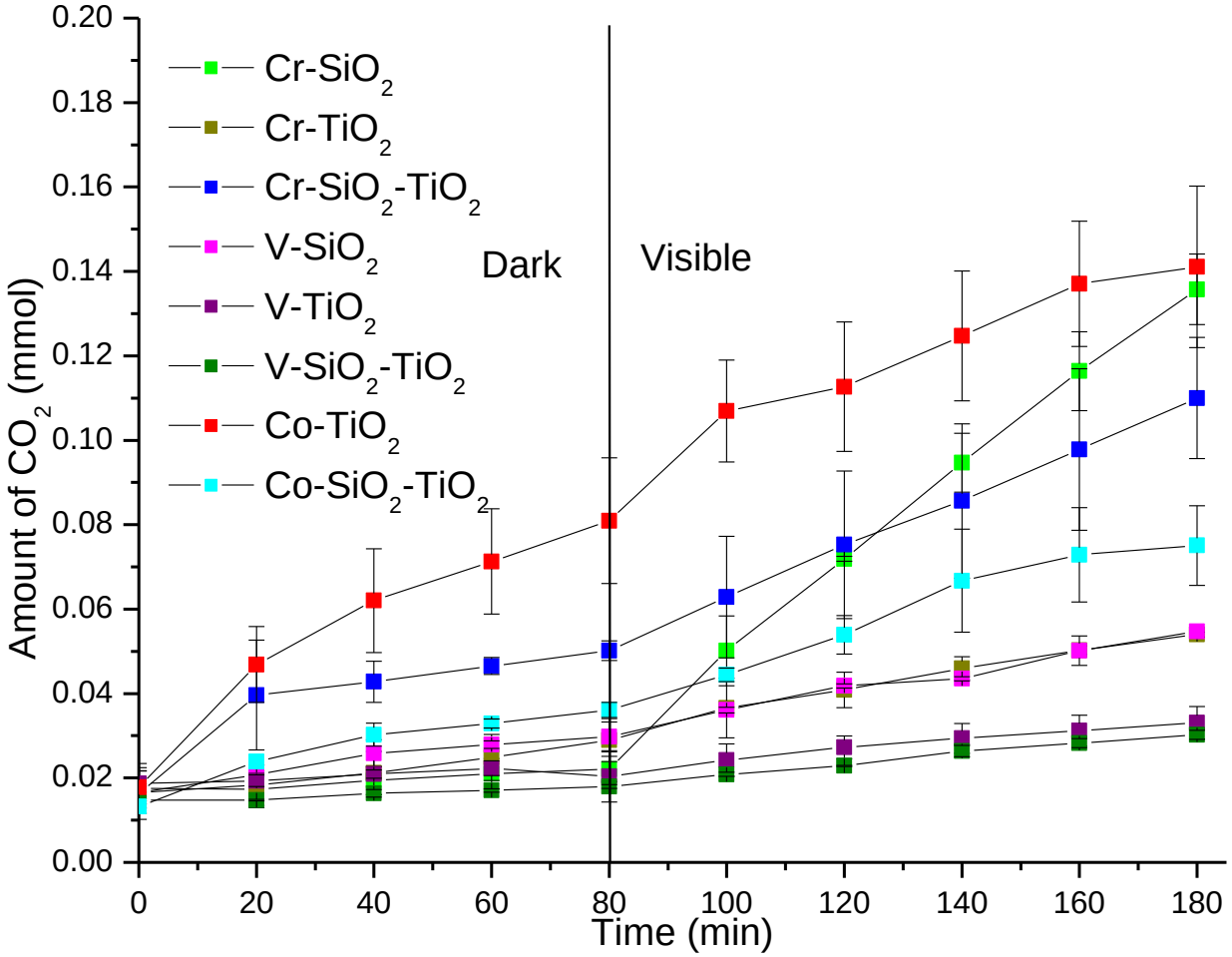

3.6. References

1. Vu, A.T.; Nguyen, Q.T.; Bui, T.H.L.; Tran, M.C.; Dang, T.P.; Tran, T.K.H., Synthesis and characterization of TiO_2 photocatalyst doped by transition metal ions (Fe+, Cr^{3+} and V^{5+}), *Adv. Nat. Sci.: Nanosci. Nanotechnol*., **2010**, 1, 15009
2. Matsumoto, Y.; Murakami, M.; Shono, T.; Hasegawa, T.; Fukumura, T.; Kawasaki, M.; Ahmet, P.; Chikyow, T.; Koshihara, S.; Koinuma, H., Room-Temperature Ferromagnetism in Transparent Transition Metal-Doped Titanium Dioxide, *Science*, **2001**,291, 854
3. Schrauben, J.N.; Hayoun, R.; Valdez, C.N.; Braten, M.; Fridley, L.; Mayer, J.M., Titanium and Zinc Oxide Nanoparticles Are Proton-Coupled Electron Transfer Agents, *Science,***2012**, 336, 1298.
4. Naik, B.; Ghosh, N.N., A Review on Chemical Methodologies for Preparation of Mesoporous Silica and Alumina Based Materials, *Recent Patents on Nanotechnology*, **2009**, 3, 213-224
5. Pinho, L.; Mosquera, M.J., Titania-Silica Nanocomposite Photocatalysts with Application in Stone Self-Cleaning, *J. Phys. Chem. C*, **2011**, 115, 22851–22862
6. Anderson, M.L.; Stroud, R.M.; Morris, C.A.; Merzbacher, C.I.; Rolison, D.R.; Tailoring Advanced Nanoscale Materials Through Synthesis of Composite Aerogel Architectures, *Advanced Engineering Materials*, **2000**, 2, 8, 481-488
7. Schneider, M.; Baiker, A., *J. Mater. Chem.*, High-surface-area Titania Aerogels: Preparation and Structural Properties, **1992**, 2, (6), 587-589
8. Campbell, L.K.; Na, B. K.; KO, E.I., Synthesis and Characterization of Titania Aerogels, *Chem. Mater.*, **1992**,4, 1329-1333
9. Liang, Y. T.; Vijayan, B.K.; Gray, K.A.; Hersam, M.C., Minimizing Graphene Defects Enhances Titania Nanocomposite-Based Photocatalytic Reduction of CO_2 for Improved Solar Fuel Production, *Nano Lett.,* **2011**, 11, 2865–2870
10. Liang, Y. T.; Vijayan, B.K.; Gray, K.A.; Hersam, M.C., Minimizing Graphene Defects Enhances Titania Nanocomposite-Based Photocatalytic Reduction of CO_2 for Improved Solar Fuel Production, *Nano Lett.,* **2011**, 11, 2865–2870
11. 220. Climate Change: The Role of Cities, United Nations Environment Programme (UNEP), **2009**
12. 210. Lim, S.H.; Phonthammachai, N.; Pramana, S.S.; White, T.J.; Simple Route to Monodispersed Silica-Titania Core-Shell Photocatalysts, *Langmuir*, **2008**, 24, 6226-6231
13. **230.** Dvoranová, D,; Brezová, V.; Mazúra, M.; Malati, M.A., Investigations of metal-doped titanium dioxide photocatalysts, *Applied Catalysis B: Environmental*, **2002**, 37, 91–105
14. 240. Gomathi Devi, L.; Girish Kumar, S., Influence of physicochemical.electronic properties of transition metal ion doped polycrystalline titania on the photocatalytic degradation of Indigo Carmine and 4-nitrophenol under UV/solar light, *Applied Surface Science*,**2011**, 257, 2779–2790
15. 250. Choi, J.; Park, H.; Hoffmann, M.R., Effects of Single Metal-Ion Doping on the Visible-Light Photoreactivity of TiO_2, *J. Phys. Chem. C*, **2010**, 114, 783–792
16. 260. Umebayashi, T.; Yamaki, T.; Itoh, H.; Asai, K., Analysis of electronic structure of 3d transition metai-doped TiO_2 based on band calculations, *Journal of physics and chemistry of solids*,**2002**, 1909-1920

17. Choi, W.; Termin, A.; Hoffmann, M.R., The Role of Metal Ion Dopants in Quantum-Sized TiO_2: Correlation between Photoreactivity and Charge Carrier Recombination Dynamics, *J. Phys. Chem.*, **1994**, 98, 13669-13679
18. 280. Chang, C.; Shen, Y., Synthesis and characterization of chromium doped SrTiO3 photocatalyst, *Materials Letters*, **2006**, 60, 129 – 132
19. 290. Yu; J.; Xiang, Q.; Zhou, M., Preparation, characterization and visible-light-driven photocatalytic activity of Fe-doped titania nanorods and first-principles study for electronic structures, Applied Catalysis B: Environmental, **2009**, 90, 595–602

Chapter 4 - Chromium(VI) Oxide Loaded Silica Aerogels: Novel Visible light Active Photocatalytic Materials for Removal of Air Pollutants

4.1. Introduction

Photocatalysis has been studied actively during the last several decades because of its application to green energy and due to the understanding of the importance of a cleaner atmosphere. As a result there are a large number of reports about applications of photocatalysis in various tasks such as environmental remediation, photocatalytic water splitting, *etc.* Photocatalysis has widely been studied to destroy organic dye compounds from industrial effluents, oxidation of indoor and outdoor organic pollutants, etc. The basic advantage of photocatalysis is its ability to mineralize a large variety of harmful organic pollutants under ambient temperature and pressure conditions.[1]

In most of the successful photocatalytic materials that have been reported earlier, consist of a supporting base material. Titania is one of the most widely used photocatalytic material that has shown success in organic material decomposition. It is believed that the supporting material facilitates the catalytic activity of the catalytic site by enhancing charge carrier separation, allowing reduced electron hole recombination and facilitating charge transfer to adsorbed species making photocatalytic processes are non-localized.[2,3] But, whether a photocatalytic process must be non-localized is a question that still needs to be answered.

Therefore, our main objective in this chapter is to discover photocatalytic systems which progress according to localized mechanisms. The study was carried out by preparing such a system using insulated silica based materials. Generally low reactivity and high band gap energy of silica makes it a suitable material to study the localized properties of photocatalysis. Furthermore, to achieve visible light activity, it is important to insert a suitable light harvesting material into silica in order to introduce photocatalytic activities. Transition metals and metal oxides have been actively used in this regard. Transition metals are very good candidates to absorb in the visible range of the spectrum, as orbital energy transfer usually lies in the visible range. According to the earlier experiments which were carried out in our lab, chromium loaded systems showed highest activities towards oxidation of organic air pollutants. Thus, for our

systems chromium was chosen as the doping agent for our more in-depth study of Cr-SiO_2.[4,5,6] Herein we report the observed UV and visible light activities of chromium ion loaded silica based materials and possible mechanisms for the observed photocatalytic performances.

4.2. Experimental Methods

4.2.1. Preparation of chromium ion loaded silica and titania aerogel samples

Chromium ion loaded silicon dioxide and titanium dioxide samples were prepared using an aerogel preparation method using a similar procedure explained in the chapter 3. The 0.5(mol)% Cr loaded samples with varying molar ratios of titania and silica was prepared to obtain molar ratios of SiO_2:TiO_2, (0:100, 20:80, 40:60, 50:50, 60:40, 80:20 and 100:0). Further the effect of higher loading chromium was studied by preparing 1(mol)%, 2(mol % and 5(mol)% loaded chromium silica samples.

4.2.2. Characterization studies

Brunauer-Emmet-Teller (BET) measurements of surface area and pore size distribution of the prepared samples were determined using a Quantachrome NOVA 1200 gas absorption/desorption analyzer after degassing the samples at 150 ^oC for two hours. Powder XRD analysis of the samples was carried out to determine the crystalline nature using a Scintag-XDS-2000 spectrometer with Cu Kα radiation with applied voltage of 40 kV and current of 40 mA. Samples were scanned 2θ from 0^o to 75^o with a scan rate of 1^o per minute. Diffuse reflectance UV-visible spectra were measured at room temperature in air on a Cary 500 scan UV-vis-NIR photometer over the range from 200 to 800 nm.

The compositions of prepared photocatalysts were determined by carrying out elemental analysis using Energy Dispersive Spectrometry using a Scanning Electron Microscope. Detailed study of the loaded chromium was carried out using a bulk elemental analysis to determine the final amounts of loaded ions. Bulk elemental analysis was carried out using simultaneous optical systems and axial or radial viewing of the plasma using Perkin Elmer Optima 5300 spectrometer at Galbraith laboratories Inc.

TEM studies were carried out using a Philips CM100 operating at 100 kV. The TEM samples were prepared by dispersing few milligrams of the catalyst in ethanol using an ultrasonic bath. Then a drop of catalyst-ethanol mixture was placed on the TEM grid and air dried. The facilities

were provided by the Microscopy and Analytical Imaging Laboratory at Department of Biology, Kansas State University.

4.2.3. Kinetic studies of photocatalytic systems

Prepared samples were tested for both UV light and visible light photocatalytic activities. Kinetics of the photocatalytic degradation was studied using a Shimadzu GCMS-QP 5000 instrument and a glass reactor with a quartz window. Acetaldehyde was used as a model pollutant and the temperature of the glass reactor was maintained at 25 ^{o}C by circulating water in the outer jacket of the reactor during all the kinetic experiments. In a typical experiment 0.10 g of the prepared sample was uniformly placed on the special glass chamber allowing UV or visible light to directly contact the prepared photocatalytic material. Then the air filled system was sealed and 0.10 ml of liquid acetaldehyde was introduced to the bottom of the reactor to avoid any direct contact of liquid acetaldehyde and the photocatalytic material. During the experiment acetaldehyde slowly gets evaporated due to its near room temperature boiling point, and gaseous acetaldehyde gets absorbed on to the reaction sites of the catalyst. Photocatalysts were then illuminated with UV or visible light using a 1000 w xenon lamp and glass filters by cutting off unnecessary light. The progress of any reaction was detected by injecting 35 µl of gas samples from the sealed reactor to the Shimadzu GCMS-QP 5000 instrument every 20 minutes. All the kinetics experiments were carried out at least two times in order to confirm the accuracy of the results and were compared with commercially available titania P25 and prepared blank samples, where no dopant elements were present.

4.2.4. Hydroxyl radical generation studies using terephthalic acid

Terephthalic acid(TPA), which is not a fluorescent compound, gives a single, fluorescent product, 2-hydroxyterephthalic acid (HTPA), by reacting with hydroxyl radicals produced during the photocatalytic reaction (Figure 4.1). HTPA emits fluorescence at around 426 nm on the excitation of its own 312 nm absorption band. The measurements of the amount of $OH^{\cdot}$ were performed for the chromium loaded titania and silica based systems carrying out photocatalytic reaction by means of this TPA fluorescence probe method as follows. For the measurements of any hydroxyl radicals generated during photocatalytic reactions the photocatalyst samples were irradiated under UV and visible light in terephthalic acid solution (2×10^{-3} M). Then the solution, after separation from the photocatalyst, was taken for fluorescence analysis. The fluorescence

measurements were carried out at the excitation wavelength of 314 nm in the range of emission wavelength from 330 nm to 600 nm with maximum peak at 425 nm.[7,8,9]

Figure 4.1: Reaction path of terephthalate and hydroxyl radicals to generate fluorescent hydroxyterephthalate[9]

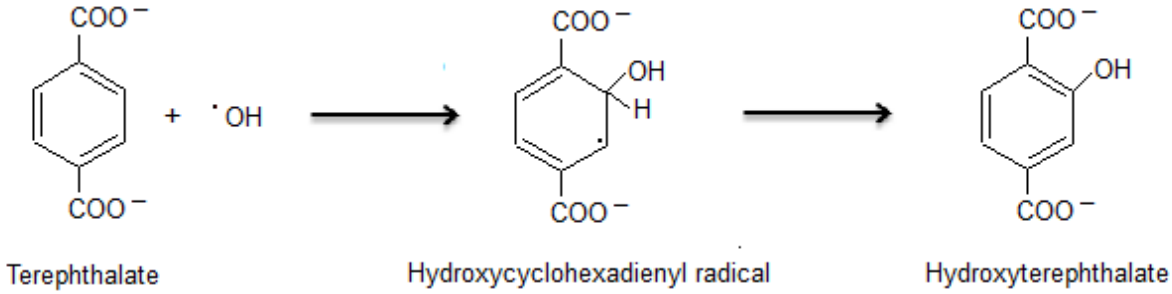

4.3. Results and Discussion

4.3.1. Structure of chromium loaded photocatalytic systems

It is well-known that the effective surface area of a material is important in deciding the photocatalytic efficiency of a material because in most of the photocatalytic systems the catalytic activity takes place on the surface of the material[10]. Therefore, the photocatalyst synthesis process was specially designed to obtain higher effective surface area using a super critical drying technique. Surface area values obtained from the BET analysis experiment show that all the samples have very high effective surface area values. Obtained effective surface area values of silica based materials are higher compared to that of titania based materials which confirm what has previously been reported.[11] Further, mixed silica and titania systems show a gradual decrease in effective surface area with increasing amounts of titania added as indicated in table 4.1. The surface area of samples increased according to a linear pattern with increasing amounts of silica (Figure 4.2).

Figure 4.2: Increase in the effective surface area with increased amounts of silica

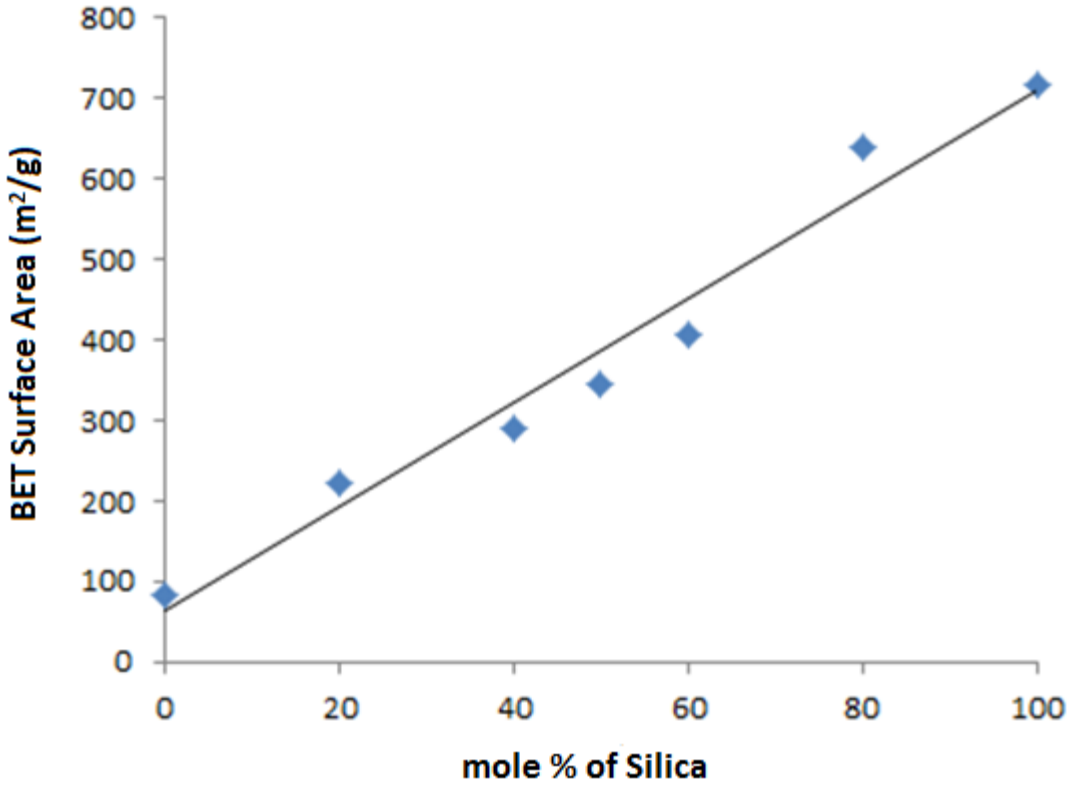

Table 4.1: Change in specific surface area of 0.5(mol)% chromium loaded silica and titania based materials

Percentage of Silica	100	80	60	50	40	20	0
Percentage of Titania	0	20	40	50	60	80	100
Effective Surface Area (m^2/g)	717	641	408	345	291	222	84

According to the EDS studies the ratios of silica to titania in mixed oxide samples matched exactly to the initial precursor concentrations. But, due to the limited sensitivity of the instrument as well as the minute amount of dopants present in these samples, percentages of chromium could not be detected (Figure 4.3) . Therefore, a bulk elemental analysis was carried out specially to determine the amounts of chromium present in the 0.5(mol)% chromium loaded sample.

According to the results obtained, the percentage of chromium is 0.369% by weight, which when converted in to reported mol % units comes around 0.43(mol)%. Thus, considering possible instrumental errors it is clear that only a minimal amount of chromium has been lost during the preparation procedure.

Figure 4.3: EDS elemental analysis data obtained for the 0.5(mol)% Cr-SiO_2 photocatalyst

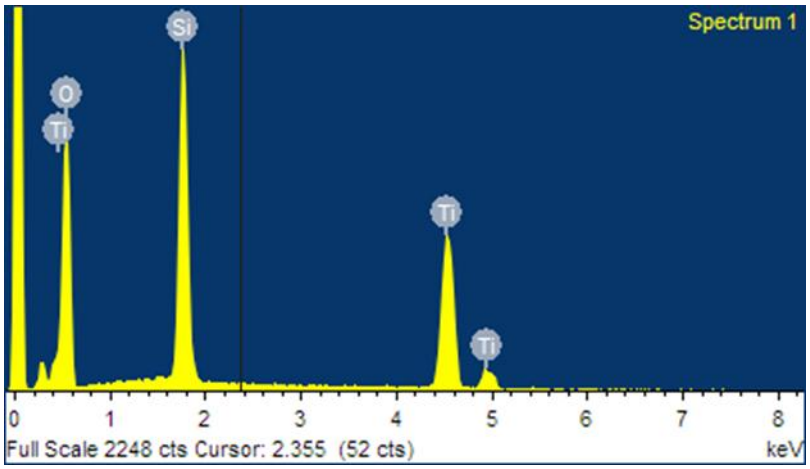

As indicated in the chapter 3, no other diffraction peaks arising from loaded chromium were observed during XRD studies. This indicates that chromium ion doping during the synthesis has no effect on the crystalline phase of the matrix material and the loaded chromium does not create any crystalline phases either. Chromium crystalline peaks may not be detectable due to lower concentrations and very smaller crystallite sizes. Detailed XRD studies were carried out with higher loading chromium silica samples prepared in the same procedure to study the reason for absence of chromium crystalline peaks. But, as indicated in the figure 4.4, no crystalline peaks arising from chromium species could be recognized for any higher loaded samples. Thus, consistent with literature reports it is clear that chromium either exist as non-crystalline forms bound to silica matrix or finely dispersed in the matrix of silica or titania as very small chromium oxide nano-particles.[4,12,13]

Figure 4.4: Powder XRD studies of 0.5(mol)% Cr-SiO_2, 1(mol)% Cr-SiO_2, 2(mol)%Cr-SiO_2 and 5(mol)% Cr-SiO_2.

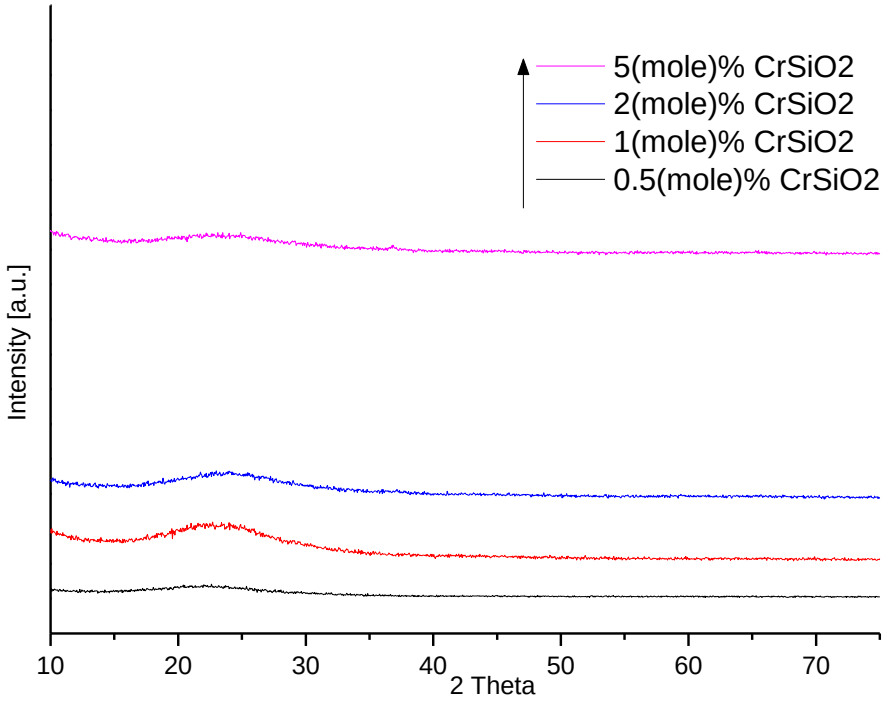

Figure 4.5 shows diffuse reflectance UV-Vis absorption spectra of chromium loaded SiO_2, TiO_2, and mixed photocatalysts. As expected, with chromium present, absorption in the visible region was observed. For silica based photocatalytic systems, bands at 240 nm, 265 nm, 360 nm, 445 nm and 650 nm, can be easily recognized in the system where no titania is present. The bands correspond to O → Cr^{6+} charge transfer transitions for Cr^{6+} ions in tetrahedral environment. These bands can be assigned as follows; the band at 445 nm (22500 cm^{-1}) is the symmetry-forbidden transition ($1t_1$ → 2e) which is partially allowed in solid salts, while the other bands at 370 nm (27000 cm^{-1}) $1t_1$ → 2e, 294 nm (34000 cm^{-1}) $1t_1$ → $7t_2$, and 241 nm (41400 cm^{-1}) $6t_2$ → 2e are symmetry allowed transitions.[14-17]

Therefore, based on the XRD and the clear UV-Vis absorption patterns which correspond to the individual Cr^{6+} state, it is evident that isolated Cr(VI) sites exist dispersed in the matrices of Silica and Titania. The use of minute amounts of chromium during the preparation of these materials also favor the formation of isolated Cr^{6+} sites.[4] Tetrahedral Cr^{6+} has been reported in three different chemical forms, such as Chromium oxide (CrO_3), Chromate ions(CrO_4^{2-}) and Dichromate ions($Cr_2O_7^{2-}$). Due to the characteristic yellow-orange coloration and according to previous reports both chromate and dichromate species are possible on silica surface[18].

Figure 4.5: Variation of UV-visible absorption bands with different ratios of 0.5(mol)% chromium loaded SiO_2 to TiO_2

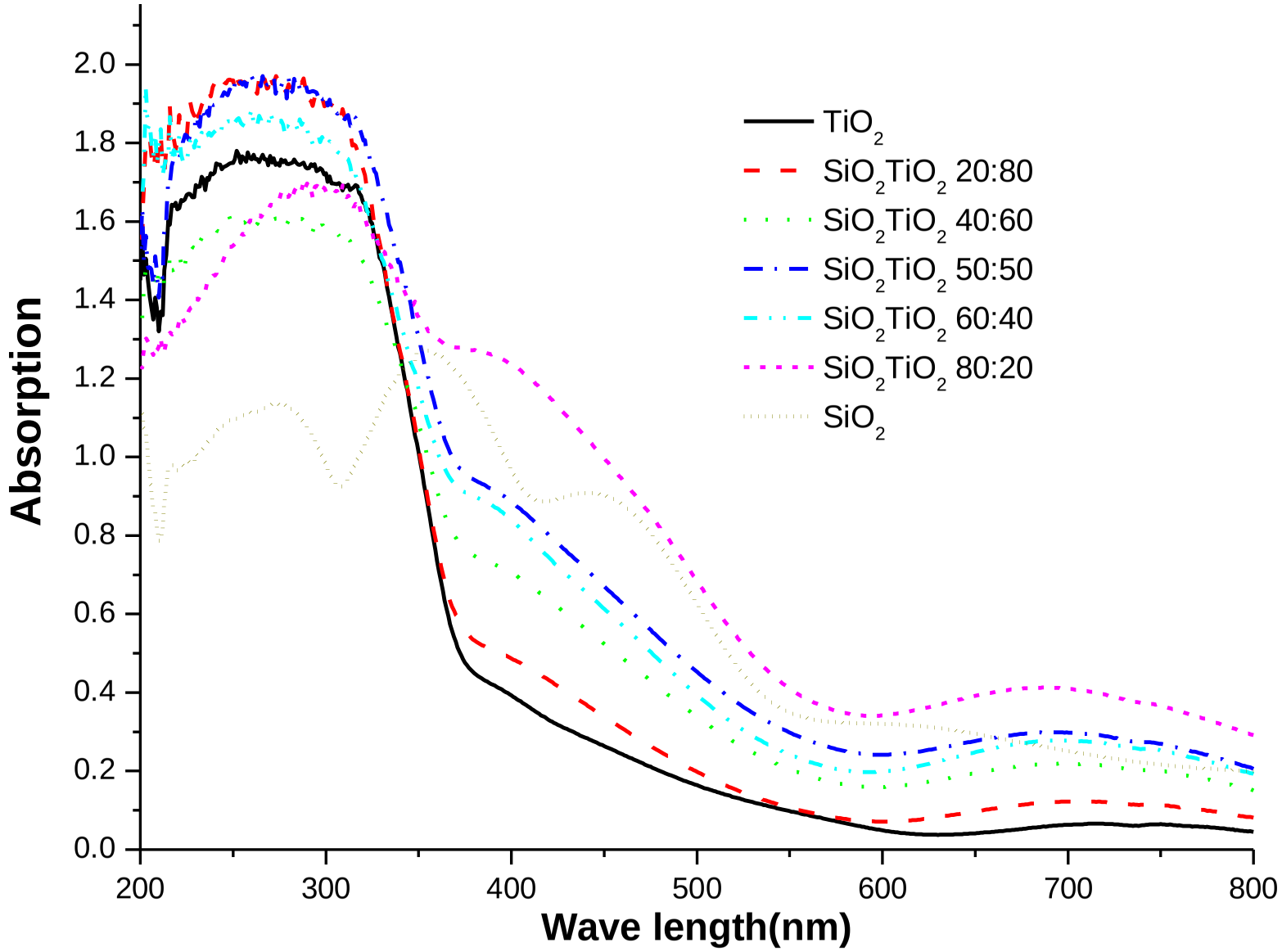

Comparison of TEM images of blank silica sample, 0.5(mol)% Cr-SiO_2, and 5(mol)% Cr-SiO_2 is shown in figure 4.6. Loaded chromium sites on silica matrix can be identified in both chromium loaded samples as ~ 2 nm size dark spots. The amount of chromium sites increase with increasing chromium loading was observed without significant increase in the size of these particles. But, no chromium sites could be observed on the surface of Cr-TiO_2 sample as shown in the figure 4.6d.

Figure 4.6: TEM images of (a) Blank Silica aerogel, (b) 0.5(mol)% Cr-SiO_2 catalyst (c) 5(mol)% Cr-SiO_2, and (d) 0.5(mol)% Cr-TiO_2

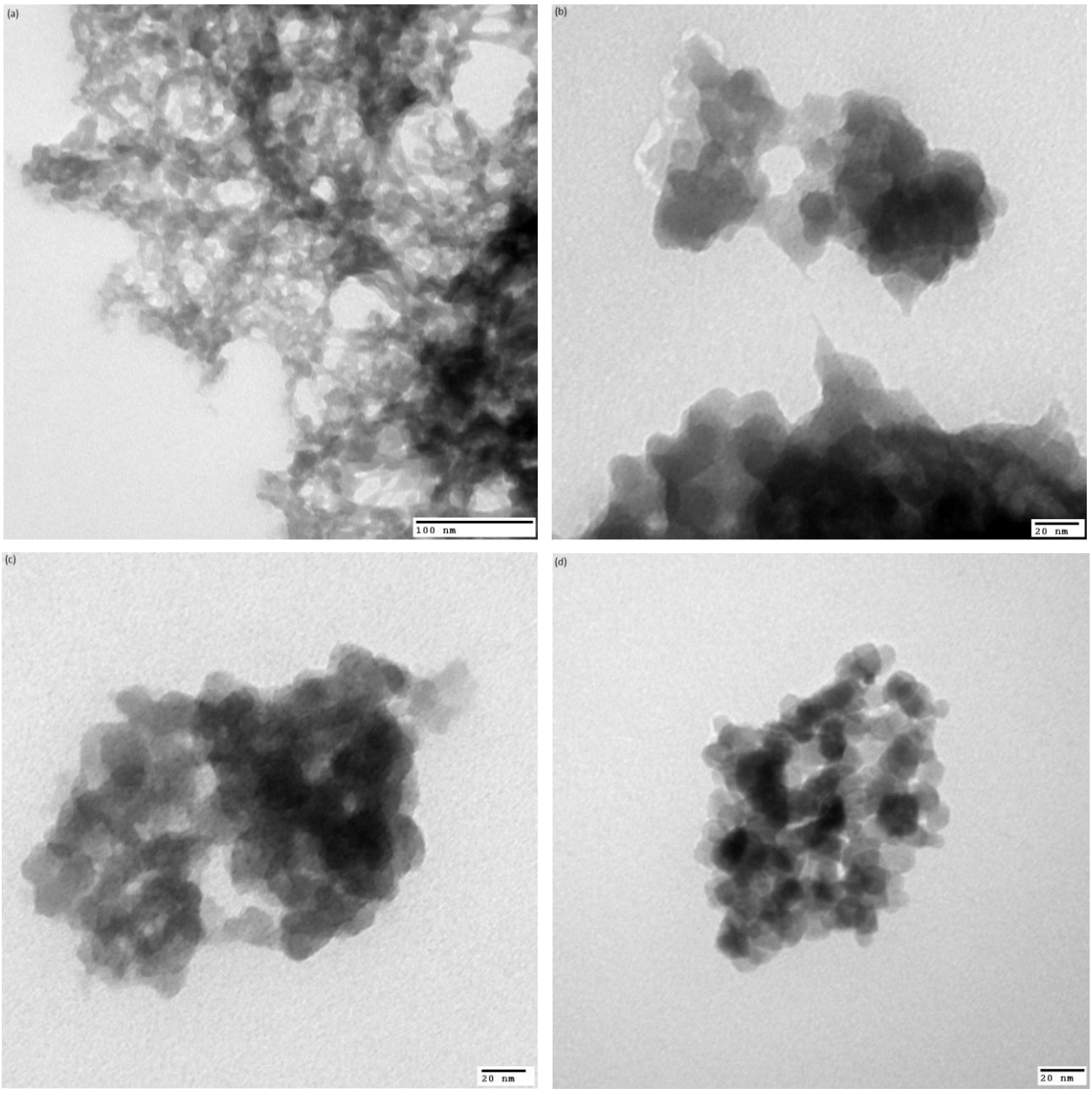

The structure of the bound chromium site is one of the important factors when studying the mechanism of photocatalytic action. There have been several attempts reported in literature to characterize the structure of isolated Cr^{6+} sites on silica. Moisii and co-workers proposed two possible structures for Cr^{6+} sites (Figure 4.7) and confirmed the structure a for their 0.5% Cr loaded silica xerogels using XANES and Raman spectroscopic studies.[19]

Figure 4.7: Possible structures for the bonding nature of chromium sites to silica

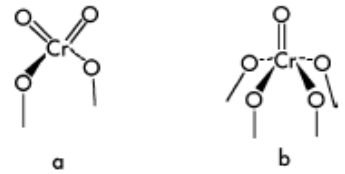

The probability of getting the same binding nature for our 0.5 (mol)% chromium loaded silica system is high due to the similar compositions and nearly same synthesis procedures that were employed during the preparation of materials. Further, it has been predicted in literature, using Pauling's criterion, that there is a high probability of isomorphous substitution, which would yield metal ions in a stable tetrahedral environment surrounded by oxygen atoms. Based on the ratio of ionic radii, ρ, of the cation and anion, the calculated value for titania and oxygen (ρ=0.515) falls out of the acceptable range (ρ= 0.225-0.414) for a tetrahedral coordination due to the larger size of Ti^{4+}(68pm). Therefore, the binding of small tetrahedral Cr^{6+}(44pm) ions to titania matrix is unlikely due to the larger distortion. But Since the ionic radii of Cr^{6+} and Si^{4+}(41pm) are much closer in value, binding of Cr^{6+} into a silica matrix is very favorable compared to Cr^{6+} binding onto titania.[21,22] But, due to the presence of the hexavalent Cr oxidation state in our catalyst, it is unlikely that Cr^{6+} could enter into the bulk lattice of silica due to charge considerations and due to the absence of four siloxy anions. Thus, it is likely that most of the loaded chromium will end up on the surface of the silica material, resulting in a large number of catalytically active sites.[19,20]

4.3.2. Kinetics of photocatalytic degradation

In chapter 3 we discussed the results obtained from basic acetaldehyde photo degradation studies of prepared silica, titania and mixed photocatalytic systems under UV and Visible light. According to the kinetic results obtained, chromium ion loaded silica shows the highest photocatalytic degradation and shows very interesting photocatalytic behaviors under UV and visible wavelengths that only start its activity upon exposure to light confirming photocatalytic nature of the material. Further, according to figure 4.8, which compares the effect of different ratios of silica and titania on kinetic activities under visible light, increasing photo degradation ability is observed when more and more silica is present. This increased photo activity could occur due to the favorable binding of Cr^{6+} in a silica matrix over that of titania.

Turnover number and the rate of catalysis were calculated using kinetic information given in figure 4.8. For calculation purposes the amount of loaded chromium was used as the catalytic active sites assuming that all the loaded chromium involved equally in catalytic oxidation process. Turnover numbers given are only for 100 minutes of catalytic time. Since the catalysts are active after 100 minutes reaction time, turnover numbers can be further improved by carrying out catalytic experiments for prolonged time durations. Thus, turnover numbers for 0.5(mol)% Cr-SiO_2 system and mixed systems clearly indicate that the acetaldehyde degradation process is photocatalytic in nature.

Figure 4.8: Kinetics of photocatalytic degradation of acetaldehyde using 0.5%(mol) chromium loaded photocatalytic systems with varying ratios of SiO_2: TiO_2 under visible light irradiation

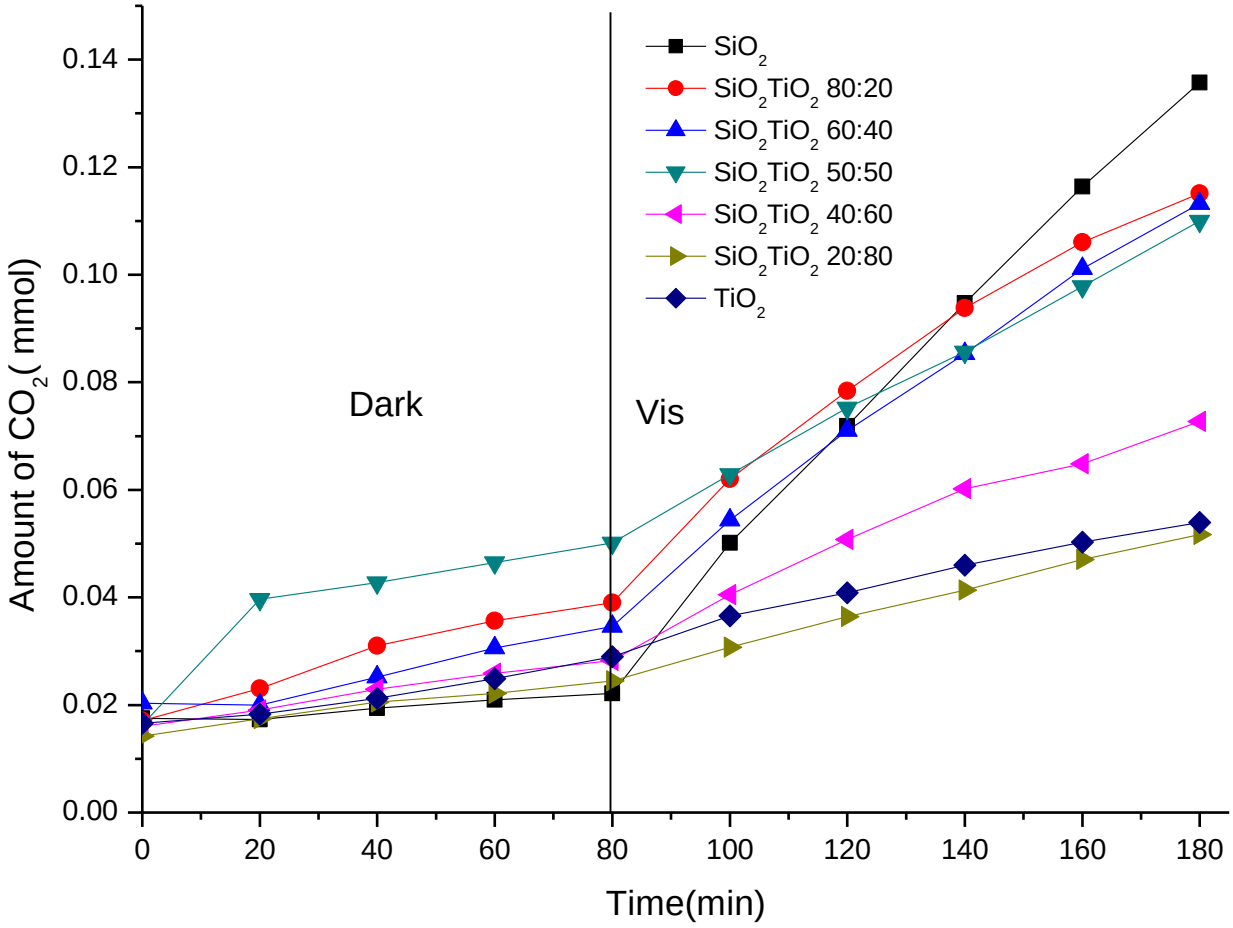

Table 4.2: Turnover numbers obtain for the acetaldehyde degradation under visible light

Catalyst	Turnover Number (First 100 minutes of catalysis)	Turnover Frequency (min^{-1})
0.5(mol)% Cr-SiO_2	17	0.17
0.5(mol)% Cr-SiO_2-TiO_2 (80:20)	11	0.11
0.5(mol)% Cr-SiO_2-TiO_2 (60:40)	12	0.12
0.5(mol)% Cr-SiO_2-TiO_2 (50:50)	8.8	0.09
0.5(mol)% Cr-SiO_2-TiO_2 (40:60)	6.5	0.07
0.5(mol)% Cr-SiO_2-TiO_2 (20:80)	4.0	0.04
0.5(mol)% Cr-TiO_2	3.7	0.04

4.4. Mechanism/s of Photocatalytic Activity

Understanding the mechanism which governs the photocatalytic activity is equally important to the study of the structure of the material, and can lead to predicting better photocatalysts. The study of hydroxyl radical generation upon exposure to UV light is widely used to confirm the mechanism of photocatalytic activity of titania based photo catalysts.[8,23] The observed intense fluorescence peaks at 426 nm indicate the oxidation ability of the generated reactive species which we believe the main component is hydroxyl radicals according to the previous reports. The results obtained from hydroxyl radical detection experiments for both titania and silica based samples studied herein, clearly indicate varying amounts of hydroxyl radicals formed (figure 4.9).

Figure 4.9: Fluorescence spectra obtained for the supernatant liquid of the irradiated a) titania b) silica suspension containing 3×10^{-3} M terephthalic acid at various irradiation periods.

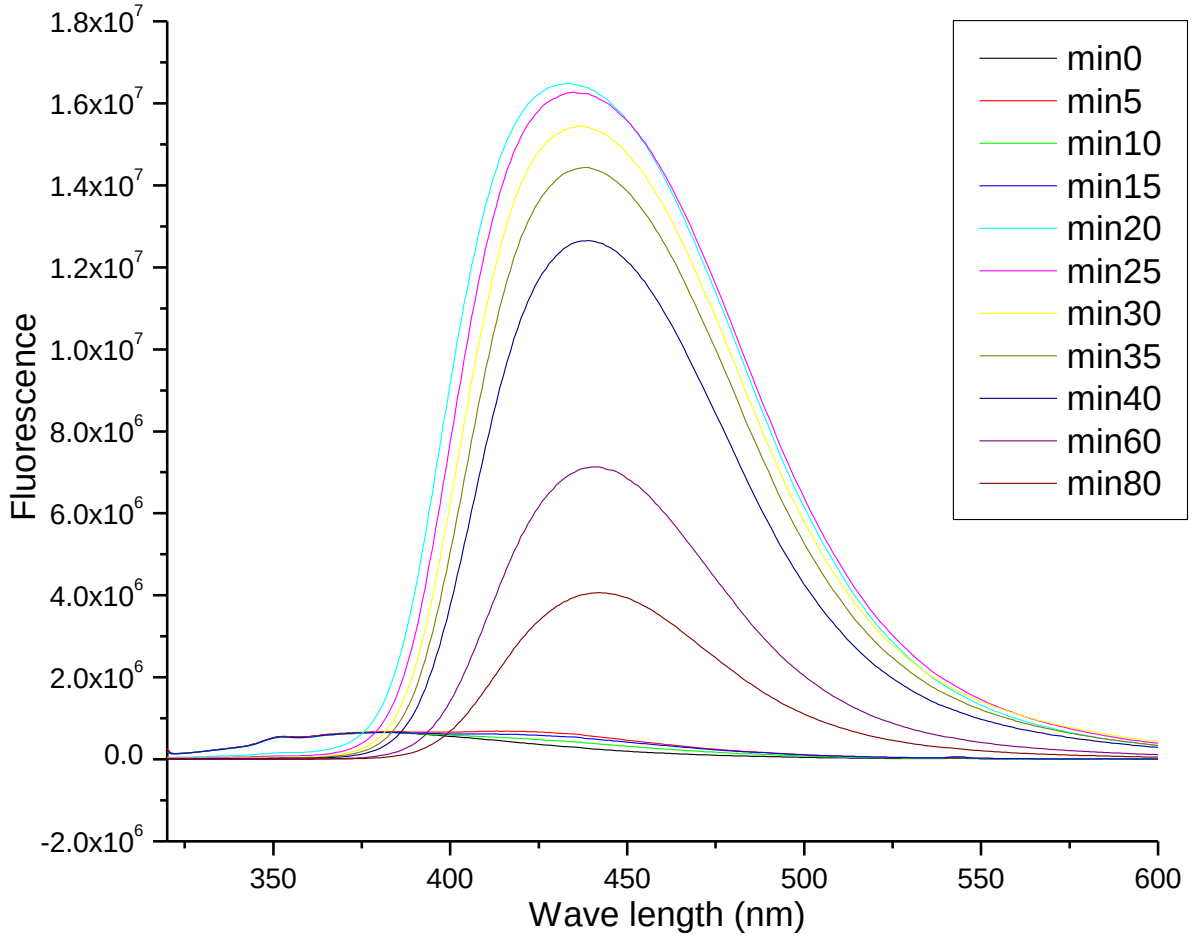

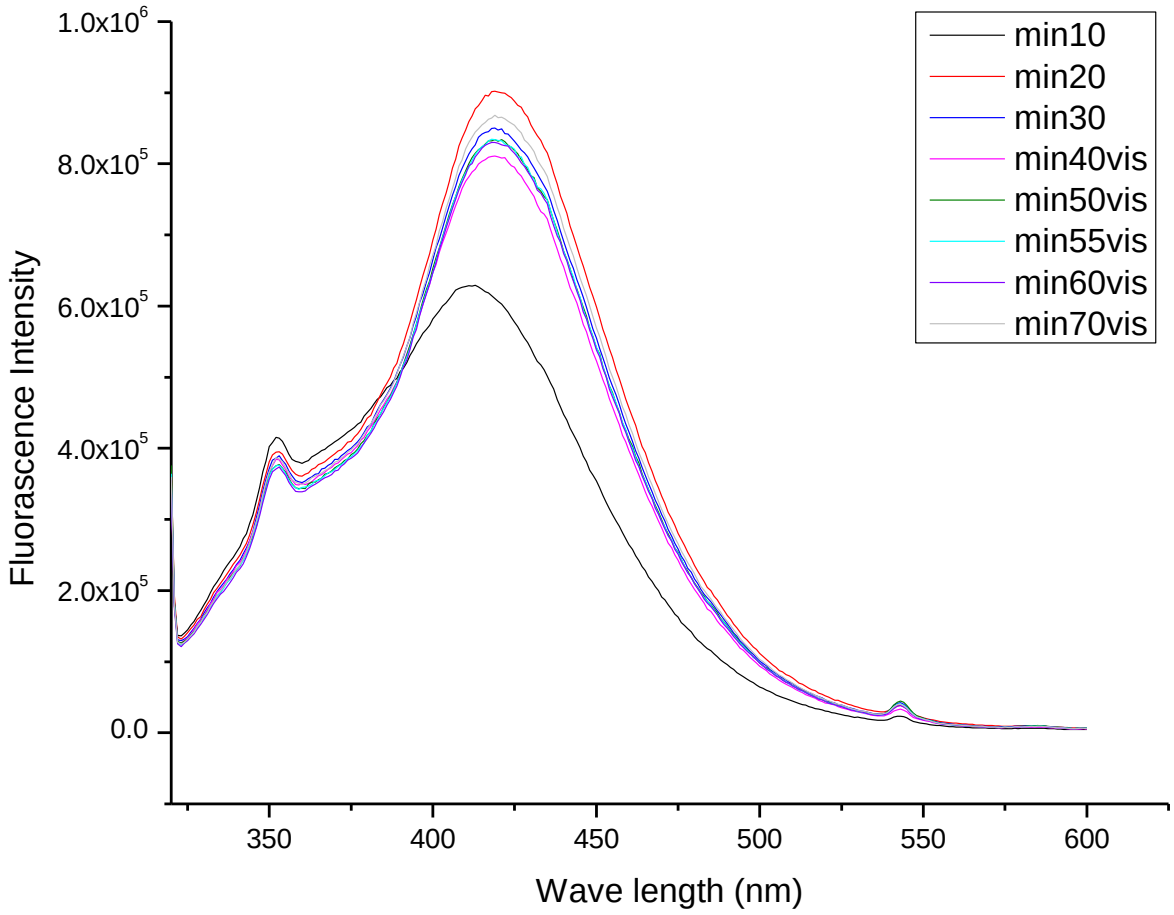

Comparing the results of kinetic studies it is clear that 0.5(mol)% Cr-SiO_2 material is able to perform best in degrading acetaldehyde into carbon dioxide. Further, according to the results obtained the catalytic activity emerges only upon irradiation of light, proving the photocatalytic nature of the catalyst. Since silica is an insulating compound with very large band gap, it cannot be excited with light photons generating reactive electron hole pairs, which is generally considered as the primary process governing any photocatalytic reaction upon exposure to UV/ visible light. But, due to the high photo sensitivity observed in the Cr loaded silica photocatalyst, there must be a different mechanism of photocatalytic degradation.

According to the evidence from UV-visible spectra, TEM and XRD analysis, chromium sites in the silica matrix are highly dispersed. In addition to that, due to the insulating silica support the active photocatalytic sites, which are metal oxide species, are localized and isolated making the photocatalytic process significantly different from that of semiconducting titania.

According to Yoshida and coworkers, a photo excitation process can occur at the molecular orbital level at localized reaction sites when loaded metal oxides are highly dispersed.[6] During

the excitation process, an electron in the ground state of the M-O bond gets excited to an unoccupied singlet orbital. Then depending of the availability of inter system crossing mechanisms, the excited electron could transfer to a triplet state yielding phosphorescence, which has been detected using a photoluminescence spectroscopic method.[6] We were able to observe similar emission fine structure which consist of intensity maxima corresponding to each vibrational energy level of the bond in the photoactive site, in our case (Cr - O). Note our solid state photoluminescence studies (Figure 4.10). According to the results indicated in the figure 4.10 (b), fine structure cannot be identified in photoluminescence spectra of blank samples. The emission peaks present in the blank photoluminescence spectra may occur due to the output of the light source in the instrument as well as outside light sources. Since, the blank samples do not show any fine structures in the region where fine structure is observed for Cr-SiO_2 sample, it is clear that peak patterns arise due to the presence of chromium. Further, the luminescence fine structures are much clear in silica based systems compared to that of titania based system which is a good evidence for higher number of reactive sites in much reactive silica based photocatalysts. Even though we can assign this peaks generally as phosphorescence fine structure due to vibrational bands, in depth studies and calculations are necessary to confirm the assignment. But, in general the observed vibrational fine structure is a clear indication of the localized excitation process taking place during the photocatalytic process.

Figure 4.10: (a) Solid state fluorescence of 0.5(mol)% Cr-SiO_2 catalyst at 300 nm excitation wave length (b) comparison of solid state fluorescence study of 0.5(mol)% Cr-SiO_2, 0.5(mol)% Cr-TiO_2 and blank samples

(a)

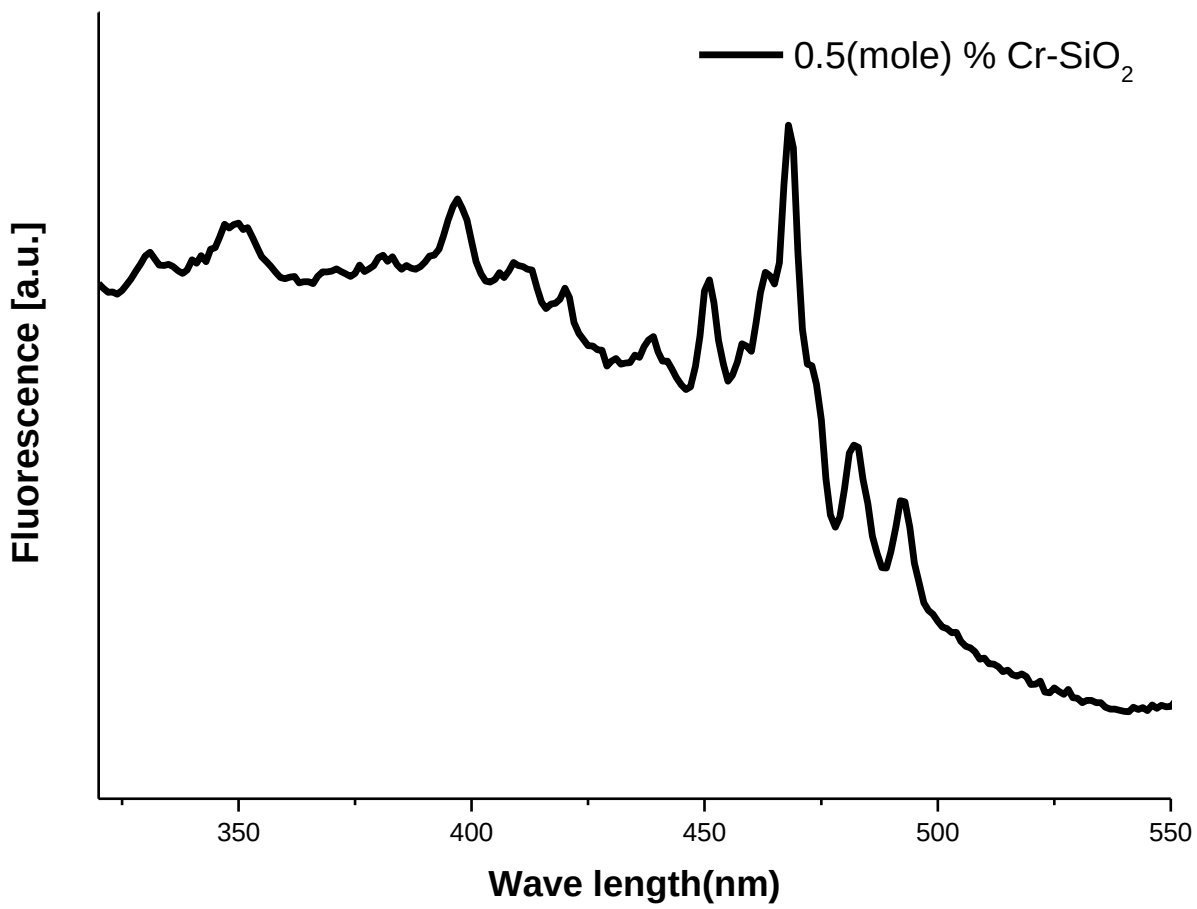

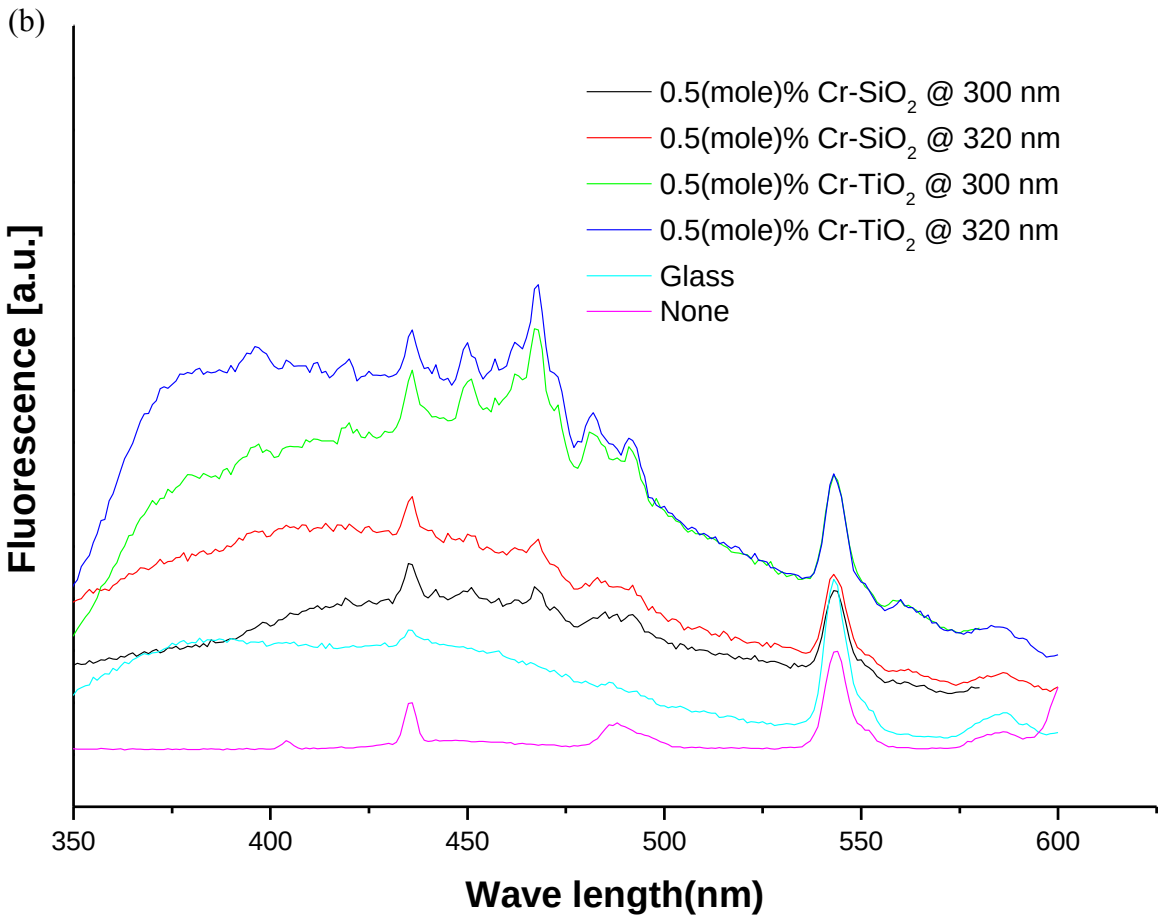

The intervals of peak maxima values obtained for the photoluminescence studies indicate the vibration energy of the photoactive sites. The calculated values are indicated in the table (4.3) below. According to the calculated values does not in agreement with the reported IR values for the Cr=O and the Cr-O-Si bonds reported in literature, but in agreement with IR values of Cr-O bonds of chromium clusters (Figure 4.11). [24-27]

Table 4.3: The intervals of the fine structure on the phosphorescence spectrum of Cr-SiO_2

Maximum Wavelength (nm)	Maximum Wavelength (cm-1)	Gap between adjacent peaks (cm-1)
438	22779.04	-
451	22222.22	606.1
468	21367.52	805.4
483	20746.89	620.6
493	20325.2	421.7

Figure 4.11: Diffuse Reflectance IR spectra of (a) blank silica, (b) 0.5(mol)% Cr-SiO_2 systems

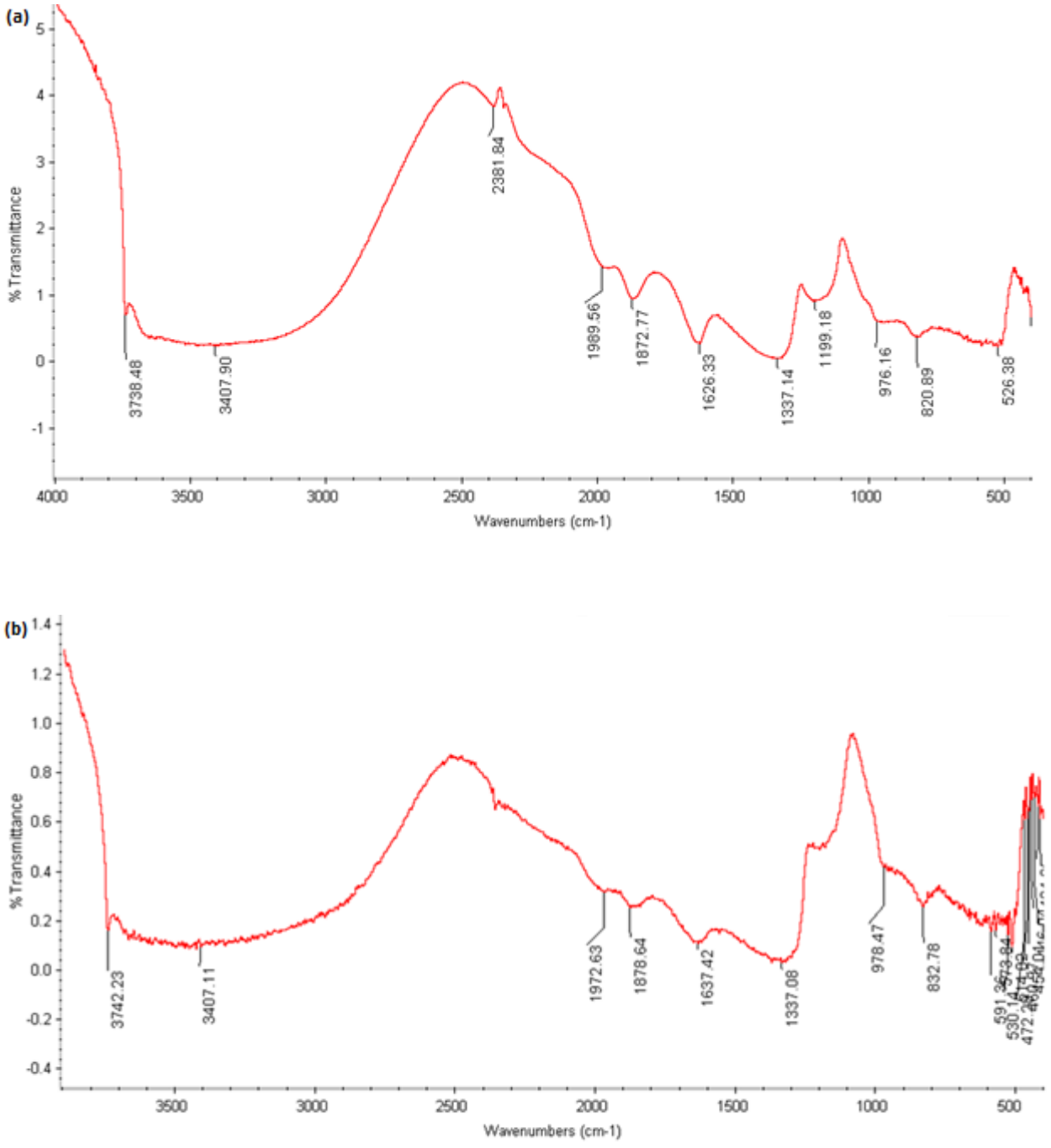

Figure 4.12: Photo excitation in a quantum photocatalyst on which the exiton is localized.[6]

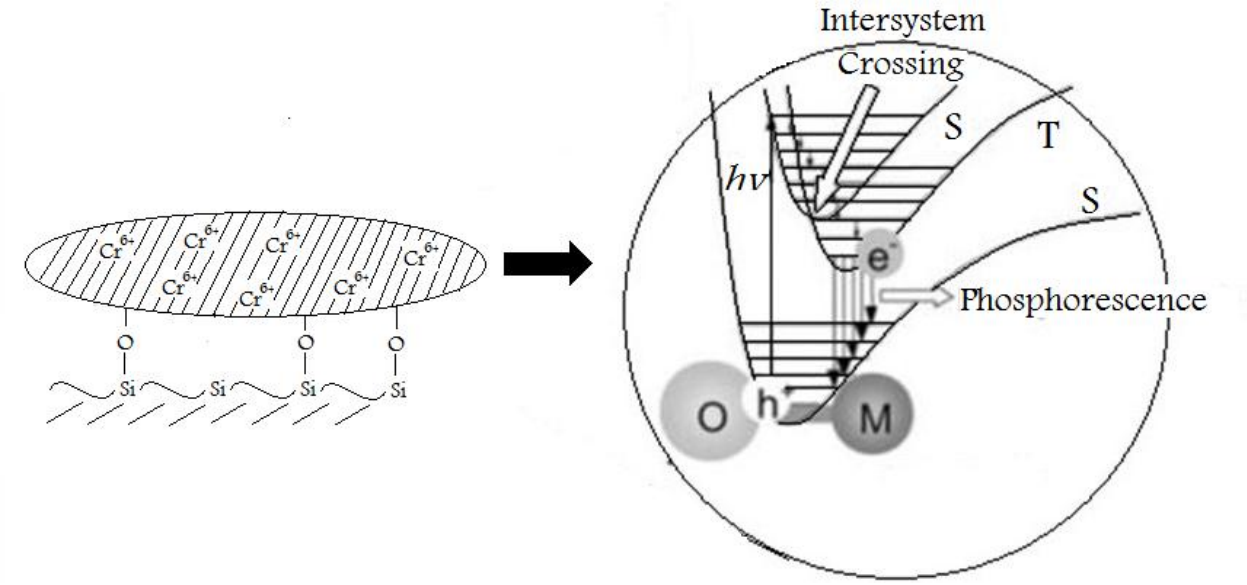

Thus, based on the above literature and experimental data it is clear that the Cr^{6+} loaded silica system is producing reactive electron hole pairs upon light irradiation. Usually, in titania based systems, generation of reactive hydroxyl radicals and oxygen species takes place by reacting surface hydroxyl groups and atmospheric oxygen with photo generated electrons and holes respectively. Similarly, according to the hydroxyl radical experiments carried out for our 0.5(mol)% Cr loaded silica sample, a fluorescence peak around 426 nm provides evidence for hydroxyl radical generation during the photocatalytic reaction (figure 4.10). However, the active site is localized, and all the chemical steps must take place rapidly at that site. Therefore, photo generation of reactive electron and holes in quantum sites of Cr—O, generate positively charged holes, which must react with surface hydroxyl groups present on the silica surface producing reactive hydroxyl radicals. These hydroxyl radicals may be involved in oxidation of acetaldehyde in the presence of oxygen to carry out complete oxidation to produce carbon dioxide.

4.5. Summary

The photocatalytic oxidation ability of chromium loaded silica, titania, and mixed systems were prepared and studied to better understand the localized nature of photocatalysis. The prepared 0.5(mol)% Cr-SiO_2 system shows interesting visible and UV light activities towards acetaldehyde degradation. Even though semiconducting titania based systems are known as

successful photocatalytic materials, insulating silica based systems showed higher oxidation abilities towards complete oxidation of acetaldehyde. Such direct comparison have not been reported before. According to the reported literature, most of the silica based systems were successful for either partial oxidation of organic materials or other reactions, such as polymerization, metathesis reactions, *etc*.[6]

Moreover, the structure and the mechanisms which govern the photocatalysis are compared separately for the chromium loaded titania system as well as for the silica based system. Hydroxyl radical generation studies further support the proposed localized electron-hole pair generation at highly dispersed chromium oxide photo active quantum sites.

4.6. References

1. Coronado, J.M.; Maira, A.J.; Conesa, J.C.; Yeung, K.L.; Augugliaro, V.; Soria, J., EPR Study of the Surface Characteristics of Nanostructured TiO2 under UV Irradiation, *Langmuir*, **2001**, 17, 5368-5374
2. Liang, Y. T.; Vijayan, B.K.; Gray, K.A.; Hersam, M.C., Minimizing Graphene Defects Enhances Titania Nanocomposite-Based Photocatalytic Reduction of CO2 for Improved Solar Fuel Production, *Nano Lett.*, **2011**, 11, 2865–2870
3. Kudo, A., Photocatalysis and solar hydrogen production, *Pure Appl. Chem.*, **2007**, 79, 11, 1917–1927
4. Wang, J.; Uma, S.; Klabunde K.J., Visible light photocatalysis in transition metal incorporated titania-silica aerogels, *Applied Catalysis B: Environmental*, **2004**, 48 151–154
5. Yoshida, H.; Active sites of silica-based quantum photocatalysts for non-oxidative reactions, *Catalysis Surveys from Asia*, **2005**, 9, 1
6. Yoshida, H.; Silica-based quantum photocatalysts for selective reactions, *Current Opinion in Solid State and Materials Science*, **2003**, 7, 435–442
7. Linxiang, L.; Abe, Y.; Nagasawa, Y.; Kudo, R.; Usui, N.; Imai, K,; Mashino, T.; Mochizuki, M. and Miyata, N, An HPLC assay of hydroxyl radicals by the hydroxylation reaction of terephthalic acid, *Biomed. Chromatogr.*, **2004**, 18, 470–474
8. Hirakawa, T.; Nosaka, Y., Properties of $O_2^{\cdot}$— and $OH^{\cdot}$ Formed in TiO_2 Aqueous Suspensions by Photocatalytic Reaction and the Influence of H_2O_2 and Some Ions, *Langmuir*, **2002**, 18, 3247-3254
9. Šnyrychová, I.; Hideg, E., First Application of Terephthalate as a Fluorescent Probe for Hydroxyl Radicals in Thylakoid Membranes, *Springer*, **2008**, 1553–1556.
10. Davis; A.P.; Huang, C. P., Effect of Cadmium Sulfide Characteristics on the Photocatalytic Oxidation of Thioacetamide, *Langmuir*, **1991**, 7, 709-713
11. Koshitani, N,; Sakulkhaemaruethai, S.; Suzuki, Y,; Yoshikawa, S.; Preparation of mesoporous titania nanocrystalsusing alkylamine surfactant templates, *Ceramics International*, **2006**, 32, 819–824
12. Jagtap, N.; Bhagwat, M.; Awati, P.; Ramaswamy, V.; Characterization of nanocrystalline anatase titania: an in situ HTXRD study, *Thermochimica Acta,* **2005**, 427, 37–41

13. Hou, J.; Cao, R.; Wang, Z.; Jiao,S.; Zhu, H., Chromium-doped bismuth titanate nanosheets as enhanced visible-light photocatalysts with a high percentage of reactive {110} facets, *J. Mater. Chem.*, **2011**, 21, 7296–7301,
14. Dvoranová, D,; Brezová, V.; Mazúra, M.; Malati, M.A., Investigations of metal-doped titanium dioxide photocatalysts, *Applied Catalysis B: Environmental,* **2002**, 37, 91–105
15. Weckhuysen, B.M.; Schoonheydt, R.A.; Recent progress in diffuse reflectance spectroscopy of supported metal oxide catalysts, *Catal. Today*, **1999**, 49, 441
16. Weckbuysen, B.M.; De Ridder, L.M.; Schoonheydt, R.A.; Quantitative Diffuse Reflectance Spectroscopy Study of Supported Chromium Catalysts, *J. Phys. Chem.*, **1993**,97, 4156-4163
17. Bensalem, A.; Weckhuysen, B.M.; Schoonheydt, R.A.; In Situ Diffuse Reflectance Spectroscopy of Supported Chromium Oxide Catalysts: Kinetics of the Reduction Process with Carbon Monoxide, *J. Phys. Chem. B*, **1997**, 101, 2824-2829
18. Weckhuysen, B.M.; Verberckmoes, A.A.; Buttiens, A.L.; Schoonheydt, R.A., Diffuse Reflectance Spectroscopy Study of the Thermal Genesis and Molecular Structure of Chromium-Supported Catalysts, *J. Phys. Chem.*, **1994**,98, 579-584
19. Moisii, C.; Deguns, E.W.; Lita, A.; Callahan, S.D.; van de Burgt, L.J.; Magana, D.; Stiegman, A.E.; Coordination Environment and Vibrational Spectroscopy of Cr(VI) Sites Supported on Amorphous Silica, *Chem. Mater*, **2006**, 18,17,3965-3975.
20. Cejka, J.; Corma, A.; Zones, S.; Zeolites and catalysis, synthesis, reactions and applications,*Wiley-VCH:Weinheim*, **2010**, 1, 714
21. Climate Change: The Role of Cities, United Nations Environment Programme (UNEP), **2009**
22. Lim, S.H.; Phonthammachai, N.; Pramana, S.S.; White, T.J.; Simple Route to Monodispersed Silica-Titania Core-Shell Photocatalysts, *Langmuir*, **2008**, 24, 6226-6231
23. Barreto, J.C.; Smith, G.S.; Strobel, N.H.P.; McQuillin, P.A.; Miller, T.A., terephthalic acid: A dosimeter for the detection of hydroxyl radicals in vitro, *Life Sciences*, **1995**, 56, 4, 89-96.
24. Hazedkamp, M.F.; Blasse, G., A Luminescence Spectroscopy Study on Supported Vanadium and Chromium Oxide Catalysts, *J. Phys. Chem.*, **1992**, 96, 3442-3446
25. Yoshida, H.; Chaskar, M.G.; Kato, Y.; Hattori, T., Active sites on silica-supported zirconium oxide for photoinduced direct methane conversion and photoluminescence, *Journal of Photochemistry and Photobiology A: Chemistry*, **2003**, 160, 47–53
26. Ivanova, T.; Gesheva, K.; Cziraki, A.; Szekeres, A.; Vlaikova, E., Structural transformations and their relation to the optoelectronic properties of chromium oxide thin films, *Journal of Physics: Conference Series*, **2008**, 113, 012030
27. Mukherjee, S.; Pal1, A.K.; Bhattacharya, S., Electron paramagnetic resonance and other allied studies of sol–gel derived nanocrystalline chromium oxides in a silica glass matrix, *J. Phys.: Condens. Matter*, 2005, 17, 3385–3403

Chapter 5 - Silica Supported Cobalt Oxide Catalyst; A Novel Nanostructured Catalyst for Destroying Indoor Air Pollutants in the Dark

5.1. Introduction

Quality of indoor air has gained the interest of many researchers as it has become a major issue with the health of humans. There are large numbers of reports about the diseases that occurs due to poor quality indoor atmospheres. Asthma, Lung cancers, respiratory irritations are some of the reported health problems that caused by poor indoor environments. Main pollutants that are responsible for the bad indoor atmospheres can be listed as semi volatile organic compounds, carbon monoxide, biological compounds from mold toxins, etc. Therefore, immediate attention is necessary to improve the indoor air quality.

Many nanostructured catalysts have been reported in the past to address this issue. Among successful nanomaterials that were used for the removal of air pollutants, transition metal ions loaded Silica, Titania and Zeolite materials are good candidates. Mainly, the mineralization of these pollutants is done by means of oxidation degradation of organic matter into relatively non harmful compounds such as carbon dioxide (CO_2).[1]

Cobalt is a well-known oxidation catalytic material that has been widely used for many years. Silicon dioxide (SiO_2) on the other hand is well-known to provide higher surface areas generating large number of absorption sites to facilitate pollutant adsorption and thereby enhance the reactivity of materials. Herein we discuss the collective use of higher surface area silica and catalytic cobalt oxides for the catalytic removal of air pollutants.[2]

5.2. Experimental Methods

5.2.1. Catalyst preparation

Silica (Silicon Dioxide; SiO_2) supported Cobalt aerogel samples were prepared using a well-known aerogel preparation method to prepare higher surface area materials. Tetra ethyl ortho silicate (TEOS) was used as the silica precursor for the synthesis. The catalytic system was prepared by mixing the silica precursor and the dopant, Cobalt(II) acetylacetonate, and co-hydrolyzing together using an acid catalyzed hydrolysis technique. All the chemicals were analytical grade and used without further purification. Samples of various loadings of cobalt ions, 0.5 (mol)%, 0.8 (mol)%, 2(mol)% and 5(mol)%, were prepared to study in depth structural properties and the effect of dopant amount. The samples were prepared using amounts equivalent to the required doping materials and the percentages were calculated with respect to the percent of silica base material assuming all the TEOS converted in to SiO_2 at the end of the process. The calculated dopant material was first dissolved in 140 ml of methanol and 20.0 mL of TEOS solution and stirred well. Then, a mixture of 0.5 ml of water and 2.5 ml concentrated nitric acid was added drop wise to hydrolyze the silica precursor. The solution mixture was then aged for about 15 minutes and then super critical drying was carried out in an autoclave. The autoclave was quickly vented soon after the temperature reached 265 ^oC and the gaseous phase solvent, Methanol, was removed without collapsing the silica network structure. Finally, the resulting powder was calcined in air at 500 ^oC for 2 hours.

5.2.2. Characterization studies

Brunauer-Emmet-Teller (BET) measurements of surface area and pore size distribution of the prepared samples were carried out using a Quantachrome NOVA 1200 gas absorption/desorption analyzer after degassing the samples at 150 ^oC for two hours. Powder XRD analysis of the samples was carried out to determine the crystalline nature of samples using a Scintag-XDS-2000 spectrometer with Cu Kα radiation with applied voltage of 40 kV and current of 40 mA. Samples were scanned 2θ from 0^o to 75^o with a scan rate of 0.5^o per minute. Diffuse reflectance UV-Visible spectra were measured at room temperature in air on a Cary 500 scan UV-Vis-NIR photometer over the range from 200 nm to 900 nm. The sample cell was made of two transparent CaF_2 discs, a Teflon O-ring and screw-type combination in which catalysts were packed between

two discs and the O-ring. Polytetrafluoroethylene (PTFE) powder of 1 μm particle size was taken as a reference material for diffuse reflectance studies.

The compositional studies of prepared systems were done by carrying out elemental analysis experiments using Energy Dispersive Spectrometry using a Scanning Electron Microscope. Detailed study of the loaded cobalt was carried out using a bulk elemental analysis to determine the final amounts of loaded cobalt ions. Bulk elemental analysis was carried out using simultaneous optical systems and axial or radial viewing of the plasma using Perkin Elmer Optima 5300 spectrometer at Galbraith laboratories Inc.

Oxidation state of cobalt before and after catalysis was determined using XPS studies. XPS data were recorded using a Perkin−Elmer PHI 5400 electron spectrometer using polychromatic Al Kα radiation (1486.6 eV). Analysis was carried under vacuum less than 2×10^{-8} Torr. The XPS binding energies were measured with a precision of 0.1 eV. The analyzer pass energy was set to 17.9 eV, and the contact time was 50 ms. the spectrometer was calibrated by setting the binding energies of Au $4f_{7/2}$ and Cu $2p_{3/2}$ to 84.0 and 932.7 eV, respectively. The sample spectra were referenced to the adventitious C 1s peak at 285.0 eV.

TEM studies were performed on a Philips CM100 operating at 100 kV. The TEM samples were prepared by placing a few milligrams of the catalyst in acetone followed by sonication. Then grids were allowed to air dry overnight. The facilities were provided by the Microscopy and Analytical Imaging Laboratory at Department of Biology, Kansas State University.

5.2.3. Kinetic studies of photocatalytic systems

Prepared samples were tested for possible catalytic activities using the primary sample, 0.5(mol)% Co-SiO_2. The kinetics of the degradation was studied using a Shimadzu GCMS-QP 5000 instrument and a glass reactor with a quartz window. Acetaldehyde was used as a model pollutant and the temperature of the glass reactor was maintained at 25 ^{o}C by circulating water in the outer jacket of the reactor during all the kinetic experiments. In a typical experiment 0.10 g of the prepared sample was uniformly placed on the special glass chamber. Then the air filled system was sealed and 0.10 ml of model pollutant was introduced to the bottom of the reactor to avoid any direct contact of liquid acetaldehyde and the photocatalytic material. During the experiment acetaldehyde slowly gets evaporated due to its near room temperature boiling point and gaseous acetaldehyde gets absorbed on to the reaction sites of the catalyst. The progress of

any reaction was detected by injecting 35 µl of gas samples from the sealed reactor to the Shimadzu GCMS-QP 5000 instrument. All the kinetics experiments were carried out at least two times in order to confirm the accuracy of the results and were compared with prepared blank samples, where no dopant elements present.

5.3. Results and Discussion

Prepared cobalt loaded samples were analyzed using powder x-ray diffraction to determine the crystalline nature of the catalysts prepared. According to powder XRD results, a broad peak correspond to amorphous silica was obtained. The 0.5(mol)% Co-SiO_2 sample did not show any crystalline peaks for any possible cobalt oxide crystalline states. This absence of XRD peak patterns can occur due to several reasons, such as fine incorporation of loaded cobalt ions in to the matrix of the system creating no chance of formation of crystalline cobalt states to detect by XRD[3,4], or the amount of crystalline cobalt present in the sample may be below the detection limit of the XRD instrument due to the very small amounts of cobalt precursors used during the synthesis of the system.

Figure 5.1: Powder x-ray diffraction studies of 0.5(mol)% Co-SiO_2 catalyst

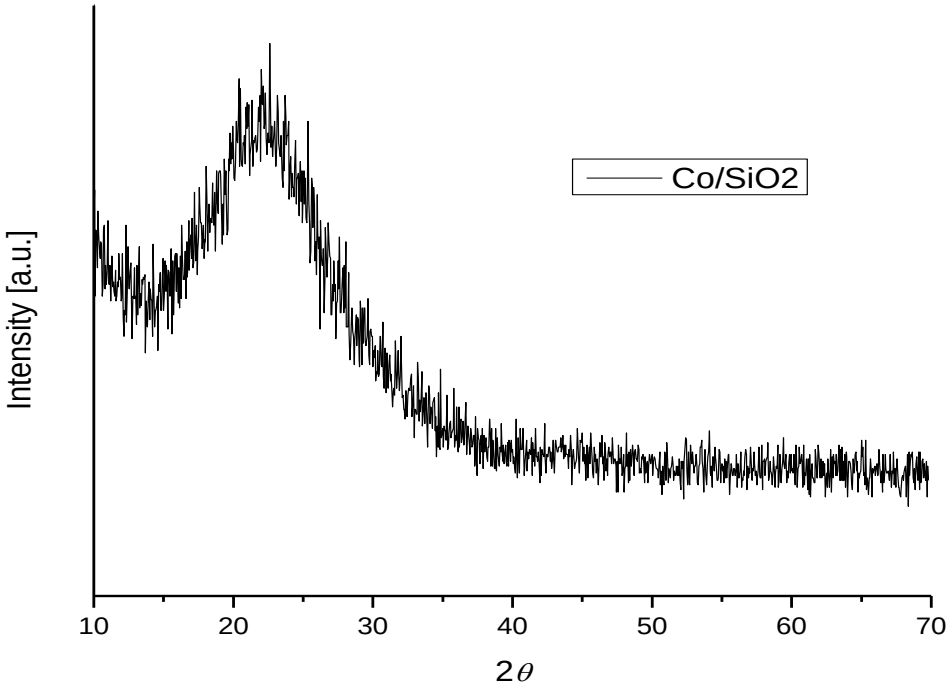

To further study the reasons for absence of any cobalt crystalline phases and to confirm the dispersed nature of cobalt in the silica matrix, further studies were carried out with silica samples with higher loadings of cobalt. The obtained XRD patterns are indicated in the figure 5.2.

Figure 5.2: XRD patterns of 0.5% Co-SiO_2, 0.8% Co-SiO_2, 2.0% Co-SiO_2 and 5.0% Co-SiO_2 catalysts

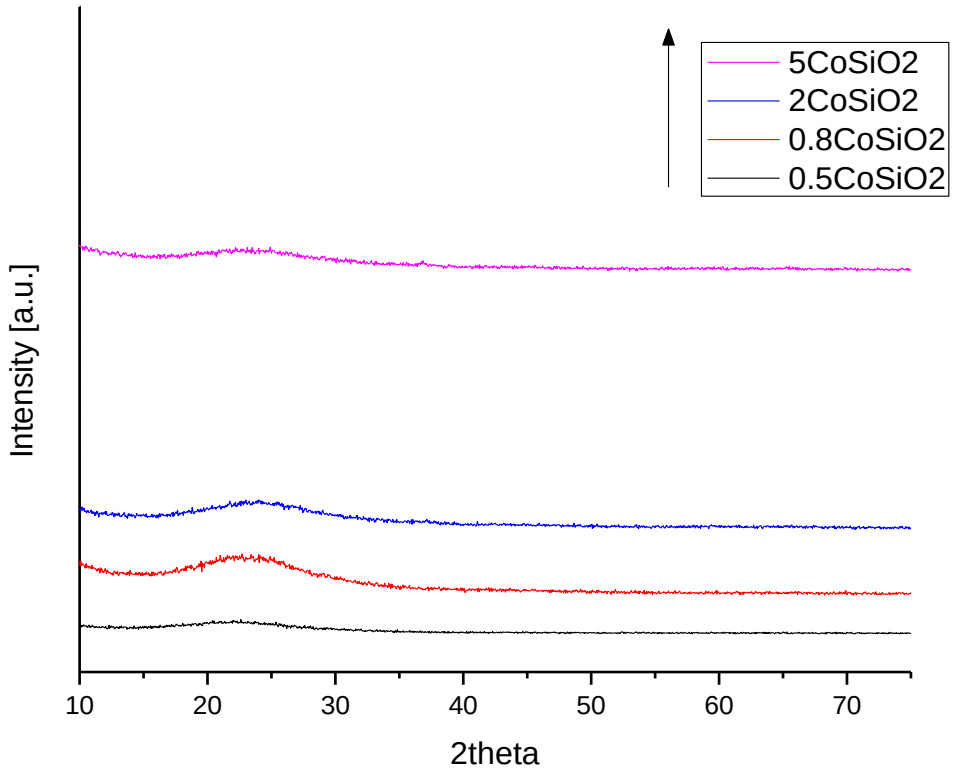

Powder XRD data obtained for the various amounts of cobalt loaded silica samples clearly indicate that there is no observable crystalline peaks present even for the highest loading sample studied which is 5(mol)% Co-SiO_2. This is a good evidence to support the high dispersion of cobalt in the silica matrix. Further, it is clear that the reason for not observing any crystalline cobalt oxide peaks in 0.5(mol)% sample is not due to below detection limit concentrations of cobalt, but due to the actual doping of cobalt in to the silica matrix. Further, these results suggest that the cobalt loaded into silica exist as non-crystalline forms such as cobalt composites with silica or as extremely small crystalline cobalt oxide particles that are undetectable by XRD.[5]

Figure 5.3: (a), (b) TEM images of Blank Silica aerogel, (c) 0.5(mol)% $CoSiO_2$, (d) 2(mol)% $CoSiO_2$, and 5(mol)% $CoSiO_2$

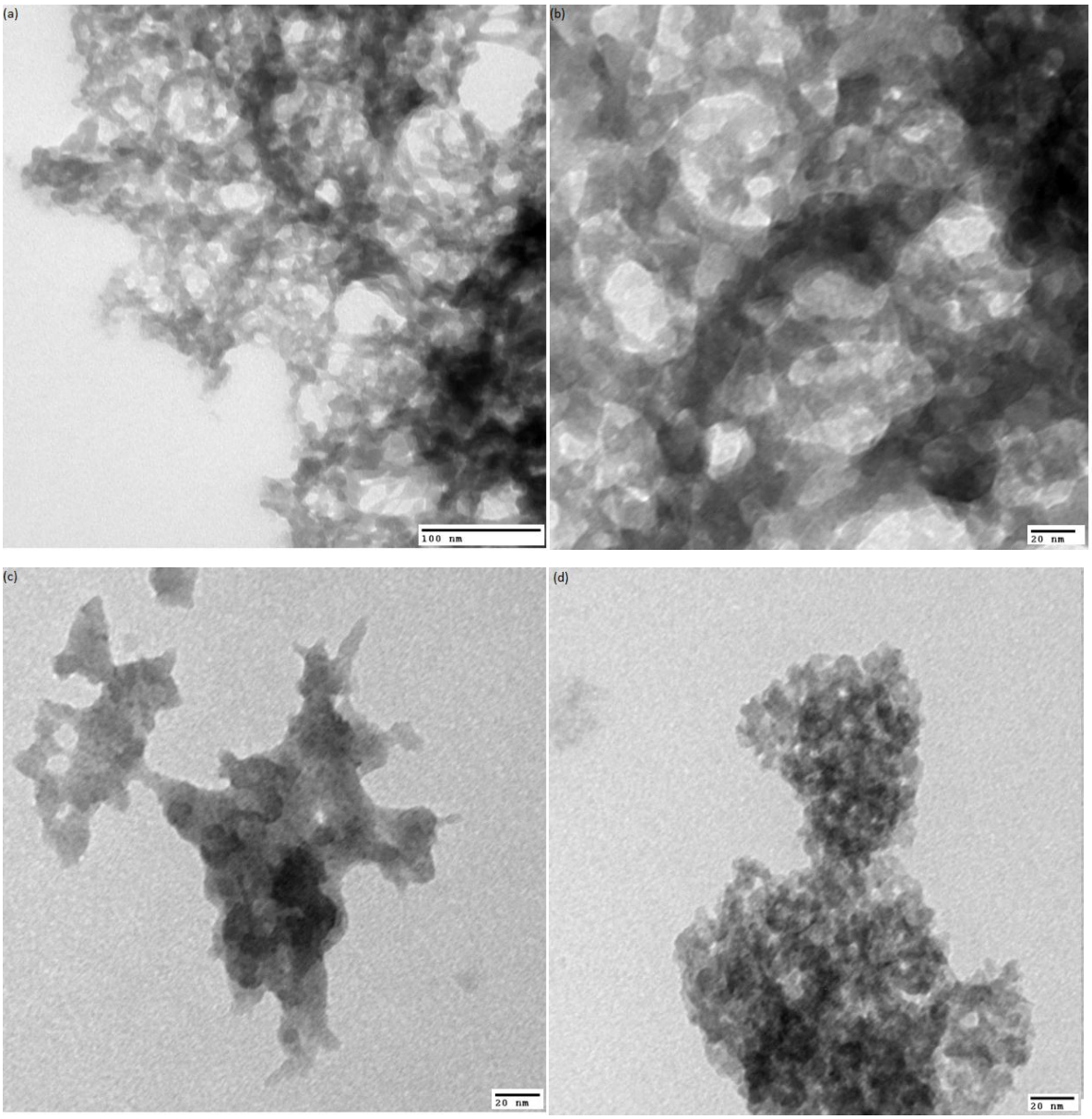

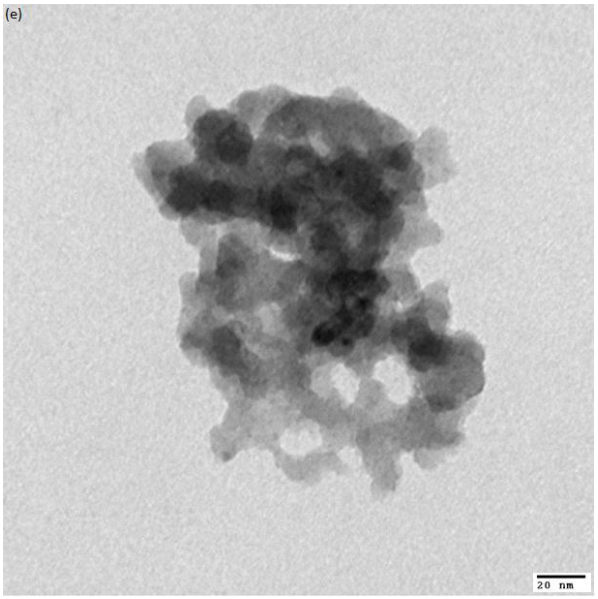

Figure 5.3 shows the TEM micrographs of as prepared blank silica and 0.5(mol)% cobalt loaded silica samples. TEM pictures clearly indicate the mesoporous nature of all the materials and irregular pore structures present in the matrix which is in agreement with very high surface area values we obtained for these silica samples. According to the size determination using TEM, finely dispersed, about 1-2 nm sized dark spots could be observed all over the silica matrix of all the Co-SiO_2 samples we studied (figure 5.3(c), (d) and (e)). Slight increase in the frequency of these dark spots could be observed with increasing cobalt loading confirming the dark spots originates due to loaded cobalt. Furthermore, it is expected to see cobalt sites dark compared to that of silica due to higher electron density of cobalt. Moreover, the presence of these small particles in TEM, but their absence in the XRD spectra suggests that they are not pure cobalt oxide nano particles, but are probably cobalt oxide-silica composites without much crystallinity. [5, 6]

Diffuse reflectance UV-vis spectra indicate peak patterns correspond to cobalt oxide states present in the system with absorptions in 400 nm to 700 nm range with peak absorptions at 520 nm, 581 nm and 648 nm wavelengths. Similar results have been reported by Stanislaw Dzwigaj and coworkers, based on their studies of cobalt catalyst supported on Si and reported that the obtained peak maxima belongs to isolated tetrahedral cobalt species and attributed to $^4A_2 \rightarrow {}^4T_1$ (^4P), $^4A_2 \rightarrow {}^4T_1$ (^4F) and $^4A_2 \rightarrow {}^4T_2$ transitions respectively.[7,8]. An additional shoulder peak is present around 478 nm in our 0.5(mol)% Co-SiO_2 sample. In line with earlier studies this low

intense peak is evidence for octahedral Co^{2+} which is attributed to the $^4T_{1g}(F) \rightarrow {}^4T_{1g}(P)$ transition [9].

UV-vis absorption spectra of pure Co_3O_4 has two characteristic broad peaks around 300 nm -500 nm region with ~400 nm peak maxima which occurs due to charge transfer transitions $O^{2-} \rightarrow Co^{2+}$ and $O^{2-} \rightarrow Co^{3+}$ and Co(III) in an octahedral site: $^1A_{1g} \rightarrow {}^1T_{2g}$, and 600 nm - 800 nm region with 700 nm peak maxima which is usually assigned to Co(III) in an octahedral site:$^1T_{1g} \leftarrow {}^1A_{1g}$.[10-13]. Even though the characteristic second band centered about 650 nm cannot be identified in our spectrum, the broad peak present around 300 nm to 400 nm could be assigned to highly dispersed Co_3O_4 species.[10,11,14]. Furthermore, in accordance with L.F. Liotta and co-workers, Co(II) ions could migrate into the silica lattice forming octahedral and tetrahedral Co(II) sites, as we suspected during our XRD studies,[15] while some of the Co(II) atoms may oxidize to Co (III) during the calcination step carried out in air due to the presence of atmospheric oxygen, giving rise to the broad absorption peak at 300 nm- 400 nm region.[14].

Figure 5.4: Curve fitted DR UV-vis spectra of 0.5(mol)%Co-SiO_2 catalyst

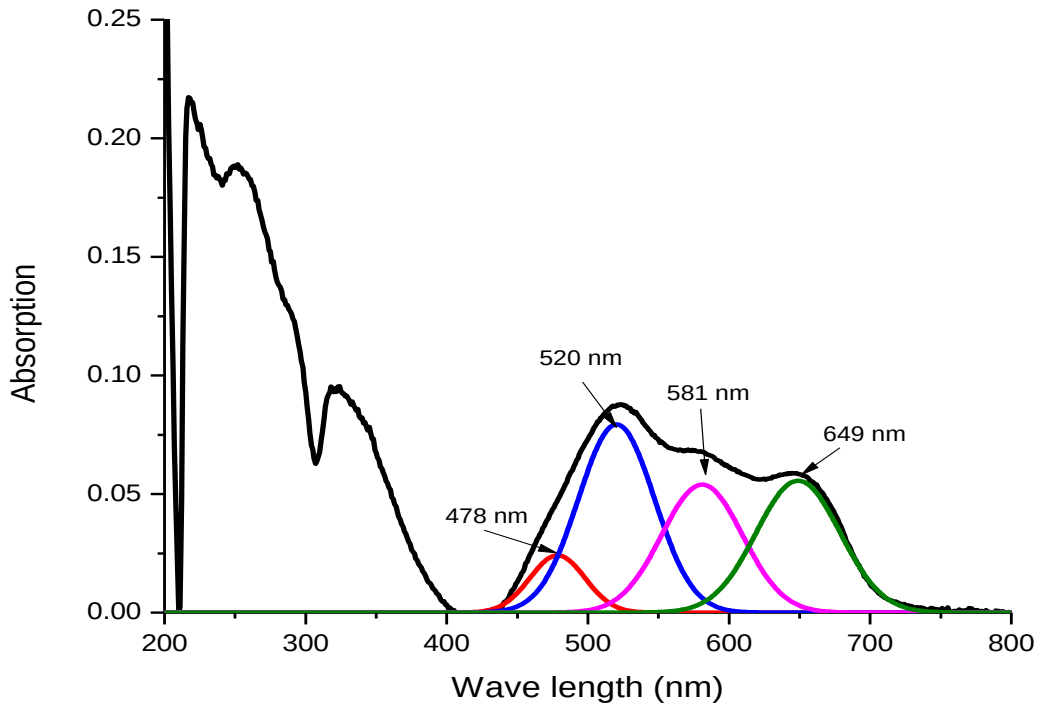

Figure 5.5 shows DR UV-Vis studies carried out for Co-SiO_2 catalyst before calcination, as prepared catalyst, after catalysis with acetaldehyde and two weeks old sample of Co-SiO_2 after

catalysis. The as prepared catalyst has a dark blue color and special textural properties. UV-vis absorption studies show a corresponding peak pattern of the as prepared sample which we discussed earlier in this text. According to further UV-vis studies, the catalyst before calcination has a crude absorption pattern due to the presence of various oxidation states and left over precursor materials. During the calcination, the catalyst seems to generate corresponding active state which is responsible for the catalysis as evidenced by UV-vis spectra obtained for the as prepared catalyst. But, upon exposure to the pollutant the catalyst changes its color from dark blue to dark green instantly. This color change could occur due to the absorption of acetaldehyde or due to some changes in the oxidation state of the cobalt due to catalytic activity.

One interesting feature of 0.5(mol)% Co-SiO_2 catalyst is its ability to re-gain its original color and texture spontaneously within about two weeks after catalytic reaction. Studies carried out later revealed that the catalyst could be regenerated quickly simply re-calcining the reacted sample. UV-Visible spectra in figure 5.5 clearly show the regeneration ability of the catalyst which is an added advantage of reusability of the catalyst.

Figure 5.5: DRUV-vis spectra of (a) 0.5(mol)%Co-SiO_2 sample before calcination, (b) after calcination at 500 ^{o}C, (c) After catalytic reaction upon exposure to acetaldehyde, (d) re-calcined sample after catalysis.

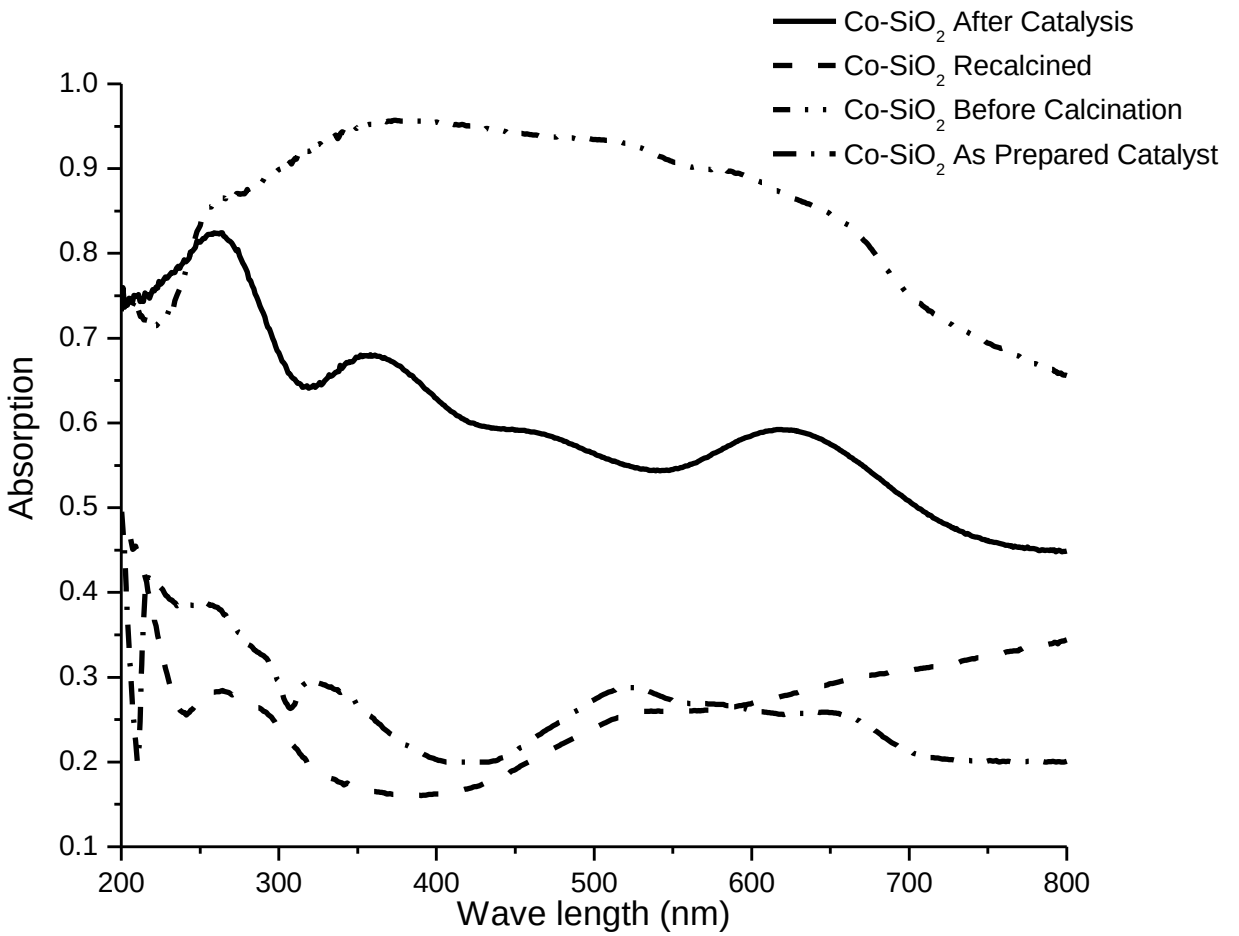

The 0.5(mol)% Co-SiO_2 sample was characterized using XPS spectroscopy in order to further confirm the electronic states and the environment of cobalt present in the as prepared system and to study any changes of oxidation states due to the catalytic oxidation process.[16]

After careful analysis of obtained XPS spectra, characteristic Cobalt $2P_{3/2}$ and $2p_{1/2}$peaks could be identified for both samples. But, these spectral peaks are common for all the possible cobalt states. Thus, a more detailed analysis is important to understand the real state of cobalt. Table 1 gives the binding energy of the Co $2p_{3/2}$ peak and the difference in binding energy between the Co $2p_{1/2}$ and the Co $2p_{3/2}$ peaks of possible cobalt states.[17]

Table 5.1: XPS binding energy values for known cobalt oxides [17]

Sample	Binding Energy (eV) of $2p_{3/2}$	ΔE (Co $2p_{1/2}$ − Co $2p_{3/2}$) (eV)
Metallic Cobalt	777.8	15.0
CoO	780.5	15.7
Co_3O_4	780.1	15.0

The experimental value obtained for the binding energy difference between two main peaks is in good agreement with the ΔE value of Co(II) reported in the table 1 in both as prepared sample and after catalysis. Both samples show spectral peak splitting of 15.8 eV indicating the presence of Co(II) state both before and after the catalytic process.[17,18] Satellite peaks can be identified in both cases as well. According to the reported XPS data, satellite peaks positioned at nearly 6 eV above the main peaks Co $2p_{3/2}$ and Co $2p_{1/2}$ indicates the presence of Co(II).[18,19] On the other hand, Satellite peaks are not present in Co 2p spectrum of normally diamagnetic and low-spin Co(III) in Co_2O_3. But, Co_3O_4 is a combination of the two oxides CoO and Co_2O_3, its spectrum is usually described by the combination of the contributions of these two oxides with a ratio Co(II):Co(III) =1:2. Therefore, Co_3O_4 species also produce satellite peaks with nearly 6 eV above the main peaks making it difficult to distinguish between CoO and Co_3O_4 states. But, the intensity of satellite peaks in Co 2p spectrum of Co_3O_4 is expected to be low due to lower amount of Co(II) present in Co_3O_4 state while CoO state 100% Co(II).[19]

The XPS spectra of Co 2p region on as prepared catalyst have lower Co $2p_{3/2}$ electron binding energy than the reported value of free Co_3O_4 and the binding energy difference listed in the table above (ΔE (Co $2p_{1/2}$ − Co $2p_{3/2}$)) does not match the ΔE value of Co_3O_4. But, careful comparison of XPS spectra obtained before and after catalysis shows increase intensity in the satellite peaks for the sample after the catalysis process. Therefore, consistent with the above explanation about the satellite peaks of Co_3O_4 and CoO we can conclude that some of the Co(III) sites present in the as prepared catalyst has reduced into Co(II). Moreover, this result confirms DRUV-vis observations about Co(III) species present in the system and give evidence about the active catalytic site of the 0.5(mol)% Co-SiO_2 catalyst.

Figure 5.6: (a)Curve fitting of XPS Co 2p spectrums of as prepared Co-SiO_2 catalyst. (b) Curve fitting of XPS Co 2p spectrums of Co-SiO_2 after catalysis. Satellite peak intensity increase significantly after the catalytic process

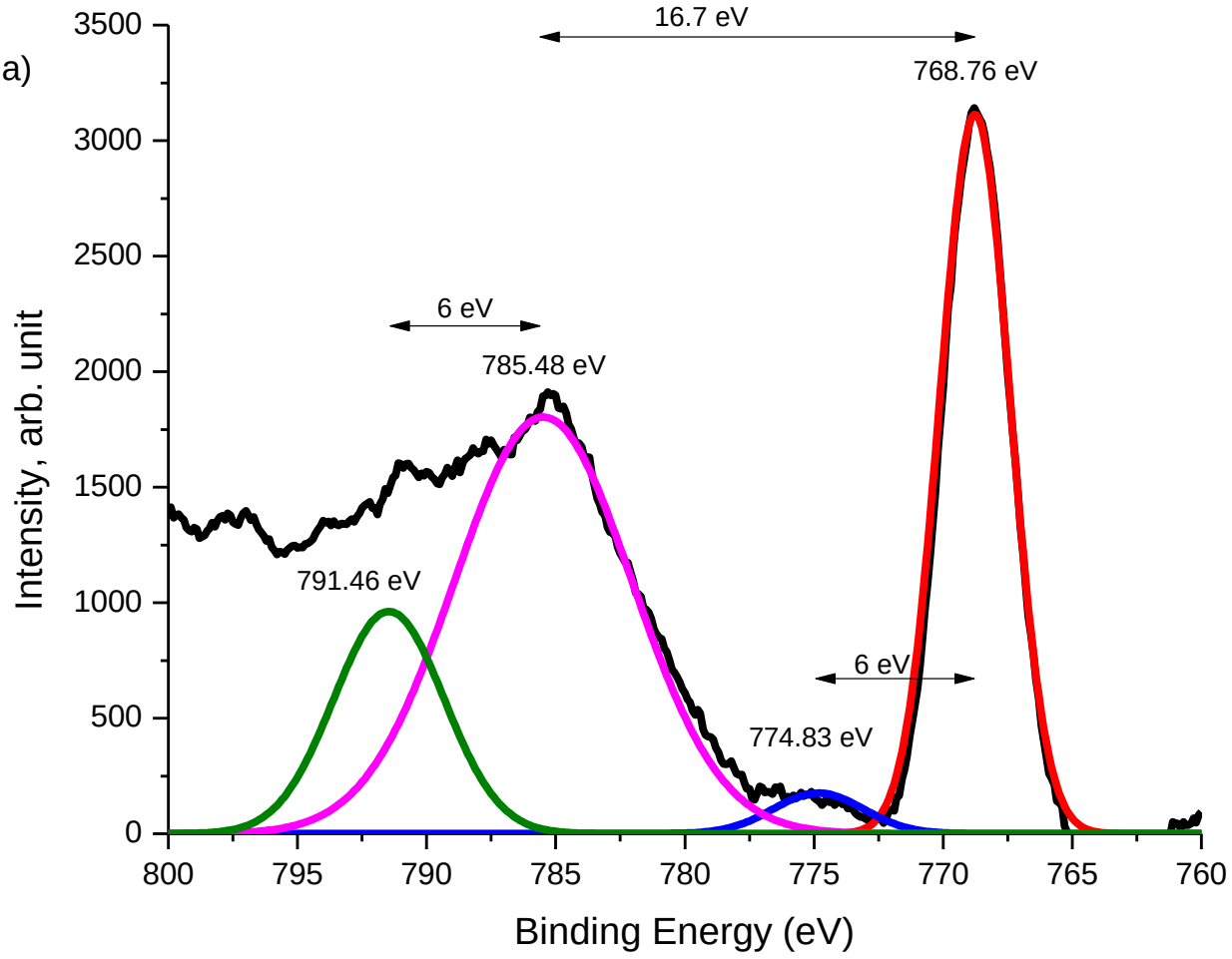

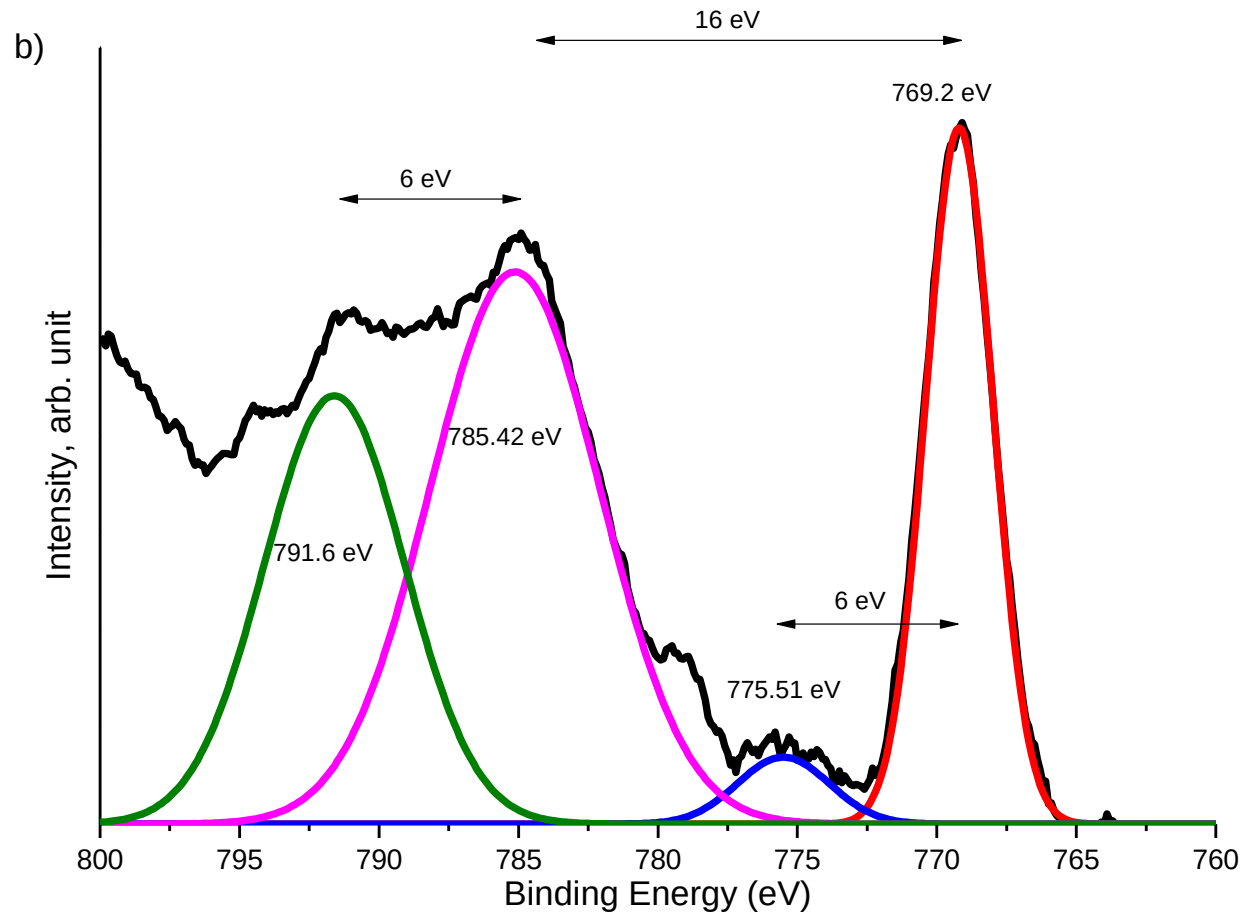

5.3.1. Kinetics of catalytic degradation

As discussed earlier in chapter 3, 0.5(mol)% cobalt loaded silica system show interesting dark catalytic activity. The catalyst does not require any light source to initiate or maintain the reaction. One interesting observation unique to the Co-SiO_2 catalyst is conversion of almost all the acetaldehyde present in the system into CO_2 within first 40 minutes of the reaction. But, after the first 40 minutes of the reaction no additional CO_2 production occurred. This can be due to two main reasons; lack of reactants or the catalyst deactivation. According to reaction scheme (1), continuous supply of oxygen is important to continue produce CO_2. But, the reactor system used for the kinetic studies is a closed system and has a limited amount of oxygen. To study the reason for CO_2 leveling off, several dark catalytic experiments were carried out by injecting more acetaldehyde and oxygen. The results are shown in figure 5.7.

Figure 5.7: Detailed kinetic studies of 0.5(mol)% Co-SiO_2 system with (a) added acetaldehyde and (b) added oxygen

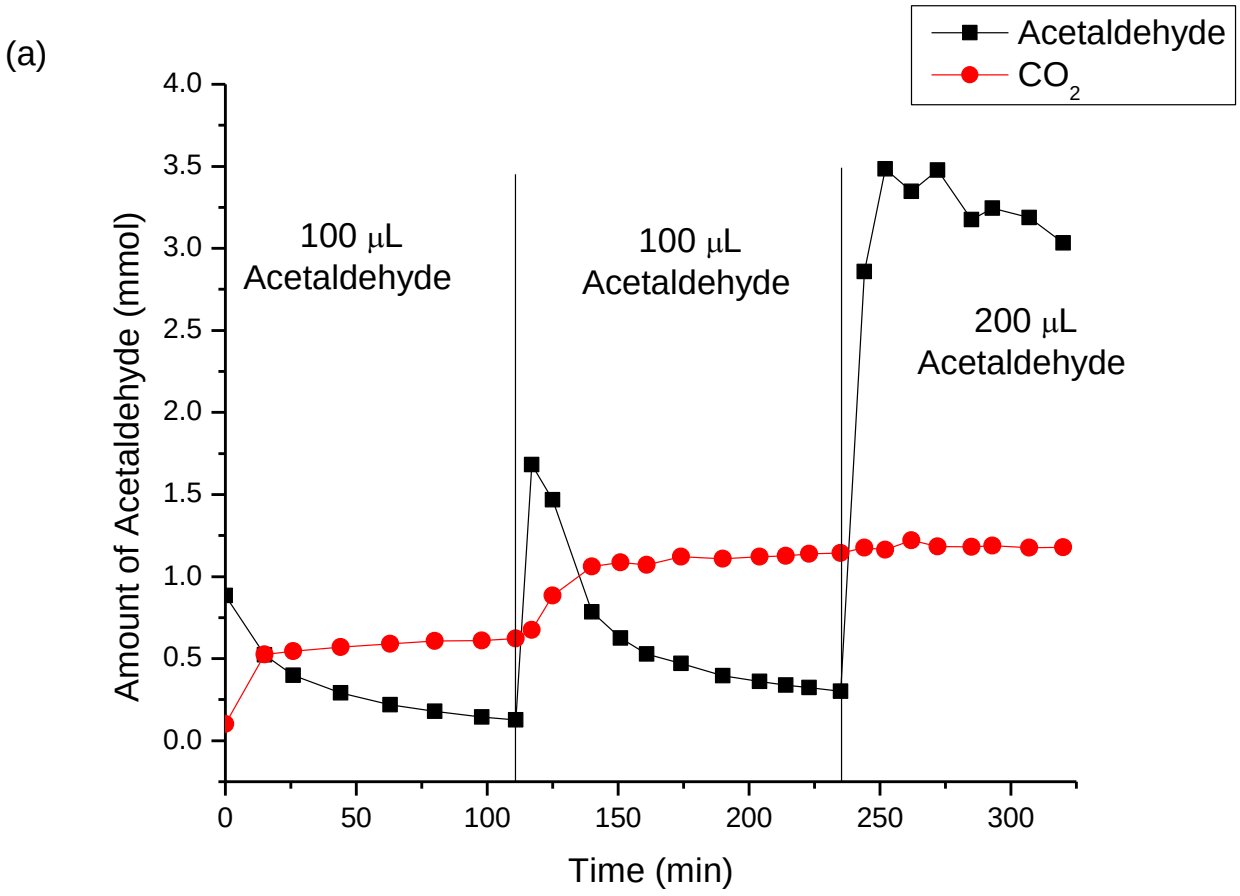

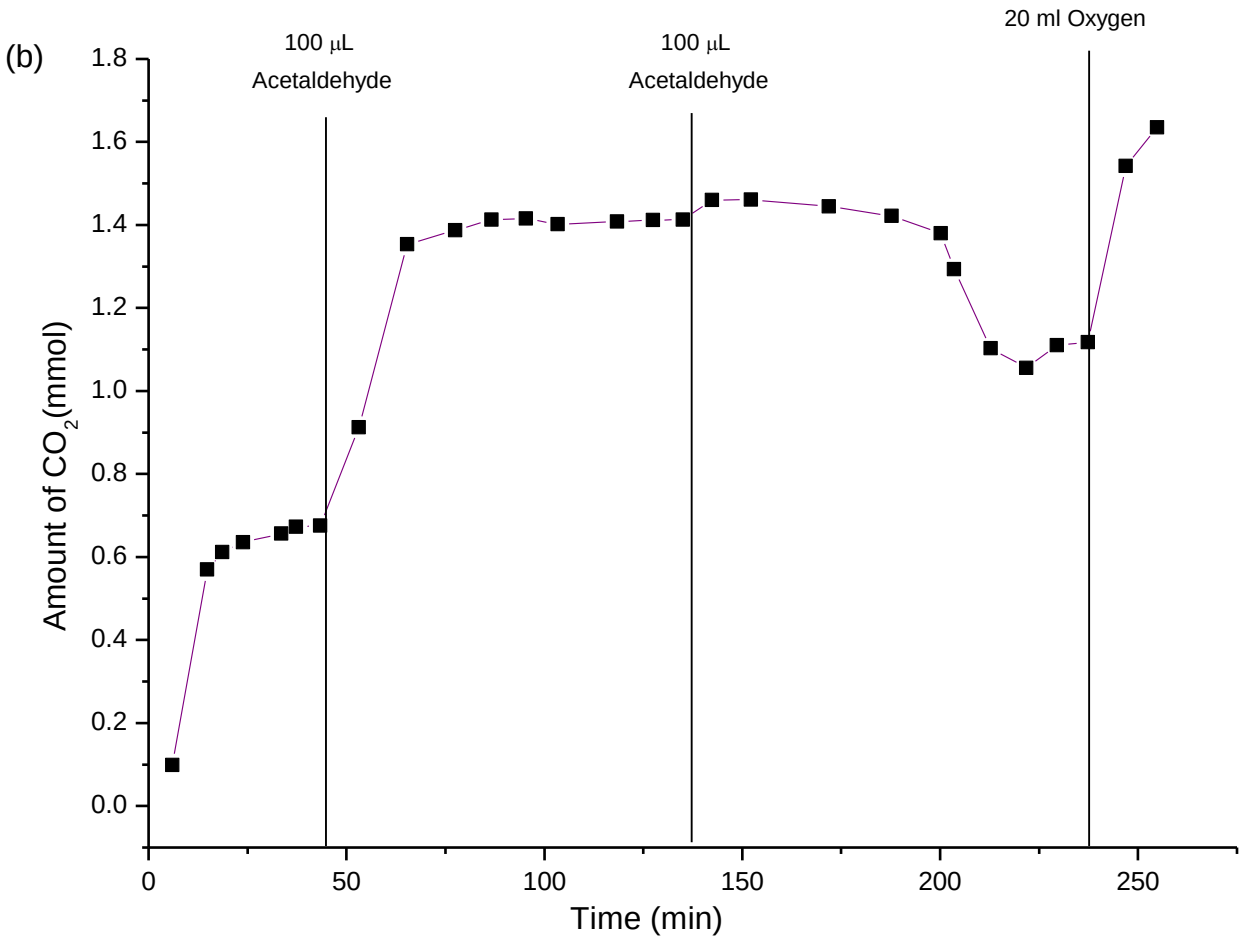

According to Figure 5.7, the reason for the carbon dioxide leveling off is not the poisoning of the catalytic sites but the lack of reactants. Detailed study of figure 5.7(b) shows that after the first catalytic cycle when acetaldehyde is introduced into the system, CO_2 production doubled and again leveled off. Since the reaction stopped after reaching nearly double the amount of CO_2, another 100 μL of acetaldehyde was introduced to observe the catalytic performance (figure 5.7 (b)). But, the third cycle did not produce an equal amount of CO_2. Even though another 100 μL of acetaldehyde was added, no increase in carbon dioxide could be observed. But, when 20 mL of pure oxygen was introduced, the system started producing CO_2 again.

The catalytic performance of Co-SiO_2 catalyst was further studied to estimate the total amount of acetaldehyde that it can convert into CO_2. During this study, the same Co-SiO_2 sample was used throughout the experiment. After constant CO_2 levels were obtained, the reactor set-up was opened and flushed with air to refresh the system and re used the same catalyst with new 200 μL acetaldehyde sample. The results obtained by this study are indicated in the figure 5.8.

Figure 5.8: catalytic cycles of 0.5(mol)% Co-SiO_2 catalyst for acetaldehyde oxidation (13 cycles over three days)

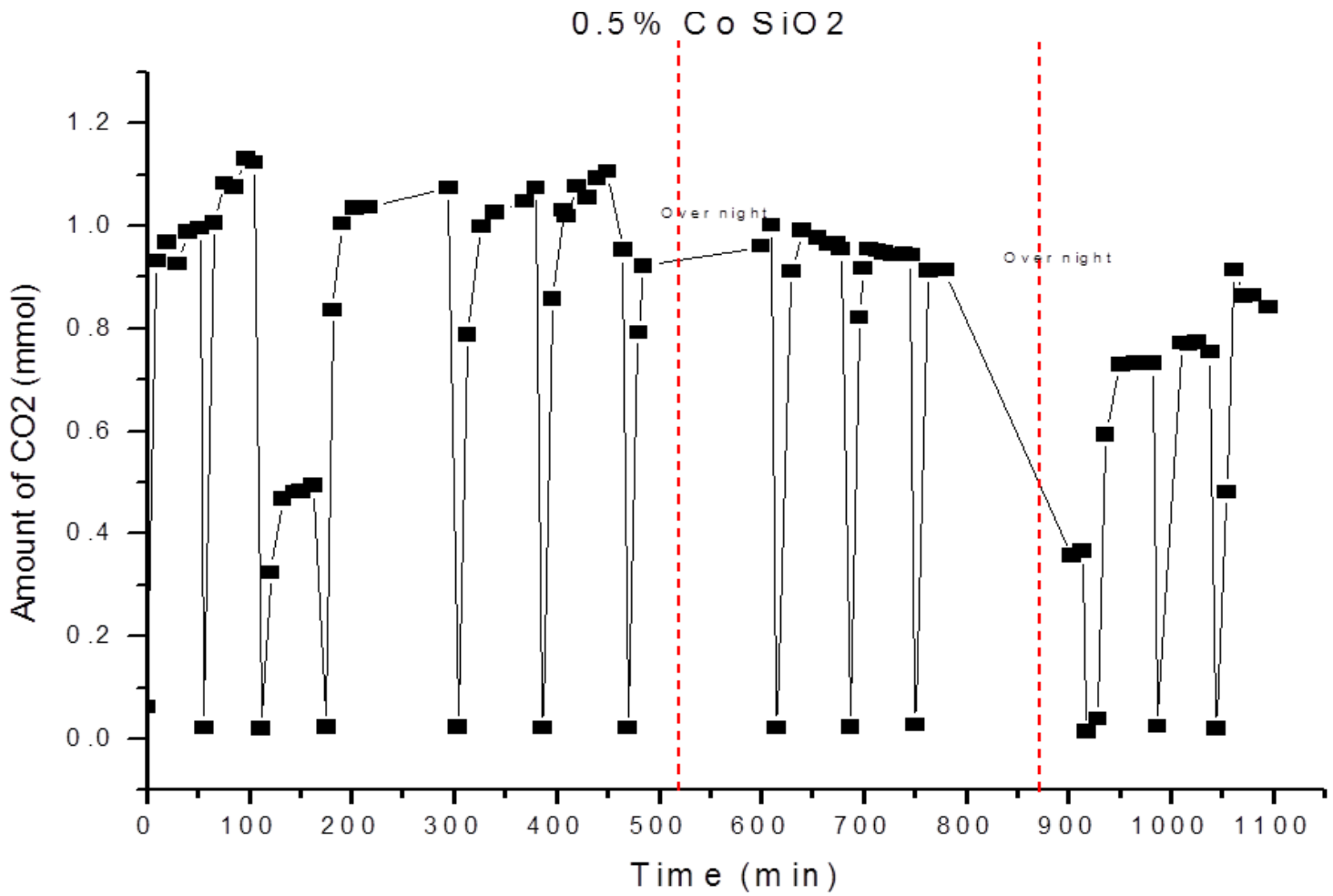

The results show that the catalytic activity of Co-SiO_2 upon degradation of acetaldehyde is extremely fast and stayed active throughout all the 13 reaction cycles that were studied. This whole experiment was carried out continuously for three days. The catalyst remained active, and CO2 production continued, with a small decrease in the third day. Turnover number and the rate of catalysis was also calculated using the experimental data and discussed earlier in the chapter 3.

After confirmed strong catalytic activity of Co-SiO_2 catalyst towards acetaldehyde, a new set of experiments were carried out to study the activity of the same catalyst on degradation of other types of pollutants which are much more difficult to oxidize compared to that of acetaldehyde. Therefore, catalytic oxidation of series of aldehydes, propanaldehyde, 2,2-dimethylpropanaldehyde, and benzaldehyde, was studied using Co-SiO_2 catalyst.

Figure 5.9: Catalytic degradation of propanaldehyde.

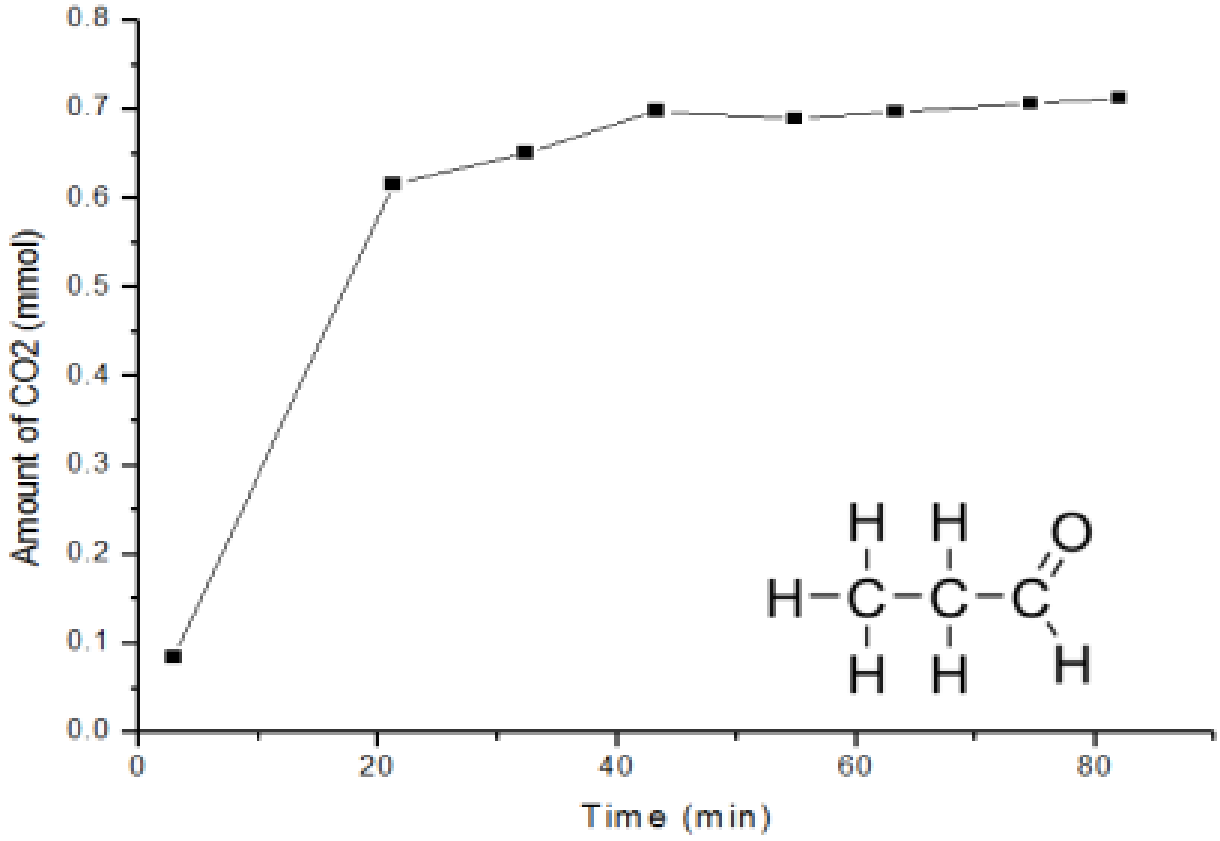

Figure 5.10: Catalytic degradation of tert-butyl aldehyde as followed by CO_2 evolution.

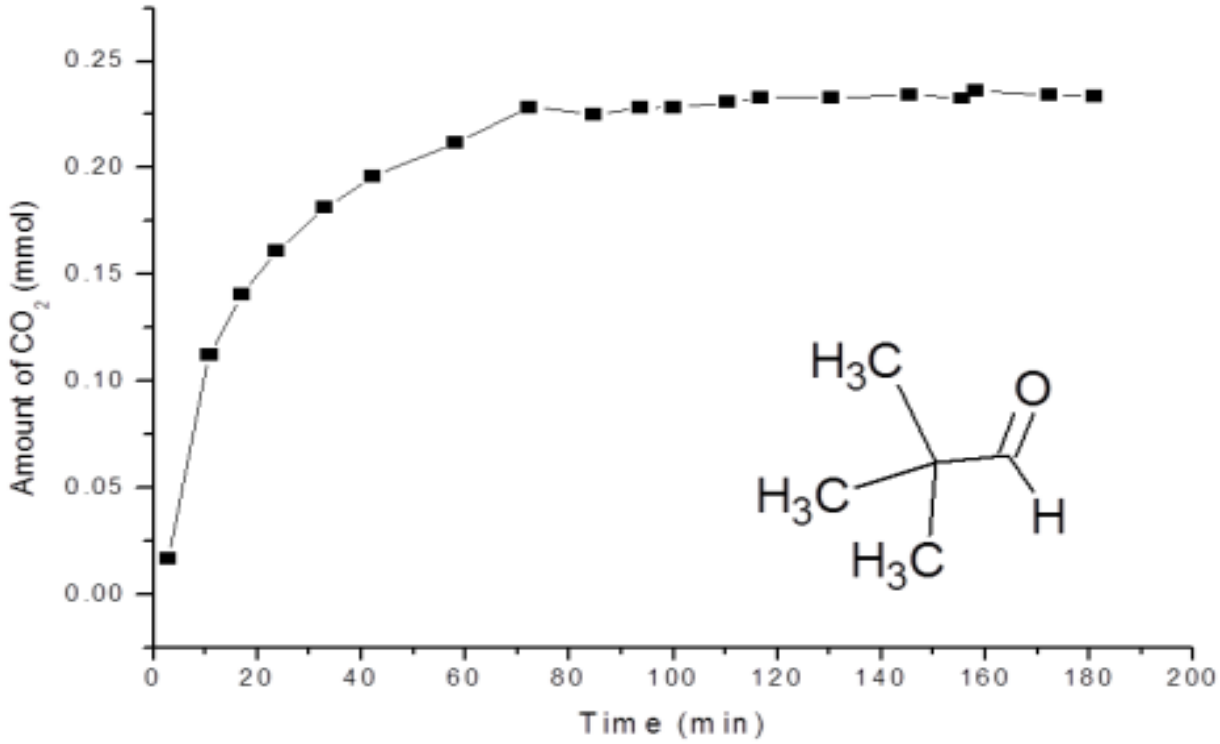

Figure 5.11: Catalytic degradation of benzaldehyde as followed by CO_2 evolution.

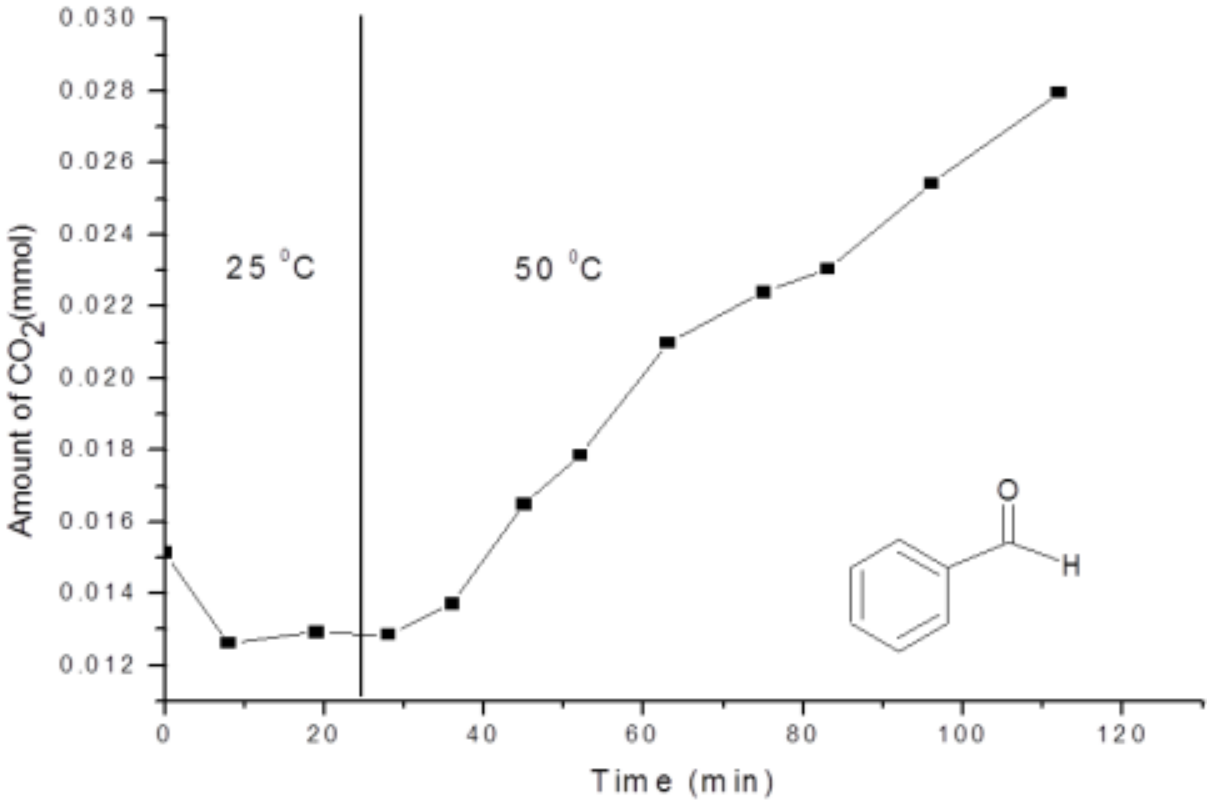

The results obtained are indicated in figure 5.10 above. The amount of CO_2 produced was less compared with that of acetaldehyde. However, the catalyst was moderately active and only benzaldehyde was resistant. But, when compared to acetaldehyde, all the other model pollutants have higher boiling points which are an important factor in our system design. In order to oxidize the pollutant, it must be able to get into the gaseous phase in order to contact the catalyst surface. Thus, when benzaldehyde was studied at slightly elevated temperature (50 ^{o}C), CO_2 production increased with time.

5.4. Mechanism of catalytic activity

It is important to understand the mechanism of the catalytic cycle of the Co-SiO_2 catalyst in order to further improve the catalyst and enhance performance. More studies are probably needed, but a general mechanism can be proposed based on the evidence available (Figure 5.12). According to our characterization studies using XPS and UV-Vis data, cobalt as Co(II) and Co(III) are both present. It has been shown earlier that both Co(II) and Co(III) oxidation states have ability to work as reactant binding sites. According to the studies carried out by Jansson and co-workers, Co(III) plays the active role in absorbing CO, while, Pollard and co-workers claimed the absorption of CO onto both Co(II) and Co(III) sites in Co_3O_4 clusters based on their IR studies.[20-22]

Figure 5.12: General mechanism of the 0.5(mol)% Co-SiO_2 catalyst

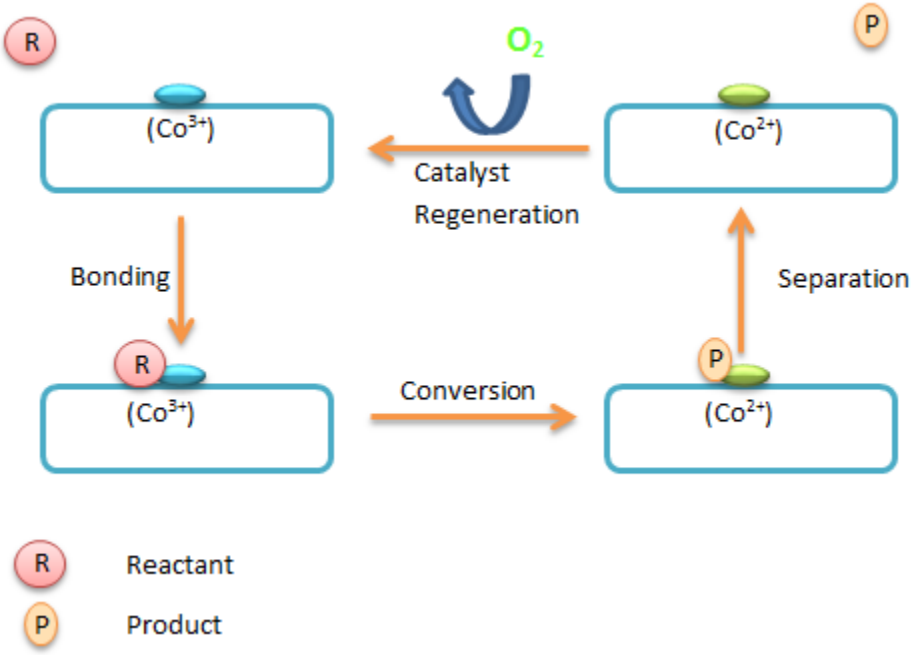

Even though our IR studies did not show any carbonyl stretching frequencies after the binding of acetaldehyde onto the catalyst (Figure 5.13), we did observe an increase in the peak area of satellite peaks in our XPS spectra which, usually occur due to increased Co(II) sites. This suggests that Co(III) site is the binding site. This is reasonable considering higher positive charge compared to that of Co(II). The bound pollutant could be oxidized at the Co(III) site using an oxygen in the lattice reducing Co(III) site in to Co(II). The reduced cobalt can be then re oxidized by gas phase oxygen after desorption of CO_2.[22,23] But, it is still unclear whether the oxidation catalytic process degrade the whole pollutant molecule or just the carbonyl group of the molecule. More detailed experiments such as studies with other types of organic pollutants as well as Isotopes labeling studies will be beneficial to further clarify the catalytic behavior of this highly active system.

Figure 5.13: Diffuse Reflectance IR studies of 0.5(mol)% $CoSiO_2$ catalyst (a) As prepared (b) after the catalysis

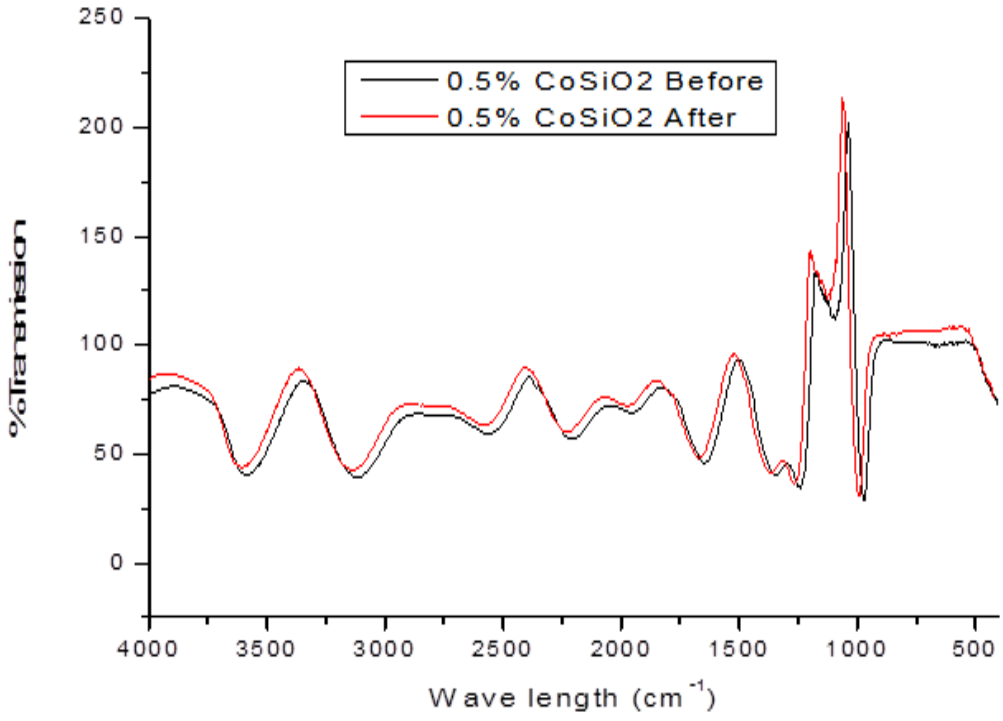

5.5. Summary

In conclusion we have discovered a very active oxidation catalyst based on cobalt and silica aerogels. Characterization studies revealed that the catalyst has a high surface area and consists of Cobalt(II) as well as Co(III) oxidation states. Even though it is not yet very clear how the pollutant binds to the catalyst, according to XPS studies the most likely binding site in the system is Co(III) site as indicated by the XPS satellite peaks. This 0.5(mol)% Co-SiO_2 system has shown excellent catalytic oxidizing ability towards all the pollutants that we have tried so far. Based on the available observations, a general catalytic mechanism is proposed.

5.6. References

1. Alanís-Oaxaca, R.; Jiménez-Becerril, J.; Titanium Oxide Modification With Oxides of Mixed Cobalt Valence for Photocatalysis, *J. Mex. Chem. Soc.*, **2010**, 54(3), 164-168
2. Narayan, R.V.; Kanniah, V.; and Dhathathreyan, A.; Tuning size and catalytic activity of nano-clusters of cobalt oxide, *J. Chem. Sci.*, **2006**, 118(2), 179–184
3. Thind, S.S.; Wu, G.; Chen, A.; Synthesis of mesoporous nitrogen–tungsten co-doped TiO_2 photocatalysts with high visible light activity, *Applied Catalysis B: Environmental*, **2012**, 111– 112, 38– 45
4. Hamadanian, M.; Reisi-Vanani, A.; Majedi, A.; Sol-Gel Preparation and Characterization of Co/TiO_2 Nanoparticles: Application to the Degradation of Methyl Orange, *J. Iran. Chem. Soc.*, **2010**, 7, S52-S58.
5. Claesson, E.M.; Philipse, A.P.; Thiol-functionalized silica colloids, grains, and membranes for irreversible adsorption of metal(oxide) nanoparticles, *Colloids and Surfaces A: Physicochem. Eng. Aspects*, **2007**, 297, 46–54
6. Krivoruchko, O.P.; Shmakov, A.N.; Zaikovskii, V.I.; Nuclear Instruments and Methods in In situ X-ray diffraction study of solid state transformations during catalytic graphitization of amorphous carbon, *Physics Research A*, **2001,** 470, 198–201
7. Dzwigaj, S.; Janas, J.; Machej, T.; Che, M.; Selective catalytic reduction of NO by alcohols on Co- and Fe-Sib catalysts, *Catalysis Today*, **2007,** 119, 133–136
8. Yin, J. S.; Wang, Z. L.; Ordered Self-Assembling of Tetrahedral Oxide Nanocrystals, *Physical Review Letters,* **1997,** 79, 13, 2570-2573.
9. He, C.; Paulus, M.; Chu, W.; Find, J.; Nickl, J.A.; Ko¨hler, K.; Selective catalytic reduction of NO by C_3H_8 over CoO_x/Al_2O_3: An investigation of structure–activity relationships, *Catalysis Today*, **2008**, 131, 305–313
10. Zhang, F.; Zhang, S.; Guan, N.; Schreier, E.; Richter, M.; Eckelt, R.; Fricke, R.; NO SCR with propane and propene on Co-based alumina catalysts prepared by co-precipitation, *Applied Catalysis B: Environmental*, **2007**, 73, 209–219
11. Osorio, A. E.; Olmos, A. V.; Berru, R.S.; Escudero, R.; Hydrothermal synthesis of co3o4 nanooctahedra and their magnetic properties, *Rev. Adv. Mater. Sci.*, **2009**, 22, 60-66
12. Leon, G.A.; van de Water, G.; Bezemer, L.; Bergwerff, J.A.; Helder, M.V.; Weckhuysen, B.M.; de Jong, K.P.; Spatially resolved UV–vis microspectroscopy on the preparation of alumina-supported Co Fischer–Tropsch catalysts: Linking activity to Co distribution and speciation, *Journal of Catalysis*, **2006,** 242, 287–298

13. Xiao, Q.; Zhang, J; Xiao, C; Tan, X; Photocatalytic degradation of methylene blue over Co_3O_4/Bi_2WO_6 composite under visible light irradiation, *Catalysis Communications*, **2008**, 9, 1247–1253
14. Fierro, G.; Eberhardt, M.A.; Houalla, M.; Hercules, D.M.; Hall, W.K.; Redox Chemistry of CoZSM-5 Zeolite, *J. Phys. Chem.*, **1996**, 100, 8468-8477
15. Liotta, L.F.; Pantaleo, G, Macaluso, A.; Di Carlo, G.; Deganello, G.; CoOx catalysts supported on alumina and alumina-baria: influence of the support on the cobalt species and their activity in NO reduction by C_3H_6 in lean conditions, *Applied Catalysis A: General*, **2003**, 245, 167–177
16. Petitto, S.C.; Marsh, E.M.; Carson, G.A.; Langell, M.A.; Cobalt oxide surface chemistry: The interaction of CoO(1 0 0), Co_3O_4(1 1 0), and Co_3O_4(1 1 1) with oxygen and water, *Journal of Molecular Catalysis A: Chemical,* **2008**, 281:1–2, 49- 58
17. Riva, R.; Miessner, H.; Vitali, R.; Del Piero, G.; Metal–support interaction in Co/SiO_2 and Co/TiO_2, *Applied Catalysis A: General*, **2000**, 196, 111–123,
18. Dillard, Schenck, and Koppelman; Surface chemistry of cobalt in calcined cobalt-kaolinite materials, *Clays and Clay Minerals*, **1983**, 31, 1, 69-72.
19. Laureti, S.; Agostinelli, E.; Scavia, G.; Varvaro, G.; Albertini, V.R.; Generosi, A.; Paci, B.; Mezzi, A.; Kaciulis, S.; Effect of oxygen partial pressure on PLD cobalt oxide films, *Applied Surface Science*, **2008**, 254, 5111–5115
20. Jansson, J.; Palmqvist, A.E.C.; Fridell, E.; Skoglundh, M,; O¨ sterlund, L.; Thorm¨ ahlen, P.; Langer, V.; On the Catalytic Activity of Co3O4 in Low-Temperature CO Oxidation, *Journal of Catalysis*, **2002**, 211, 387–397
21. Pollard, M.J.; Weinstock, B.A.; Bitterwolf, T.E.; Griffiths, P.R.; Newbery, A.P.; Paine, J.B.; A mechanistic study of the low-temperature conversion of carbon monoxide to carbon dioxide over a cobalt oxide catalyst, *Journal of Catalysis*, **2008**, 254, 218–225
22. Xie, Y.; Dong, F.; Heinbuch, S.; Roccab, J.J.; Bernstein, E.R.; Oxidation reactions on neutral cobalt oxide clusters: experimental and theoretical studies, *Phys. Chem.Chem. Phys.*, **2010,** 12, 947–959
23. Luo, J.; Meng, M.; Li, X.; Li, X.; Zha, Y.; Hu, T.; Xie, Y.; Zhang, J.; Mesoporous Co3O4–CeO2 and Pd/Co3O4–CeO2 catalysts: Synthesis, characterization and mechanistic study of their catalytic properties for low-temperature CO oxidation, *Journal of Catalysis*, **2008**, 254, 310–324

Chapter 6 - Photocatalysts for Elimination of Toxins on Surfaces and in Air Using UV and Visible Light

Abstract

Among the materials that have been studied to eliminate harmful air pollutants, photocatalytic systems get a high priority due to the use of clean, renewable, solar energy to drive the reactions involved.

Various types of photocatalytic systems have been reported for the degradation of harmful air pollutants. Most of the reported systems are based on semiconducting materials. Titania (TiO_2) is the most widely studied semiconducting compound in photocatalysis. Various types of modifications to titania systems have been reported to achieve visible light activity. Not only semiconducting systems but also insulating materials have been studied. The exact mechanism of photoactivity is still an ambiguity for insulator based photocatalytic systems. But, some reports suggest that photocatalysis occurs at the molecular orbital level, which generate reactive electron-hole pairs which then drive the chemical decomposition of pollutants.

Herein, a comparison of these types of photocatalysts is made.

6.1. Introduction

Over the last several decades there has been great concern about environmental pollution due to the fact that it is one of the primary causes for various health problems as well as for possible changes in the global climate. Generally, environmental pollution can be defined as contamination of air, water and land due to manmade waste and can be divided into three major groups; air pollution, water pollution and soil pollution. From these three major groups, air pollution has received the attention of many researchers due to the seriousness of the impact on climate change, acid rain, smog, and human and animal health. Air pollution can be sub grouped in two main categories; as indoor and outdoor. Both categories are equally important as they can create very unhealthy conditions to humans as well as to animals and plants.[1]

These environmental problems are related to energy use, and clean renewable energy is needed, such as solar energy, wind, geothermal, *etc.* Out of all these renewable energy sources, solar energy has the most potential. In fact, it has been calculated that the amount of solar energy arriving at the earth's surface in a minute is sufficient to meet the energy demand of the world

for a year. But, the lack of efficient solar energy harvesting and storing methods is one of the main drawbacks that we face. So, there are thousands of researchers around the globe experimenting on efficient methods to harvest and store solar energy. Solar energy can be used to heat, or to produce electricity. Solar energy can also be converted into chemical energy or can be used to catalyze important reactions.[2]

Photocatalysis is one of the very successful and active areas of research that have provided important ways to harvest readily available solar energy to destroy harmful organic air contaminants to overcome environment pollution. Usually, any chemical reaction requires a certain amount of activation energy to initiate the reaction. In normal chemical reactions the activation energy will usually be supplied by simple methods such as heating, mechanical stirring, *etc*. But, in photochemical reactions, light is used for this purpose. Upon exposure to certain wavelengths of light, photocatalytic material can be used to catalyze specific chemical reactions based on the oxidation and reduction potentials of the photo generated charge carriers. Thus, in photocatalytic reactions, the catalytic material plays an intermediate role in absorbing light energy and promoting desired chemical reactions. According to the literature, various photocatalytic materials have been employed to drive water splitting to produce hydrogen and oxygen gases, mineralizing harmful organic pollutants, as well as to remove organic dye molecules from industrial effluents. Even though, there are many materials that have been reported, the number of materials that have become successful on an industrial scale is very limited.[3]

There are various factors that determine the efficiency of a photocatalyst. These are efficiency of charge separation, energy range of the solar spectrum suitable for the excitation of the material, optimum intensity of the light photons, environment of active sites, *etc*. Usually, during the preparation of photocatalytic materials the energy levels of the conduction and valance bands of the materials are modified, or the chemical environment of the active site is changed by doping with suitable doping agents. These changes to photocatalytic systems usually enhance the light absorption, electron hole pair generation and the overall activity. Surface acidity is another important factor that determines the specificity, efficiency and the mechanism of action of a photocatalytic material. For example, acidity of titania based materials is strongly related to the amount of surface hydroxyl groups present on the surface and these groups play a major role in

trapping photo generated holes and thereby decrease the recombination of electron hole pairs, which in turn increase the quantum efficiency of the photocatalyst.[4]

Most of the successful photocatalytic materials that have been reported consist of a supporting base material. Usually compounds such as zeolite, titania and silica are popular as successful base materials due to their high stability under high temperature and pressure conditions, low toxicity, low cost and the ability to obtain various physico-chemical properties simply by changing particle dimensions. Usually the supporting material facilitates the catalytic activity of the catalytic site by enhancing charged carrier separation, providing reduced electron hole recombination and facilitating charge transfer to an adsorbed species.[5]

On the other hand, most of the catalytic systems reported in the past are primarily based on at least one semiconducting base material. Semiconducting materials are required to obtain good photocatalytic activities due to the ability of semiconductors to create reactive electron hole pairs upon irradiation of UV or Visible light. But, whether comparable photocatalytic activity can be obtained without using semiconducting base materials is an important question that still remains unanswered. Thus, it is very important to directly compare other available options, such as insulators based materials, in order to determine the photocatalytic activities of these materials.

6.2. Titanium Dioxide Based Photocatalysis

Titanium dioxide photocatalysis is the most studied and well understood photocatalytic system. Thus, studying the mechanistic details of how titania behaves is important. Titanium dioxide, also known as Titania, is a white colored compound that is widely used as a photocatalyst, catalytic support, sensor material, and hydrogen adsorber. Titania is a semiconductor with a band gap of 3.2 eV, and has been shown to promote mineralization of organic pollutants, water splitting, and carbon dioxide reduction upon exposure to UV light. Titanium dioxide occurs in nature in three well-known mineral forms known as anatase, rutile and brookite. Among these mineral forms, anatase typically exhibits higher photocatalytic activity than the other two forms. But, in some cases it has been reported that even higher photocatalytic activity is possible with precise mixtures of both anatase and rutile. One such example is commercially available Degussa P25 TiO_2, which consists of 80% anatase phase and 20% rutile phase. Because of a relatively wide band gap, titania absorbs light corresponding to wavelengths shorter than 388 nm, which is only 3-4% of the solar energy that reaches the earth. Thus, in principle, photocatalytic activity

should be enhanced by adjusting the band gap toward visible light energies by doping, since visible light is readily available in the solar spectrum. Doping has been carried out in earlier research using various methods and materials. Common doping materials used have been inorganic compounds, noble metals, transition metal oxides, organic dye molecules, anionic compounds *etc*.[5,6,7]

6.3. Non-Metal Doping

Doping with various non-metallic compounds has been carried out to obtain visible light photoactivity of titania photocatalysts usually by introducing new energy states in between the band gap. Low-band gap, nitrogen modified titania based visible light photocatalysts prepared by Kisch and coworkers and Panayoto and coworkers are good examples of photocatalytic materials based on titania that has been doped with non-metallic material. According to these reports, nitrogen doped titania photocatalyst clearly shows an intense band-to-band absorption in the range of 400-500 nm visible range of the solar spectrum, which brings the modified band gap of titania to 2.46 - 2.20 eV and very high photocatalytic activity towards formic acid mineralization under visible light (figure 6.1).[8,9]

Figure 6.1: Diffuse reflectance spectra of (a) TiO_2, (b) TiO_2-N, (c) TiO_2-N1 calcined 1 h, and (d) TiO_2-N2 calcined 0.5 h.[8]

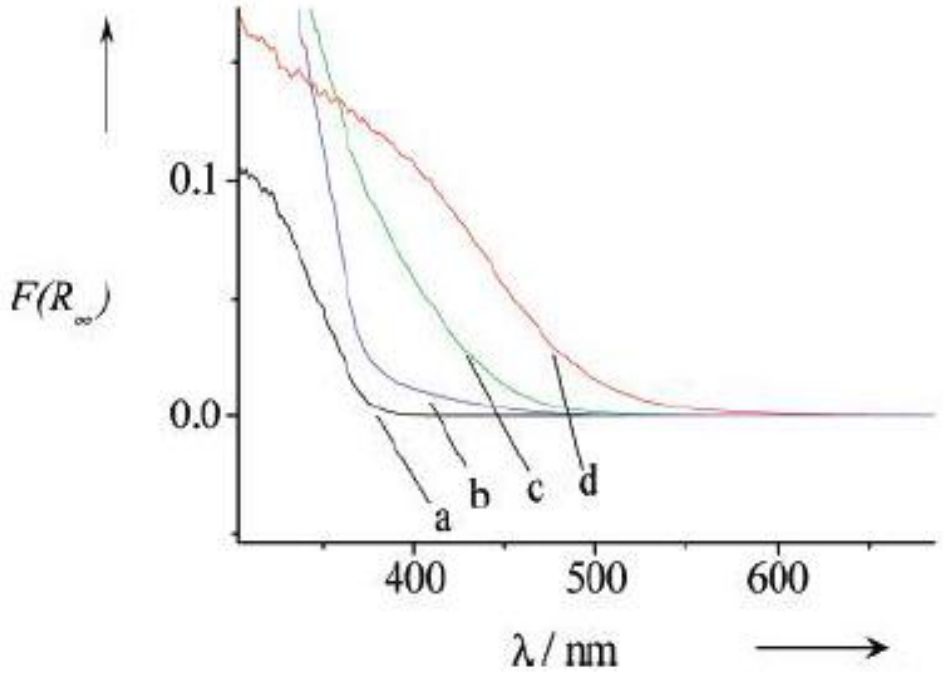

Tang and coworkers also reported on highly crystalline and ordered mesoporous TiO_2 thin films doped with carbon, synthesized via a highly cost effective route, that exhibit high photocatalytic activity. In this material carbon inclusion plays a major role to stabilize the framework of titania during thermal crystallization process. Moreover, according to their findings high crystallinity and ordered mesoscopic structures always help to enhance the efficiency of photocatalysis.[10]

Figure 6.2: TEM images of a TiO_2 thin film crystallized at 550 °C with pure post induced carbon as the confining material. The zoom-in image is also shown on the right. The inset is a selected area electron diffraction pattern (SAED) indexed as the anatase phase[10]

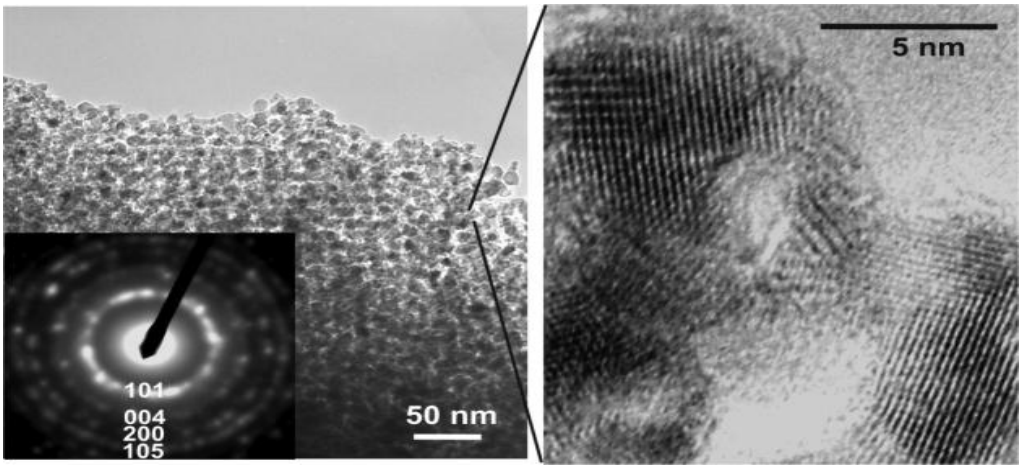

Further, there are reports about titania based photocatalytic materials co-doped with several non-metallic compounds. Xiang and coworkers as well as Hamal and coworkers, have separately reported successful preparation methods for visible light active titania photocatalysts using more than one non-metal.[11,12] According to the literature, doping with nitrogen and sulfur co-dopants can induce the formation of new energy levels in the band gap. These new energy levels result in visible light response of co-doped photocatalysts due to the requirement of lower energy of photons to generate new electron hole pairs. Under lower energy visible light irradiation, electrons can easily transfer from the valance band to impurity states, and the electrons in the impurity states can move to the conduction band after secondary excitation.[12] The density of states diagram represented in figure 6.3 clearly indicates the insertion of intermediate energy levels due to the addition of S and N.[12]

Figure 6.3: Total density of states for N,S co-doped TiO_2 at 2.08 at.% doping levels[12]

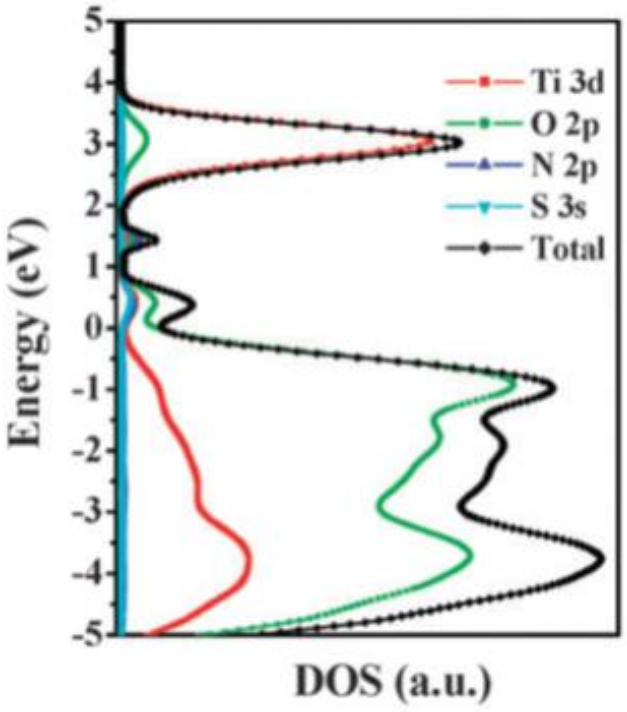

6.4. Metal Doping

Visible light photo degradation activity of titania can also be obtained by introducing various metals and metal oxides. Transition metals and respective metal oxides have been actively used in this regard due to the ability to absorb in the visible range of the spectrum, as orbital energy transfer usually lies in the matching wavelength range. There are a large number of reports about effects of metal ion doping on titania photocatalysis. Some metal ions like Co^{3+} and Al^{3+} decrease the photocatalytic activity while metal ion such as Fe^{3+}, Ru^{3+}, V^{4+} to enhance the photocatalytic activity. According to Choi and co-workers the relative photocatalytic efficiency of a metal-ion dopant depends on whether the metal ion serves as a mediator of interfacial charge transfer or a recombination center.[13] Furthermore, they have carried out an interesting study of titania based photocatalysis using various metal ion dopants to study the effect of each dopant on visible light photocatalytic activity of titania prepared by the well-known sol-gel method.[13] According to the findings of Choi and co-workers, the ionic radii of the dopant metal ion play an important role in the final structure of the photocatalytic material and have a direct effect on the photoactivity. The final structure of a doped photocatalyst is highly affected by the nature of the doped metal ion and its size. Usually, metal ions such as Pt^{4+}(0.765 Å), Cr^{3+}(0.755 Å), and

V^{3+}(0.78 Å) ions, which have similar ionic radii to Ti^{4+}(0.745 Å) ions in titania, are most likely substituted in the titania framework with less amounts of distortions, thus forming favorable structures. In contrast, metal-ion dopants such as Co^{2+}(0.89 Å), Cu^{2+}(0.87 Å) and Pt^{2+}(0.94 Å) ions usually end up located in interstitial positions of the titania lattice, rather than directly in Ti^{4+} sites, because of the relatively large size difference between dopant ions and Ti^{4+}. Also, much larger dopant ions such as Ag^{+}, Rb^{+}, Y^{3+} and La^{3+} ions do not get incorporated in the titania framework due to the larger size variation between the metal ion and Ti^{4+}. Thus, they are more likely to be found as dispersed metal oxides within the crystal matrix or dispersed on the surface of TiO_2.[13]

Usually, visible light activity in metal ion doped titania aerogels can occur due to two main reasons. (1) the excitation of electrons from the dopant ions to the conduction band of titania (*i.e.*, a metal to conduction band charge transfer) or (2) defects associated with oxygen vacancies that give rise to colored centers, or a combination of both. However, the changes that occur to titania due to dopant metals can be clearly identified using diffuse reflectance UV-Vis studies, as reported by Choi and coworkers (figure 6.4). According to their observations there is no significant difference between the absorption spectra of pure titania and Ag, Rb, Y and La ion doped titania samples, since these larger ions did not incorporate into the titania framework (spectra are identical to undoped TiO_2). But in figure 6.4 a,b,c it is very clear that the metal ions of similar size as Ti^{4+} have successfully been incorporated into the matrix of titania creating additional bands which induce absorption in the visible range of photons.[13,14]

Figure 6.4: UV-Vis diffuse reflectance spectra for various Metal-TiO_2 samples. Absorption spectra for Ag^{+}, Rb^{+}, Y^{+}, and La^{+} TiO_2 samples, which are not shown here, are identical with that of undoped TiO_2.[13]

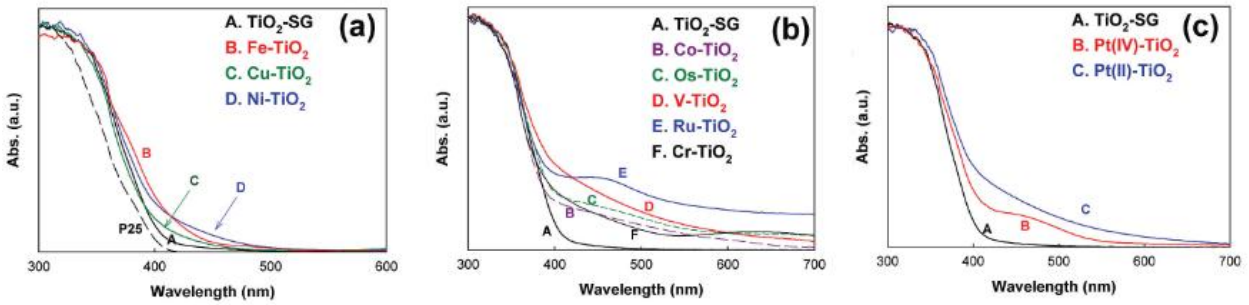

Rates of the mineralization of various organic pollutants using photocatalysis have been obtained by many researchers. Titania based photocatalysts have been employed mainly in oxidation

catalysis. There are reports about polymerization mechanisms and reduction mechanisms as well. According to the collective results of photocatalytic activities of titania reported in the literature, metal ion doping seems to be not important under UV light, as the increases in the activity compared to pure titania based samples are very small. Under UV light irradiation, the majority of the reactive species are created by semiconducting titania itself. But when it comes to visible light active titania photocatalysts, doping agents play an important role by introducing additional energy levels within the band gap of titania, introducing trap states and by stabilizing the titania framework.[13,14,]

The next topic to be discussed is the chemistry that photocatalysts induce. The study of hydroxyl radical generation upon exposure to UV light is widely used to confirm the mechanism of photocatalytic activity of titania based photocatalysts.[15,16,17] According to the reported results of hydroxyl radical detection experiments, titania based samples clearly indicate the formation of hydroxyl radicals upon exposure to UV light and Visible light (figure 6.5).

Figure 6.5: Fluorescence spectra obtained for the supernatant liquid of the irradiated TiO_2 suspension containing terephthalic acid at various irradiation periods PL spectral changes with irradiation time under UV and Vis light[15,17]

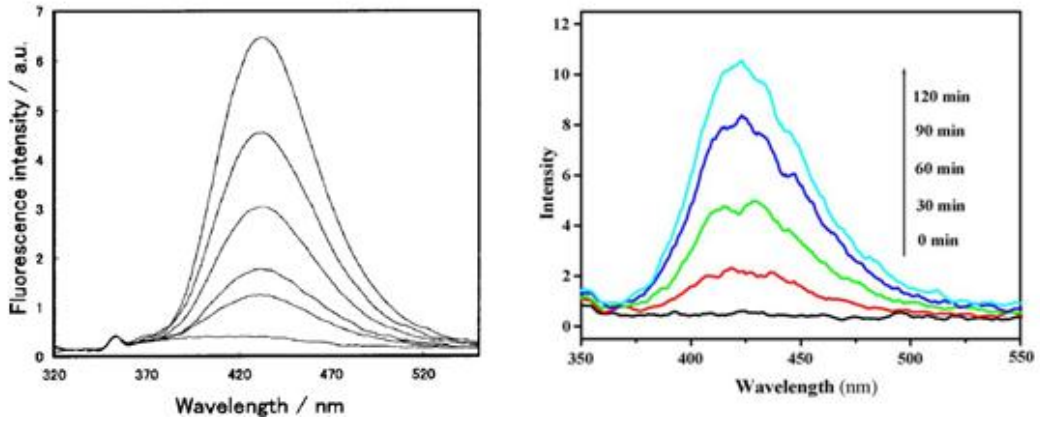

Since titania is a semiconducting pigment, its valence electrons can be promoted into the conduction band, resulting in the formation of an electron-hole pair upon irradiation with suitable light. But, the created electron hole pair needs to be spatially separated in order to allow the formed electron hole pair to undergo chemical reactions. In titania, charge carrier recombination is usually avoided by immobilizing the created excited electron or hole or both in the trap states available in between the conduction and valance bands.[7] Formed excited electrons usually have a higher effective mass compared to the holes, and moderate reduction potential. So, electrons

tend to remain in their free state or in some cases get trapped at the surface. On the other hand, holes usually have high oxidation potential and get trapped at the semiconductor surface. Usually a light excited hole can follow two paths. The holes either oxidize the hydroxyl groups available on the surface of titania to produce hydroxyl radicals, or oxidize lattice oxygen atoms from -2 to 0 valence state to create oxygen vacancies in titania. Therefore, in supported photocatalytic materials titania plays two major roles by itself providing a support to the system as well as providing active catalytic sites. Thus, the entire material is involved in photocatalysis, making the photocatalysis process non-localized.[18]

Therefore, according to the general mechanism of titania based photocatalysis, upon exposure to UV light positively charged holes and negatively charged electrons will be created in valence and conduction bands of titania respectively as described by Eq1.

$TiO_2 + h\nu \rightarrow TiO_2\ (e^-\ \text{and}\ h^+)$ ..... Eq 1

$h^+_{vb} \rightarrow h^+_{trap}$ ..... Eq 2

$O_2 + e^- \rightarrow O_2^{\cdot -}$ ..... Eq 3

In the second step positively charged holes will be trapped by surface hydroxyl groups of titania generating reactive hydroxyl radicals (Eq2). In the meantime negatively charged electrons in the valence band can interact with oxygen gas to generate reactive oxygen species (Eq3). The oxidation ability of $^{\bullet}OH$ radicals is very high so that they can easily react with various organic pollutants according to various reaction schemes.[15,19]

$O_2^{\cdot -} + O_2^{\cdot -} + 2H^+ \rightarrow H_2O_2 + O_2$ ..... Eq 4

$O_2^{\cdot -} + h^+_{vb} \rightarrow O_2$ ..... Eq 5

$O_2^{\cdot -} + h^+_{trap} \rightarrow O_2$ ..... Eq 6

$OH^- + h^+_{vb} \rightarrow OH^{\cdot}$ ..... Eq 7

$OH^{\cdot}\ \ OH^{\cdot} \rightarrow H_2O_2$ ..... Eq 8

$e^-\ \ h^+_{trap} \rightarrow \text{recombination}$ ..... Eq 9

Even though the above equations explain the behavior of semiconducting titania under UV light, the photocatalytic mechanism must be slightly modified when explaining visible light activity of metal/non-metal doped titania photocatalysts. There are various ways that doped metals/non-metals help improve the visible light photocatalytic activity. The most popular way of inducing visible light activity in a titania network is by introducing new localized electronic states and

surface structures. These changes to the titania network can eventually change the electronic structure, absorption properties, redox potential and charge carrier mobility of the photocatalyst *etc.* Introduction of such energy states and surface structures in the band gap induces a red shift in the band gap and visible light absorption through charge carrier transfer between a dopant and conduction band (CB) or valence band (VB) or a d—d transition in the crystal field[24]. The charge transfer transition between transition metal ion 3d electrons and conduction band of titania is known to be responsible for the red shift evident in UV-Vis spectra of most of the transition metal doped titania samples.[20-24]

According to the studies carried out by Umebayashi and co-workers, for transition metal doped titania photocatalysts two types of electron transitions are possible (Figure 6.6). The first transition is a donor transition from the metal t_2g level into the CB which can be explained using Eq10, and the other transition is the acceptor transition from the VB to the metal t_2g level given by Eq11.[23]

Charge carrier generation:

$$M^{n+} \quad h\nu \rightarrow M^{(n+1)+} + e^{-}_{CB} \quad \cdots\cdots\cdots\cdots \quad \text{Eq 10}$$

$$M^{n+} + h\nu \rightarrow M^{(n-1)+} + h^{+}_{VB} \quad \cdots\cdots\cdots\cdots \quad \text{Eq 11}$$

Figure 6.6: Schematic diagram to illustrate the photoexcitation process under visible light of the metal-doped TiO_2: (a) Chromium doped Titania, (b) Vanadium doped Titania, (c) Manganese doped Titania[23]

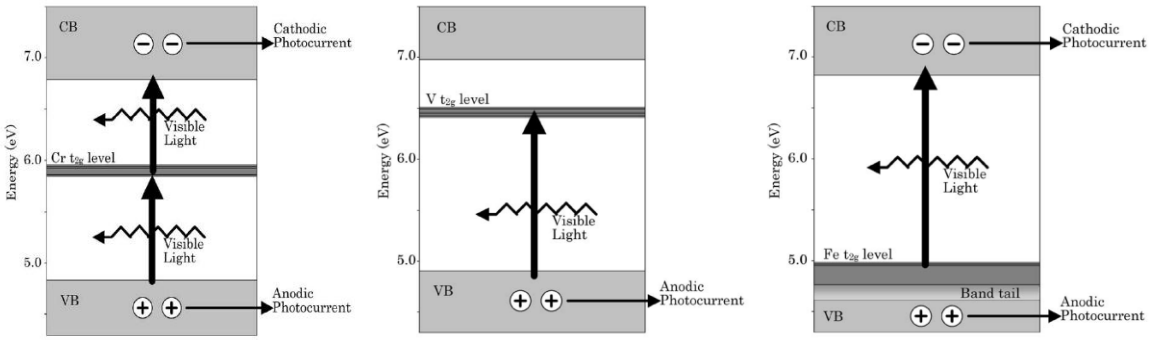

Furthermore, doped metal ions can also enhance the efficiency of TiO_2 by providing electron (or hole) trapping/defect sites and thereby decreasing generated electron hole pair recombination when the energy levels for $M^{n+}/M^{(n-1)+}$ lies below the conduction band edge and the energy level for $M^{n+}/M^{(n+1)+}$ above the valence band edge. This can be illustrated using the following equations.[17,21,23]

Charge trapping:

$Ti^{4+} + e^- \rightarrow Ti^{3+}$ ..... Eq 12

$M^{n+} + e^- \rightarrow M^{(n-1)+}$ ..... Eq 13

$M^{n+} + h^+ \rightarrow M^{(n\ 1)}$ ..... Eq 14

$OH^- + h^+ \rightarrow OH^{\bullet}$ ..... Eq 15

Therefore, considering all the possible effects of doped transition metals and as well as according to the mechanism proposed by Devi and co-workers, it is possible to explain the enhanced visible light photocatalytic activity of metal ion doped Titania photocatalysts. The following equations explain the remaining steps during a photocatalytic decomposition of organic pollutants.[20]

Charge release and migration:

$Ti^{4+} + M^{(n-1)} \rightarrow Ti^{3+} + M^{n+}$ ..... Eq 16

$M^{(n+1)+} + OH^- \rightarrow M^{n+}\ OH^{\cdot}$ ..... Eq 17

Recombination:

$e^- + h^+ \rightarrow$ heat ..... Eq 18

$Ti^{3+}\ OH^{\cdot} \rightarrow Ti^{4+} + OH^-$ ..... Eq 19

$M^{(n-1)} + h^+ \rightarrow M^{n+}$ ..... Eq 20

$M^{(n-1)}\ OH^{\cdot} \rightarrow Mn^{+} + OH^-$ ..... Eq 21

$M^{(n+1)+} + e^- \rightarrow M^{n}$ .....Eq 22

$M^{(n+1)+} + Ti^{3+} \rightarrow M^{n+} + Ti^{4+}$ ..... Eq 23

Interfacial charge transfer process:

e^- (or Ti^{3+}, $M^{(n-1)}$) $O \rightarrow O^-$ ..... Eq 24

h^+ (or OH•, $M^{(n+1)+}$) $R \rightarrow R^+$ ..... Eq 25

6.5. Photocatalytic Mineralization of Organic Pollutants with Titania Based Mixed Oxide Supports

Even though pure titania and titania with small amounts of various dopants have been successful in photocatalysis, they are not the only materials that show high photocatalytic activities. According to the article by Cheng and coworkers the photocatalytic efficiency of titania based materials can be enhanced by introducing secondary materials such as silica.[24] Interestingly, there are many reports that discuss enhanced activity of titania when associated with another metal oxide such as silica, zirconia, *etc*.[4] Examples for other such metal oxide combinations

reported are ZrO_2/TiO_2, WO_3/TiO_2, SnO_2/TiO_2, ZnO/TiO_2, PbS/TiO_2, Al_2O_3/TiO_2, $CdSe/TiO_2$, and SiO_2/TiO_2 .[19,24]

Mixed metal oxides help promote photocatalytic activity in various ways. In some cases the binary material was used as a solid acid support for titania based systems to improve the absorption of reactants and thereby to increase the concentration of reactants near the active centers of the catalysts.[19,24]

The mixed oxide system of silicon dioxide with titanium dioxide has been widely studied as compared to other reported systems because of the promising properties of silica. Silica materials are nontoxic and able to provide high surface area to the photocatalyst, acting as a carrier of titania, and helps produce suitable pore structures to favor photocatalytic activity. Moreover, the increased photocatalytic efficiency arises due to the improved adsorption of reactants and the concentration of the reactants near the active centers of mixed silica/titania catalysts. [19,24]

According to the findings of Anpo and co-workers, when titania is finely dispersed on another support surface, higher photocatalytic activity is observed due to the decreased non-radiative transfer of light energy absorbed by titania. Also, when titania is dispersed on the surface of other types of supporting materials, the presence of coordinately unsaturated surface titania sites are promoted compared to that of bulk titania which makes the mixed titania system perform better in photocatalysis.[25,26] According to another interesting study carried out by Anpo and co-workers, titania supported Alumina mixed oxide systems show enhanced photocatalytic activities due to the formation of surface layers where titania species are surrounded by the Al_2O_3 carrier, which acts as co-catalyst for the respective reaction.[26,27]

Use of TiO_2-SiO_2 mixed oxides doped with transition metal ions to achieve visible light photocatalytic activity has also been reported.[28]

Figure 6.7: The modal pollutant, Acetaldehyde, photocatalytic oxidation by 0.5 mol% Cr loaded mixed SiO_2 and TiO_2 photocatalysts with varying SiO_2 and TiO_2 ratios[28]

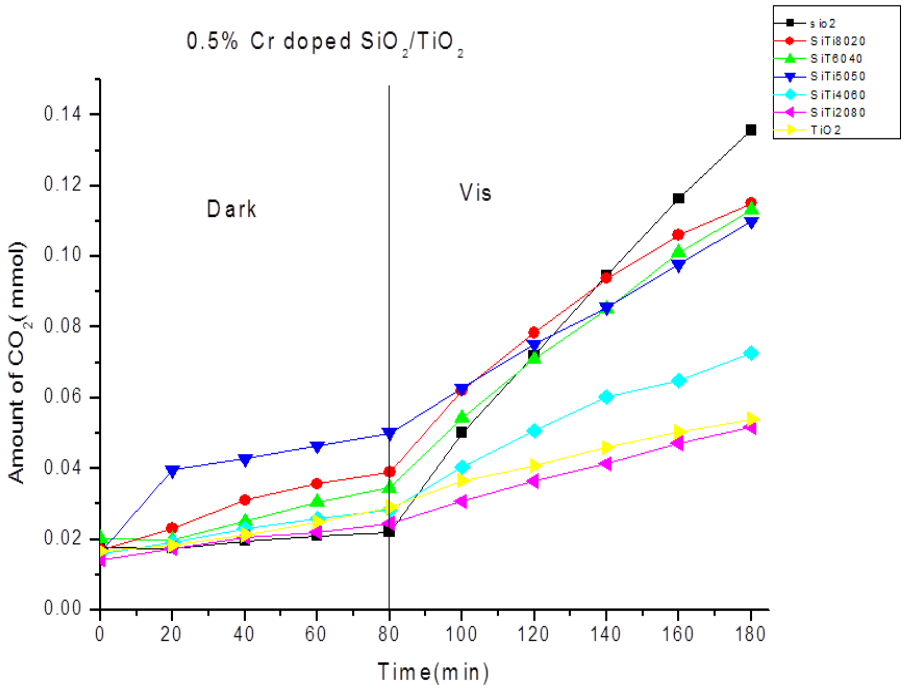

The 0.5% chromium loaded mixed silica and titania system and the 100% silica based systems show very high photocatalytic activities under visible light compared to all the other systems. Further, according to figure 6.7, which compares the effect of different ratios of silica and titania on kinetic activities under visible light, higher photo degradation takes place when more silica is present.[28]

Enhanced reactant specificity is not the only factor affected using mixed oxides. The formation of new trapping or recombination centers can be found upon addition of a foreign material to a semiconducting compound such as titania. According to XPS characterization experiments (figure 6.8) carried out by Anpo and coworkers, clear shifts of Ti($2p^{3/2}$) and Si($2p^{1/2}$) peaks were observed for varying ratios of titania and silica photocatalytic samples. The shift towards the higher binding energy values occurs due to smaller relaxation energy for highly dispersed titania, compared to that of the bulk. Because of the higher dispersion a large number of coordinative unsaturated titania sites are present on the surface, which results in high photoactivity.[25,26]

Figure 6.8: XPS signals for titanium-silicon oxide catalysts at 298 K.[25]

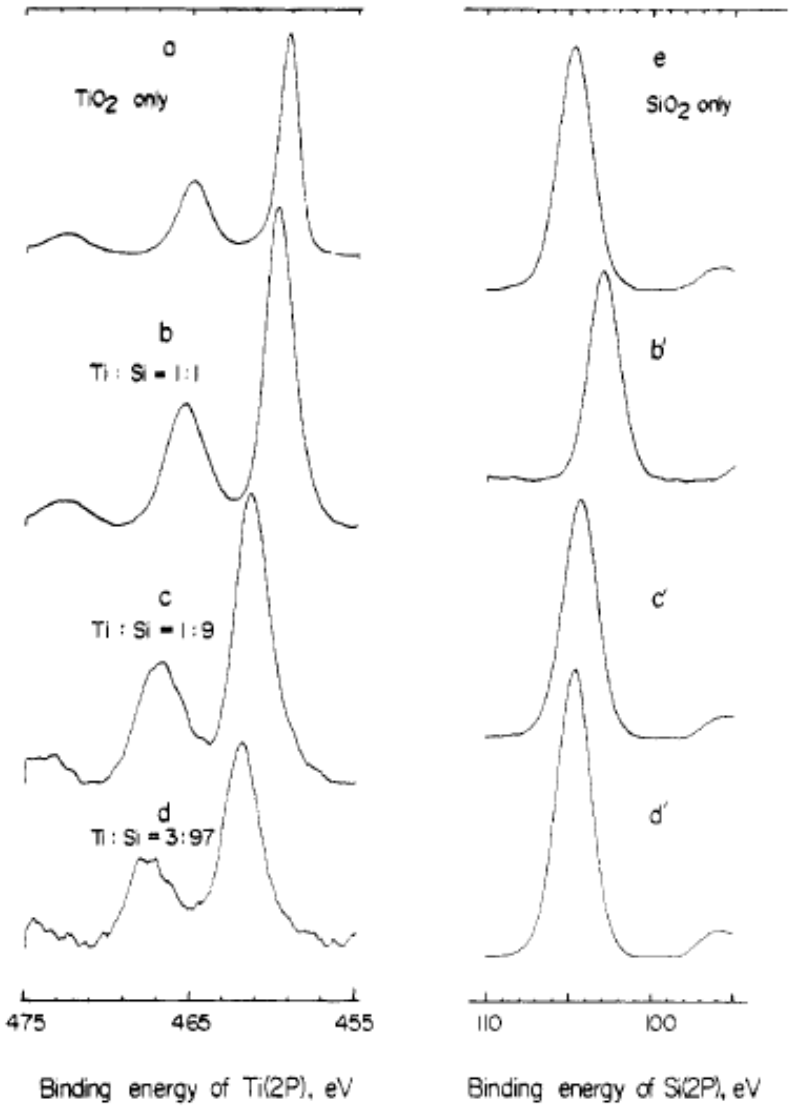

Anderson and Bard have reported a mechanism to explain the enhanced photocatalytic activity of mixed oxide systems based on titania prepared by sol-gel methods (Scheme 1). Even though they have not considered all the possible effects of mixed oxides, they have been able to address the complex puzzle of mechanism of activity up to a certain extent. During the photocatalytic reaction titania behaves as the photocatalytic center, which absorb photons and create reactive electron hole pairs and thereby generate reactive hydroxyl radicals. Supporting silica or alumina provide efficient absorption sites closer to photoactive titania sites and help increase the overall photoactivity of the system.[26]

Figure 6.9: Schematic representation of the TiO_2/SiO_2 or TiO_2/Al_2O_3 photocatalyst with no interaction between the TiO_2 and SiO_2 or Al_2O_3 phases.[26]

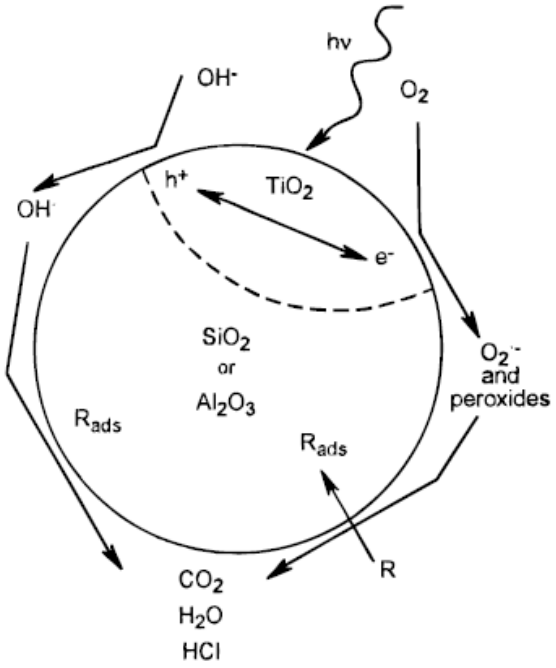

6.6. Silica Based Photocatalysis

For many years titania has been recognized as the most useful photocatalyst and various types of applications have been developed. But, recent research has focused more on photocatalytic systems other than titania. Some experiments of this kind have focused on various types of semiconductors, while some dealt with the use of different insulating materials.[29] Compared to the reported titania based photocatalytic systems the number of insulator based materials are small in number. But, some of these reported systems have shown interesting photocatalytic activities towards removal of harmful air pollutants. Herein we will discuss several such materials and their special structure and function related properties. In most of the reported literature, photoactive sites of insulator based photocatalysis occur due to the presence of highly dispersed metal oxide species of quantum size. But, according to the findings of Yoshida and coworkers it is possible to obtain photocatalytic abilities because of the presence of surface quantum defects on silica surfaces.[29] When photocatalysis occurs due to the presence of quantum defects, the usual electron hole pair generation mechanism is somewhat different from that of a semiconducting material. Usually when silica is loaded with highly dispersed metal oxides, photoexcitation occurs as shown in the scheme 2a. Quantum defects on the silica surface

can allow photoexcitation to occur in a similar manner. According to scheme 2a, photoexcitation occurs on a molecular orbital level. Upon exposure to a desired wavelength of photons, an electron in the ground state of the M-O bond is excited to an unoccupied singlet orbital state. Later, this singlet state can be transferred into the triplet state via intersystem crossing, if available. Scheme 2b is an illustration of electron-hole pair generation upon exposure to certain photons of energy. The metal oxide species have been represented as a tetrahedral MO4 arrangement.[30]

Figure 6.10: (a) Photoexcitation in a quantum photocatalyst, (b) an illustration of photoexcitation state of active sites on a silica-based photocatalyst on which the exciton is localized[30]

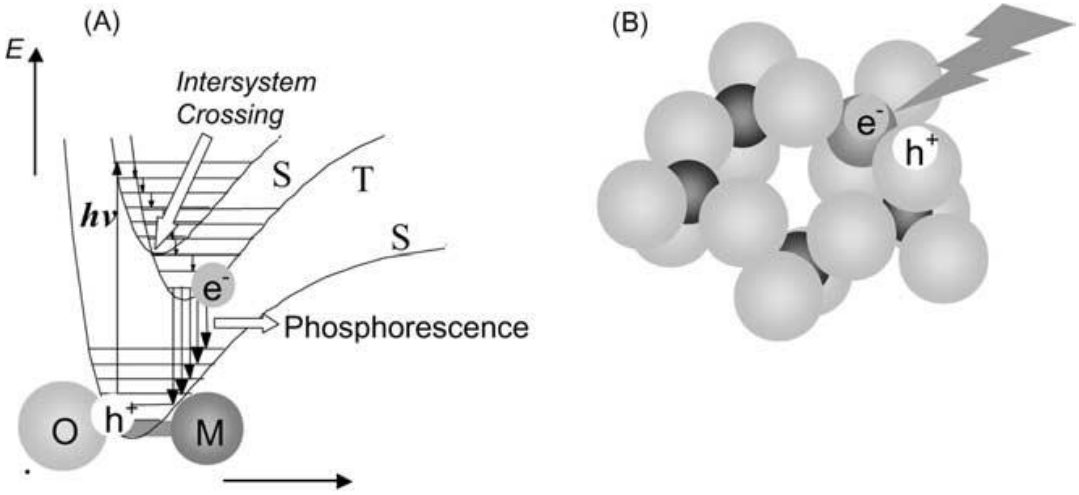

The photoactive sites on silica materials such as FSM-16, MCM-41 and sol-gel prepared SiO_2 have been revealed by various spectroscopic techniques. According to the observed results active sites were generated on silica material by dehydroxylation of surface isolated hydroxyl groups at high temperatures above 673K as indicated in scheme 3. According to FTIR studies, catalytic active sites could be recognized as 'strained siloxane bridges'. Active sites of each silica material were common and showed similar activities. But the efficiency varies from one silica material to another due to the amounts of active sites present in each material.[30]

Further, according to the results obtained from ESR studies, the presence of four different signals, which correspond to Si −O˙, Si−O−O˙, Al−O˙, and .Si w ere observed. Further collective use of IR and ESR results suggested the reaction in scheme 3a. The reaction at scheme 3b occurs according to the charge transfer transitions at 258 nm wavelength, which occurs from a bonding orbital of Si-O to 2P nonbonding bridging oxygen. Thus, the photosensitivity of silica

materials arises because of the light sensitivity of this reaction that can be photoexcited under UV light below ≈390 nm.[30,31]

Figure 6.11: Photocatalytic active sites generation mechanism in pure silica based materials[30]

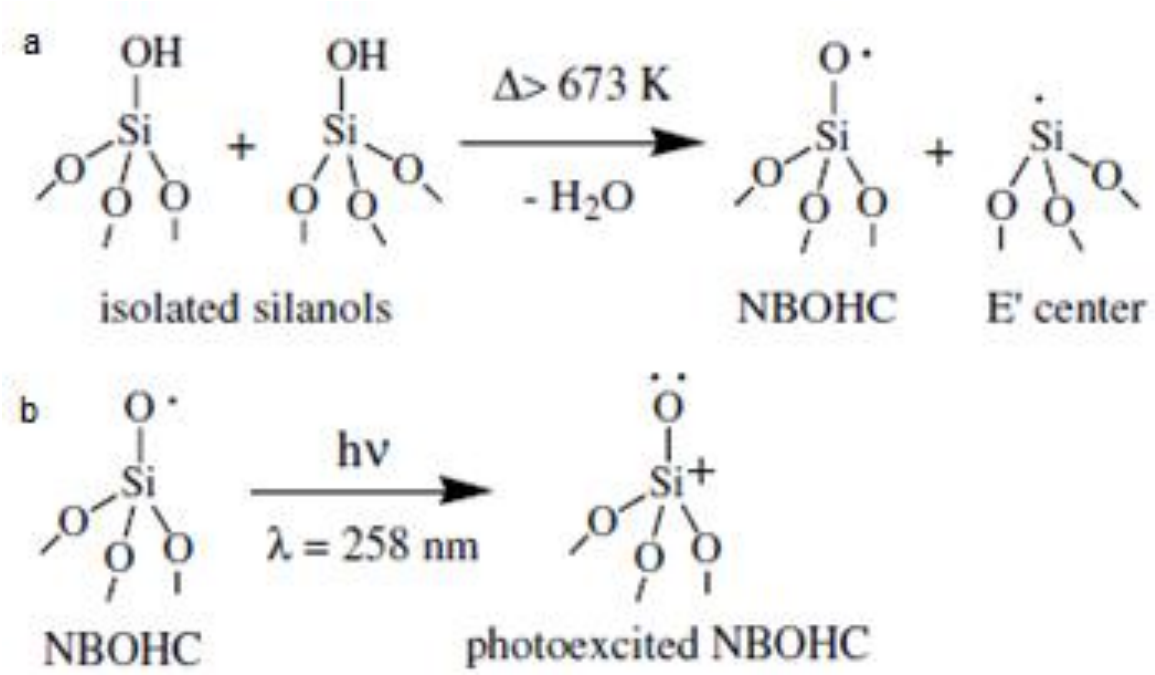

On the other hand, introduction of suitable dopant elements to the silica material can enhance the absorption in the visible region of the spectrum because as is evident from scheme 3b, higher energy UV light is required in order to generate photoactive sites in silica.[30,33,34] In literature there are many reports about successful transition metal ions loaded silica based systems. Usually, the required amount of metal oxide dopants are very small as highly dispersed transition metal oxides tend to show enhanced oxidation abilities compared to that of highly concentrated photocatalysts.[30, 32, 33]

Wang and coworkers studied the effect of various transition metal ions doping on high surface area silica based systems. From various transition metals (M= Co, Cr, Mn, V, Fe, Cu, and Ni) that were studied, cobalt and chromium were found to be the most photocatalytically active under visible light. Further, according to the studies of Moisii and co-workers, chromium oxides show promising visible light active photocatalytic performances.[32, 33] Further, according to in-depth kinetic studies 0.5 (mol)% Cr loaded Silica aerogel material is able to perform best in mineralizing acetaldehyde into carbon dioxide (Figure 6.10).[28]

Figure 6.12: Kinetics of photocatalytic degradation of acetaldehyde using 0.1%(mol) chromium loaded silica, titania, mixed systems, blank samples and commercially available titania aerogel(P25) (a) under UV light irradiation (b) Visible light irradiation[28]

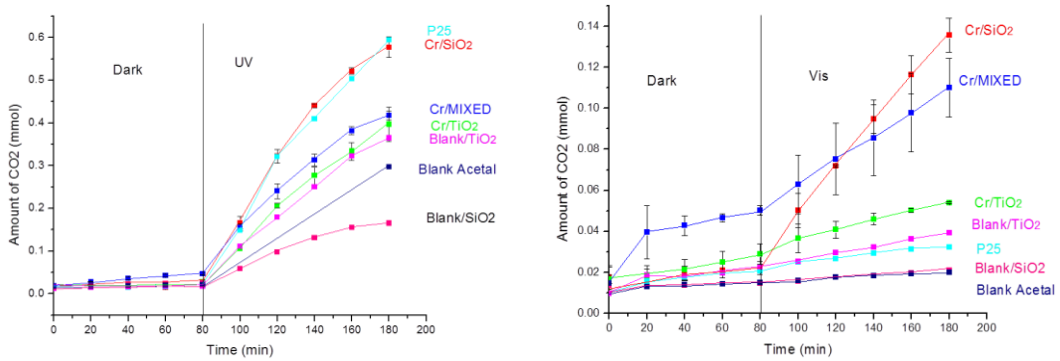

The structure of the bound chromium site is one of the important factors when studying the mechanism of photocatalytic mechanism. There have been several attempts reported in literature to characterize the structure of isolated chromium oxide sites on silica and titania. Moisii and co-workers carried out an interesting series of experiments to distinguish the correct structure from two possible structures for Cr^{6+} sites, one structure is dimeric oxygen bound to silica matrix (scheme 4a) and one oligomeric (Scheme 4b) chromate species. In most of the reports dimeric chromium bonding has been used to explain the structure of the Cr^{6+} site and the oligomeric structure were reported in a few cases. But, Moisii and coworkers confirmed structure 4a as the most favorable structure for their 0.5% Cr loaded silica xerogels using XANES and Raman spectroscopic studies.[32]

Figure 6.13: possible structures for the bonding nature of chromium sites to silica [32]

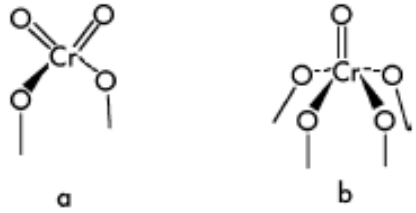

Therefore, chromium loaded silica photocatalysts should be able to generate high energy electron- hole pairs upon exposure to a desired wavelength of photons by exciting an electron in the ground state of the Cr-O bond to an unoccupied singlet orbital state.[30]

On the other hand, according to the recent article by Yi and co-workers, photochromism effects have also been proposed to play a major role in Cr^{6+} based photocatalytic materials. They observed a clear color change from purple to yellow in their $SrTiO_4$:Cr catalyst upon exposure to sunlight.[34]

Thus, the Cr^{6+} ions present on the surface of the sample undergo change in oxidation states due to the exposed light. According to the standard potentials in aqueous solutions reported by Petr Vany´sek and coworkers highly oxidizing Cr^{6+} can be easily reduced to Cr^{3+} ions.[35]

Figure 6.14: Structural and oxidation state changes of Cr^{6+} loaded silica in to Cr^{3+} as a result of photochromism

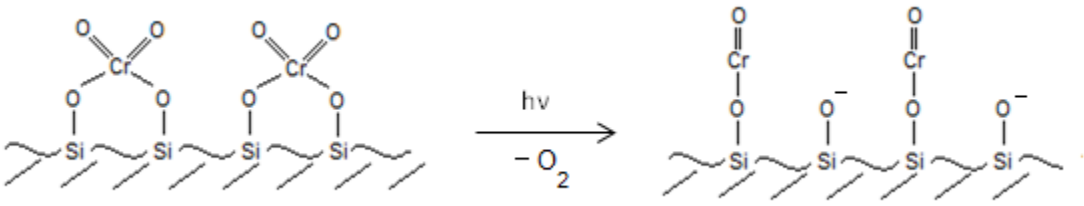

According to Pradier and coworkers, there are two possible ways for Cr^{3+} species to exist in the silica matrix due to different charge effects, either present as Cr_2O_3 crystallites (O = Cr-O-Cr = O), which are around 100Å in size, or as single chromium containing surface grafted species (-Si-O-Cr = O).[36] Usually, the correct phase of chromia can be identified by using FTIR and XPS. In most of the reported highly dispersed chromia loaded silica based photocatalysts, chromia is present as surface grafted species. Further, there are many reports of chromia species acting as very good oxidation catalysts for various organic compounds, which proves the possibility of generated chromia sites to act as catalytic sites for incoming air pollutants.[36-39]

On the other hand, there is an enhanced activity observed when silica is present compared to that of titania(figure 6.9). This increased photo activity may occur due to the favorable binding of Cr^{6+} to silica compared to titania. The probability of isomorphous substitution has been clearly predicted in the literature, and the stability of a metal ion in a tetrahedral environment surrounded by oxygen atoms by using Pauling criterion. Based on the ratio of ionic radii, ρ, of the cation and anion, the calculated value for titania and oxygen (ρ=0.515) falls out of the acceptable range (ρ= 0.225-0.414) of a tetrahedral coordination due to the larger size of Ti^{4+} (68pm). Therefore, the isomorphous binding of small Cr^{6+} (44 pm) ions to a titania matrix is

unlikely due to the larger distortion. But Since the ionic radii of Cr^{6+} and Si^{4+} (41pm) is much closer in values, isomorphous insertion of Cr^{6+} into silica matrix is highly favorable.[40] Photocatalysis is not restricted only to semiconducting materials, but photocatalysis is also possible with pure insulating materials as well as with mixtures of both. Thus, it is important to design novel systems in order to enhance photo degradation activities in the visible light range. New doping agents as well as new methods of preparation will benefit the future of photocatalysis.

6.7. References

1. Environmental Pollution and Impacts on Public Health, United Nations Environment Programme (UNEP)
2. Climate Change: The Role of Cities, United Nations Environment Programme (UNEP), **2009**
3. Kudo, A.,Photocatalysis and solar hydrogen production, *Pure Appl. Chem.,* **2007**, 79, 11, 1917–1927.
4. Fu, X.; Clark, L.; Yang, Q.; Anderson, A., Enhanced Photocatalytic Performance of Titania-Based Binary Metal Oxides: TiO_2/SiO_2 and TiO_2/ZrO_2, *Environ. Sci. Technol.* **1996**, 30, 647-653
5. Liang, Y. T.; Vijayan, B.K.; Gray, K.A.; Hersam, M.C.; Minimizing Graphene Defects Enhances Titania Nanocomposite-Based Photocatalytic Reduction of CO2 for Improved Solar Fuel Production, *Nano Lett.*, **2011**, 11, 2865–2870
6. Lim, S.H.; Phonthammachai, N.; Pramana, S.S.; White, T.J.; Simple Route to Monodispersed Silica-Titania Core-Shell Photocatalysts, *Langmuir*, **2008**, 24, 6226-6231
7. Yu, M.; Yao, H.; Jia, H.; Chihc, C.; Chien, C.; Andikal, W., Photocatalytic Activity for Degradation of Nitrogen Oxides over Visible Light Responsive Titania-Based Photocatalysts, *Environ. Sci. Technol.*, **2006**, 40, 1616-1621
8. Kisch,H.; Sakthivel, S.; Janczarek, M.; Mitoraj, D., A Low-Band Gap, Nitrogen-Modified Titania Visible-Light Photocatalyst, *J.Phys.chem. C,* **2007**, 111, 30, 11445-11449
9. (a)Ksibi, M.; Rossignol, S.; Tatibouët, J.M.; Trapalis, C., Synthesis and solid characterization of nitrogen and sulfur-doped TiO_2 photocatalysts active under near visible light, *Materials Letters*, **2008**, 62, 4204–4206 (b)Panayotov, D.; Yates, J.J.; —N Type doping of TiO_2 with atomic hydrogen-observation of the production of TiO_2 with atomic hydrogen-observation of the production of conduction band electrons by infrared spectroscopy, *Chem. Phys. Letters,***2007**, 436, 204-208
10. Tang, J.; Wu, Y.; McFarlandc, E.W.; Stucky, G.D., Synthesis and photocatalytic properties of highly crystalline and ordered mesoporous TiO_2 thin films, *Chem. Commun.*, **2004**, 1670-1671
11. Hamal, D.B.; Klabunde, K.J., Synthesis, characterization, and visible light activity of new nanoparticle photocatalysts based on silver, carbon, and sulfur-doped TiO_2, *Journal of colloidal and interface science,* **2007**, 311, 514-522

12. Xiang, Q.; Yu, J.; Jaroniec, M., Nitrogen and sulfur co-doped TiO_2 nanosheets with exposed {001} facets: synthesis, characterization and visible-light photocatalytic activity, *Phys. Chem. Chem. Phys.*, **2011**, 13, 4853–4861
13. Choi, J.; Park, H.; Hoffmann, M.R., Effects of Single Metal-Ion Doping on the Visible-Light Photoreactivity of TiO_2, *J. Phys. Chem. C,* **2010**, 114, 783–792
14. Kuznetsov, V.N.; Serpone, N., Visible Light Absorption by Various Titanium Dioxide Specimens, *J. Phys. Chem. B*, **2006**, 110, 25203-25209
15. Hirakawa, T.; Nosaka, Y., Properties of O2- and $OH^{\cdot}$ Formed in TiO_2 Aqueous Suspensions by Photocatalytic Reaction and the Influence of H2O2 and Some Ions, *Langmuir*, **2002**, 18, 3247-3254
16. Šnyrychová, I.; Hideg, E., First Application of Terephthalate as a Fluorescent Probe for Hydroxyl Radicals in Thylakoid Membranes, *Springer*, **2008**, 1553–1556.
17. Yu; J.; Xiang, Q.; Zhou, M., Preparation, characterization and visible-light-driven photocatalytic activity of Fe-doped titania nanorods and first-principles study for electronic structures, *Applied Catalysis B: Environmental*, **2009**, 90, 595–602
18. Szczepankiewicz, S.H.; Moss, J.A.; and Hoffmann, M.R.; Electron Traps and the Stark Effect on Hydroxylated Titania Photocatalysts, *J. Phys. Chem. B,* **2002**, 106, 7654-7658
19. Dvoranová, D.; Brezová, V.; Mazúra, M; Malati, M.A, Investigations of metal-doped titanium dioxide photocatalysts, *Applied Catalysis B: Environmental*,**2002**, 37, 91–105
20. Gomathi Devi, L.; Girish Kumar, S., Influence of physicochemical.electronic properties of transition metal ion doped polycrystalline titania on the photocatalytic degradation of Indigo Carmine and 4-nitrophenol under UV/solar light, *Applied Surface Science,***2011**, 257, 2779–2790
21. Choi, W.; Termin, A.; Hoffmann, M.R., The Role of Metal Ion Dopants in Quantum-Sized TiO_2: Correlation between Photoreactivity and Charge Carrier Recombination Dynamics, *J. Phys. Chem.*, **1994**, 98, 13669-13679
22. Chang, C.; Shen, Y., Synthesis and characterization of chromium doped SrTiO3 photocatalyst, *Materials Letters,* **2006**, 60, 129 – 132
23. Umebayashi, T.; Yamaki, T.; Itoh, H.; Asai, K., Analysis of electronic structure of 3d transition metai-doped TiO_2 based on band calculations, *Journal of physics and chemistry of solids*,**2002**, 1909-1920
24. Cheng, P.; Zheng, M.; Jin, Y.; Huang, Q.; Gu, M., Preparation and characterization of silica-doped titania photocatalyst through sol–gel method, *Materials Letters*, **2003**, 57, 2989– 2994
25. Anpo, M.; Nakaya, H.; Kodama, S.; Kubokawa, Y.; Domen, K.; Onishi, T., Photocatalysis over Binary Metal Oxides. Enhancement of the Photocatalytic Activity of TiO, in Titanium-Silicon Oxides, *J. Phys. Chem.*, **1986**, 90, 1633-1636
26. Anderson, C.; Bard, A.J., Improved Photocatalytic Activity and Characterization of Mixed TiO_2/SiO_2 and TiO_2/Al_2O_3 Materials, *J. Phys. Chem. B,* **1997**, 101, 2611-2616
27. Anpo, M.; Kawamura, T.; Kodama, S.; Maruya, K.; Onishi, T., Photocatalysts on Ti-Al Binary Metal Oxides: Enhancement of the Photocatalytic Activity of TiOp Species, *J. Phys. Chem.* **1988**, 92, 438-440
28. Peiris Weerasinghe, M.N., Klabunde, K.J.; Unpublished lab work from Kansas State University
29. Yoshida, H.; Active sites of silica-based quantum photocatalysts for non-oxidative reactions, *Catalysis Surveys from Asia,* **2005**, 9, 1

30. Yoshida, H.; Silica-based quantum photocatalysts for selective reactions, *Current Opinion in Solid State and Materials Science,* **2003**, 7, 435–442
31. Yoshida H, Murata C, Inaki Y, Hattori T., Photooxidation of propene by molecular oxygen over FSM-16., *Chem Lett*, **1998**, 1121–1122
32. Moisii, C.; Deguns, E.W.; Lita, A.; Callahan, S.D.; Van de Burgt, L.J.; Magana, D.; Stiegman, A. E., Coordination Environment and Vibrational Spectroscopy of Cr(VI) Sites Supported on Amorphous Silica, *Chem. Mater.*, **2006**, 18, 3965-3975
33. Wang J.; Uma, S.; Klabunde, K.J., Visible light photocatalytic activities of transition metal oxide/silica aerogels, *Microporous and Mesoporous Materials*, **2004**, 75, 143–147
34. Yi, Z.G.; Iwai,H.; Ye, J.H., Photochromism and visible light induced H2 generation in Sr2TiO4:Cr complexes, *Appl. Phys. Lett.*, **2010**, 96, 114103
35. Vany´sek, P., ELECTROCHEMICAL SERIES, **2000**, CRC PRESS LLC
36. Pradier, C.M.; Rodrigues, F.; Marcus, P.; Landau, M.V.; Kaliya, M.L.; Gutman, A.; Herskowitz, M., Supported Chromia catalysts for oxidation of organic compounds: The state of chromia phase and catalytic performance, *Applied CatalysisB: Environmental*, **2000**, 27, 73-85
37. Solymosi, F.; Rasko, J.; Papp, E.; Oszko, A.; Bansagi, T.; Catalytic decomposition and oxidation of CH3Cl on Cr2O3-doped SnO2, *Applied Catalysis A: General*, **1995**, 131 55-72
38. Delmon, B.; and Froment, G.F., Studies in Surface Science and Catalysis, Catalyst Deactivation, 1994, 88
39. Padilla, A.M.; Corella, J.; Toledo, H.M., Total oxidation of some chlorinated hydrocarbons with commercial chromia based catalysts, *Applied Catalysis B: Environmental*,**1999**, 22, 107-121
40. Cejka, J.; Corma, A.; Zones, S.; Zeolites and catalysis, synthesis, reactions and applications, **2010**, publisher – Wiley-VCH